ISSN: 2152-7385 Vol.1, No.2, July 2010

Scientific Research

Applied Mathematics

ISSN: 2152-7385
9 772152 738001 02

www.scirp.org/journal/am

Journal Editorial Board

ISSN 2152-7385 (Print) ISSN 2152-7393 (Online)
http://www.scirp.org/journal/am

Applied Mathematics, **2010, 1, 87-136**
Published Online July 2010 in SciRes (http://www.SciRP.org/journal/am/)

TABLE OF CONTENTS

Volume 1 Number 2 July 2010

Applied Mathematics (AM)

Journal Information

SUBSCRIPTIONS

Applied Mathematics (Online at Scientific Research Publishing, www.SciRP.org) is published bimonthly by Scientific Research Publishing, Inc., USA.

Subscription rates:

Print: $50 per issue.
To subscribe, please contact Journals Subscriptions Department, E-mail: sub@scirp.org

SERVICES

Advertisements
Advertisement Sales Department, E-mail: service@scirp.org

Reprints (minimum quantity 100 copies)
Reprints Co-ordinator, Scientific Research Publishing, Inc., USA.
E-mail: sub@scirp.org

COPYRIGHT

PRODUCTION INFORMATION

For manuscripts that have been accepted for publication, please contact:
E-mail: am@scirp.org

Applied Mathematics, 2010, 1, 87-93
doi:10.4236/am.2010.12011 Published Online July 2010 (http://www. SciRP.org/journal/am)

A Subclass of Harmonic Functions Associated with Wright's Hypergeometric Functions

Gangadharan Murugusundaramoorthy, Kalliyapan Vijaya
School of Advanced Sciences, Vellore Institute of Technology University, Vellore, India
E-mail: *gmsmoorthy@yahoo.com*, *kvavit@yahoo.co.in*
Received May 7, 2010; *revised May* 21, 2010; *accepted June* 25, 2010

Abstract

We introduce a new class of complex valued harmonic functions associated with Wright hypergeometric functions which are orientation preserving and univalent in the open unit disc. Further we define, Wright generalized operator on harmonic function and investigate the coefficient bounds, distortion inequalities and extreme points for this generalized class of functions.

Keywords: Harmonic Univalent Starlike Functions, Harmonic Convex Functions, Wright Hypergeometric Functions, Raina-Dziok Operator, Distortion Bounds, Extreme Points

1. Introduction

A continuous function $f = u + iv$ is a complex-valued harmonic function in a complex domain G if both u and v are real and harmonic in G. In any simply-connected domain $D \subset G$, we can write $f = h + \overline{g}$, where h and g are analytic in D. We call h the analytic part and g the co-analytic part of f. A necessary and sufficient condition for f to be locally univalent and orientation preserving in D is that $|h'(z)| > |g'(z)|$ in D (see [1]).

Denote by H the family of functions

$$f = h + \overline{g} \tag{1}$$

which are harmonic, univalent and orientation preserving in the open unit disc $U = \{z : |z| < 1\}$ so that f is normalized by $f(0) = h(0) = f_z(0) - 1 = 0$. Thus, for $f = h + \overline{g} \in$ H, we may express

$$f(z) = z + \sum_{m=2}^{\infty} a_m z^m + \overline{\sum_{m=1}^{\infty} b_m z^m}, \quad |b_1| < 1, \tag{2}$$

where the analytic functions h and g are in the forms

$$h(z) = z + \sum_{m=2}^{\infty} a_m z^m, \; g(z) = \sum_{m=1}^{\infty} b_m z^m \quad (|b_1| < 1).$$

We note that the family H of orientation preserving, normalized harmonic univalent functions reduces to the well known class S of normalized univalent functions if the co-analytic part of f is identically zero, that is $g \equiv 0$.

Let the Hadamard product (or convolution) of two power series

$$\phi(z) = z + \sum_{m=2}^{\infty} \phi_m z^m \tag{3}$$

and

$$\psi(z) = \sum_{m=2}^{\infty} \psi_m z^m \tag{4}$$

in S be defined by

$$(\phi * \psi)(z) = \sum_{m=2}^{\infty} \phi_m \psi_m z^m \quad .$$

For positive real parameters α_1, $A_1, \ldots, \alpha_p$, A_p and β_1, $B_1, \ldots, \beta_q$ B_q ($p, q \in N = 1, 2, 3, \ldots$) such that

$$1 + \sum_{m=1}^{q} B_m, - \sum_{m=1}^{p} A_m \geq 0 \quad , \qquad z \in U. \tag{5}$$

The Wright's generalized hypergeometric function [2]

$$p\Psi_q\left[(\alpha_1, A_1), \cdots, (\alpha_p, A_p); (\beta_1, B_1) \cdots (\beta_q, B_q); z\right] = p\Psi_q\left[(\alpha_m, A_m)_{1,p} (\beta_m, B_m)_{1,q}; z\right]$$

is defined by

$${}_p\Psi_q\left[(\alpha_t, A_t)_{1,p} (\beta_t, B_t)_{1,q}; z\right] = \sum_{m=0}^{\infty} \left\{\prod_{t=0}^{p} \Gamma(\alpha_t + mA_t)\right\} \left\{\prod_{t=0}^{q} \Gamma(\beta_t + mB_t)\right\}^{-1} \cdot \frac{z^m}{m!}, \quad z \in U.$$

If $A_t = 1$ ($t = 1, 2, p$) and $B_t = 1$ ($t = 1, 2, q$) we have the relationship:

$$\begin{aligned}&\Omega_p\Psi_q\left[(\alpha_t,A_t)_{1,p}(\beta_t,B_t)_{1,q};z\right]\\&={}_pF_q\left(\alpha_1,\cdots\alpha_p;\beta_1\cdots,\beta_q;z\right)\\&=\sum_{m=0}^{\infty}\frac{(\alpha_1)_m,\cdots(\alpha_p)_m}{(\beta_1)_m\cdots,(\beta_q)_m}\frac{z^m}{m!},\end{aligned}\tag{6}$$

$(p\le q+1;\, p.q\in N_0=N\cup\{0\};\, z\in U)$ is the generalized hypergeometric function (see for details [3]) where N denotes the set of all positive integers and $(\alpha)_n$ is the Pochhammer symbol and

$$\Omega=\left\{\prod_{t=0}^{p}\Gamma(\alpha_t)\right\}^{-1}\left\{\prod_{t=0}^{q}\Gamma(\beta_t)\right\}\tag{7}$$

By using the generalized hypergeometric function Dziok and Srivastava [3] introduced the linear operator. In [4] Dziok and Raina extended the linear operator by using Wright generalized hypergeometric function. First we define a function

$$\begin{aligned}&{}_p\Phi_q\left[(\alpha_t,A_t)_{1,p}(\beta_t,B_t)_{1,q};z\right]\\&=\Omega_p\Psi_q\left[(\alpha_t,A_t)_{1,p}(\beta_t,B_t)_{1,q};z\right]\end{aligned}$$

Let $W\left[(\alpha_t,A_t)_{1,p}(\beta_t,B_t)_{1,q}\right]:S\to S$ be a linear operator defined by

$$\begin{aligned}&W\left[(\alpha_t,A_t)_{1,p}(\beta_t,B_t)_{1,q}\right]\varphi(z)\\&:=z_p\Phi_q\left[(\alpha_t,A_t)_{1,p}(\beta_t,B_t)_{1,q};z\right]*\varphi(z)\end{aligned}$$

We observe that, for $f(z)$ of the form (1), we have

$$\begin{aligned}&W\left[(\alpha_t,A_t)_{1,p}(\beta_t,B_t)_{1,q}\right]\varphi(z)\\&:=z+\sum_{m=2}^{\infty}\sigma_m(\alpha_1)\,\varphi_m z^n,\end{aligned}\tag{8}$$

where $\sigma_m(\alpha_1)$ is defined by

$$\begin{aligned}&\sigma_m(\alpha_1)\\&=\frac{\Omega\Gamma(\alpha_1+A_1(m-1))\cdots\Gamma(\alpha_p+A_p(m-1))}{(m-1)!\Gamma(\beta_1+B_1(m-1))\cdots\Gamma(\beta_q+B_q(m-1))}\end{aligned}\tag{9}$$

If, for convenience, we write

$$\begin{aligned}&W[\alpha_1]\phi(z)\\&=W\left[(\alpha_1,A_1),\cdots(\alpha_p,A_p);(\beta_1,B_1)\cdots(\beta_q,B_q)\right]\phi(z)\end{aligned}\tag{10}$$

introduced by Dziok and Raina [4].

It is of interest to note that, if $A_t = 1$ (t = 1, 2, ..., p), B_t = 1 (t = 1, 2, ...,q) in view of the relationship (6) the linear operator (8) includes the Dziok-Srivastava operator (see [3]), for more details on these operators see [3,4,6,7] and [8]. It is interesting to note that Wright generalized hypergeometric function contains, Dziok-Srivastava operator as its special cases, further other linear operators the Hohlov operator, the Carlson-Shaffer operator [6], the Ruscheweyh derivative operator [7], the generalized Bernardi-Libera-Livingston operator, the fractional derivative operator [8], and so on. For example if p = 2 and q = 1 with $\alpha_1=\delta+1$ $(\delta>-1)$, $\alpha_2=1$, $\beta_1=1$, then

$$\begin{aligned}&W_1^{\,2}(\delta+1,1;1)\,\phi(z)\\&=D^{\delta}f(z)=\frac{z}{(1-z)^{\delta+1}}*\phi(z)\end{aligned}$$

is called Ruscheweyh derivative of order δ $(\delta>-1)$.

From (8) now we define, Wright generalized hypergeometric harmonic function $f=h+\overline{g}$ of the form (1), as

$$W_q^{\,p}[\alpha_1]f(z)=W_q^{\,p}[\alpha_1]h(z)+\overline{W_q^{\,p}[\alpha_1]g(z)}\tag{11}$$

and we call this as Wright generalized operator on harmonic function.

Motivated by the earlier works of [1,5,9-13] on the subject of harmonic functions, we introduce here a new subclass $WS_H([\alpha_1],\gamma)$ of H.

For $0\le\gamma<1$, let $WS_H([\alpha_1],\gamma)$ denote the subfamily of starlike harmonic functions $f\in H$ of the form (1) such that

$$\frac{\partial}{\partial\theta}(\arg W_q^{\,p}[\alpha_1]f(z))>\gamma\tag{12}$$

equivalently

$$\mathrm{Re}\left\{\frac{z(W_q^{\,p}[\alpha_1]h'(z))-\overline{z(W_q^{\,p}[\alpha_1]g'(z))}}{W_q^{\,p}[\alpha_1]h(z)+\overline{W_q^{\,p}[\alpha_1]g(z)}}\right\}>\gamma\tag{13}$$

where $W_q^{\,p}[\alpha_1]f(z)$ is given by (11) and $z\in U$.

We also let $WV_H([\alpha_1],\gamma)=WS_H([\alpha_1],\gamma)\cap V_H$ where V_H the class of harmonic functions with varying arguments introduced by Jahangiri and Silverman [10], consisting of functions f of the form (1) in H for which there exists a real number φ such that

$$\begin{aligned}&\eta_m+(m-1)\varphi\\&\equiv\pi(\mathrm{mod}\,2\pi),\ \ \delta_m+(m-1)\varphi\\&\equiv 0,\ \ m\ge 2,\end{aligned}\tag{14}$$

where $\eta_m=\arg(a_m)$ and $\delta_m=\arg(b_m)$.

In this paper we obtain a sufficient coefficient condition for functions f given by (2) to be in the class $WS_H([\alpha_1],\gamma)$. It is shown that this coefficient condition is necessary also for functions belonging to the class

$WV_H([\alpha_1],\gamma)$. Further, distortion results and extreme points for functions in $WV_H([\alpha_1],\gamma)$ are also obtained.

2. The Class $WS_H([\alpha_1],\gamma)$

We begin deriving a sufficient coefficient condition for the functions belonging to the class $WS_H([\alpha_1],\gamma)$.

Theorem 1. Let $f=h+\overline{g}$ be given by (2). If

$$\sum_{m=2}^{\infty}\left(\frac{m-\gamma}{1-\gamma}|a_m|+\frac{m+\gamma}{1-\gamma}|b_m|\right)\cdot \sigma_m(\alpha_1)\le 1-\frac{1+\gamma}{1-\gamma}b_1 \tag{15}$$

$0\le\gamma<1$, Then $f\in WS_H([\alpha_1],\gamma)$.

Proof. We first show that if the inequality (15) holds for the coefficients of $f=h+\overline{g}$, then the required condition (13) is satisfied. Using (11) and (13), we can write

$$\operatorname{Re}\left\{\frac{z(W_q^p[\alpha_1]h'(z))-\overline{z(W_q^p[\alpha_1]g'(z))}}{W_q^p[\alpha_1]h(z)+\overline{W_q^p[\alpha_1]g(z)}}\right\}$$

$$=\operatorname{Re}\frac{A(z)}{B(z)}$$

where

$$A(z)=z(W_q^p[\alpha_1]h'(z))-\overline{z(W_q^p[\alpha_1]g'(z))}$$

and

$$B(z)=W_q^p[\alpha_1]h(z)+\overline{W_q^p[\alpha_1]g(z)}$$

In view of the simple assertion that $\operatorname{Re}(w)\ge\gamma$ if and only if $|1-\gamma+w|\ge|1+\gamma-w|$, it is sufficient to show that

$$|A(z)+(1-\gamma)B(z)|-|A(z)-(1+\gamma)B(z)|\ge 0. \tag{16}$$

Substituting for $A(z)$ and $B(z)$ the appropriate expressions in (16), we get

$$|A(z)+(1-\gamma)B(z)|-|A(z)-(1+\gamma)B(z)|$$

$$\ge(2-\gamma)|z|-\sum_{m=2}^{\infty}(m+1-\gamma)\sigma_m(\alpha_1)|a_m|\cdot$$

$$|z|^m-\sum_{m=1}^{\infty}(m-1+\gamma)\sigma_m(\alpha_1)|b_m||z|^m$$

$$-\gamma|z|-\sum_{m=2}^{\infty}(m-1-\gamma)\sigma_m(\alpha_1)|a_m|\cdot$$

$$|z|^m-\sum_{m=2}^{\infty}(m+1+\gamma)\sigma_m(\alpha_1)|b_m||z|^m$$

$$\ge 2(1-\gamma)|z|\left\{1-\sum_{m=2}^{\infty}\frac{m-\gamma}{1-\gamma}\sigma_m(\alpha_1)|a_m|\cdot |z|^{m-1}-\sum_{m=2}^{\infty}\frac{m+\gamma}{1-\gamma}\sigma_m(\alpha_1)|b_m||z|^{m-1}\right\}$$

$$\ge 2(1-\gamma)|z|\left\{1-\frac{1+\gamma}{1-\gamma}b_1-\left(\sum_{m=2}^{\infty}\left[\frac{m-\gamma}{1-\gamma}\sigma_m(\alpha_1)|a_m|+\frac{m+\gamma}{1-\gamma}\sigma_m(\alpha_1)|b_m|\right]\right)\right\}\ge 0.$$

by virtue of the inequality (15). This implies that $f\in WS_H([\alpha_1],\gamma)$.

Now we obtain the necessary and sufficient condition for function $f=h+\overline{g}$ be given with condition (14).

Theorem 2. Let $f=h+\overline{g}$ be given by (2) and for $0\le\gamma<1$, then $f\in WV_H([\alpha_1],\gamma)$ if and only if

$$\sum_{m=2}^{\infty}\left(\frac{m-\gamma}{1-\gamma}|a_m|+\frac{m+\gamma}{1-\gamma}|b_m|\right)\sigma_m(\alpha_1)\le 1-\frac{1+\gamma}{1-\gamma}b_1 \tag{17}$$

Proof. Since $WV_H([\alpha_1],\gamma)\subset WS_H([\alpha_1],\gamma)$, we only need to prove the necessary part of the theorem. Assume that $f\in WV_H([\alpha_1],\gamma)$, then by virture of (11) to (13), we obtain

$$\operatorname{Re}\left\{\frac{z(W_q^p[\alpha_1]h'(z))-\overline{z(W_q^p[\alpha_1]g'(z))}}{W_q^p[\alpha_1]h(z)+\overline{W_q^p[\alpha_1]g(z)}}-\gamma\right\}\ge 0.$$

The above inequality is equivalent to

$$\operatorname{Re}\left\{\frac{z+\sum_{m=2}^{\infty}(m-\gamma)\sigma_m(\alpha_1)|a_m|z^m-\sum_{m=1}^{\infty}(m+\gamma)\sigma_m(\alpha_1)|b_m|\overline{z}^m}{z+\sum_{m=2}^{\infty}\sigma_m(\alpha_1)|a_m|z^m+\sum_{m=1}^{\infty}\sigma_m(\alpha_1)|b_m|\overline{z}^m}\right\}$$

$$=\operatorname{Re}\left\{\frac{(1-\gamma)+\sum_{m=2}^{\infty}(m-\gamma)\sigma_m(\alpha_1)|a_m|z^{m-1}-\frac{\overline{z}}{z}\sum_{m=1}^{\infty}(m+\gamma)\sigma_m(\alpha_1)|b_m|\overline{z}^{m-1}}{1+\sum_{m=2}^{\infty}\sigma_m(\alpha_1)|a_m|z^{m-1}+\frac{\overline{z}}{z}\sum_{m=1}^{\infty}\sigma_m(\alpha_1)|b_m|\overline{z}^{m-1}}\right\}\ge 0.$$

This condition must hold for all values of z, such that $|z| = r < 1$. Upon choosing φ according to (14) we must have (18).

If (17) does not hold, then the numerator in (18) is negative for r sufficiently close to 1. Therefore, there exists a point $z_o = r_o$ in (0, 1) for which the quotient in (18) is negative. This contradicts our assumption that $f \in WV_H([\alpha_1],\gamma)$. We thus conclude that it is both necessary and sufficient that the coefficient bound inequality (17) holds true when $f \in WV_H([\alpha_1],\gamma)$. This completes the proof of Theorem 2.

If we put $\varphi = \frac{2\pi}{k}$ in (14), then Theorem 2 gives the following corollary.

Corollary 1. A necessary and sufficient condition for $f = h + \overline{g}$ satisfying (17) to be starlike is that $\arg(a_m) = \pi - 2(m-1)\pi/k$, and $\arg(b_m) = 2\pi - 2(m-1)\pi/k$, $(k = 1, 2, 3, \ldots)$.

3. Distortion Bounds and Extreme Points

In this section we obtain the distortion bounds for the functions $f \in WV_H([\alpha_1],\gamma)$ that lead to a covering result for the family $WV_H([\alpha_1],\gamma)$.

Theorem 3. If $f \in WV_H([\alpha_1],\gamma)$ then

$$f(z) \le (1+|b_1|)r + \frac{1}{\sigma_2(\alpha_1)}\left(\frac{1-\gamma}{2-\gamma} - \frac{1+\gamma}{2-\gamma}|b_1|\right)r^2$$

and

$$f(z) \ge (1-|b_1|)r - \frac{1}{\sigma_2(\alpha_1)}\left(\frac{1-\gamma}{2-\gamma} - \frac{1+\gamma}{2-\gamma}|b_1|\right)r^2.$$

Proof. We will only prove the right-hand inequality of the above theorem. The arguments for the left-hand inequality are similar and so we omit it. Let $f \in WV_H \cdot ([\alpha_1],\gamma)$ taking the absolute value of f, we obtain

$$\begin{aligned} &|f(z)| \\ &\le (1+|b_1|)r + \sum_{m=2}^{\infty}\left(|a_m|+|b_m|\right)r^m \\ &\le (1+|b_1|)r + r^2\sum_{m=2}^{\infty}\left(|a_m|+|b_m|\right). \end{aligned}$$

This implies that

$$\begin{aligned} |f(z)| &\le (1+|b_1|)r + \frac{1}{\sigma_2(\alpha_1)}\left(\frac{1-\gamma}{2-\gamma}\right)\cdot \\ &\sum_{m=2}^{\infty}\left(\left(\frac{2-\gamma}{1-\gamma}\right)\sigma_2(\alpha_1)|a_m| + \left(\frac{2-\gamma}{1-\gamma}\right)\sigma_2(\alpha_1)|b_m|\right)r^2 \\ &\le (1+|b_1|)r + \frac{1}{\sigma_2(\alpha_1)}\left(\frac{1-\gamma}{2-\gamma}\right)\left[1 - \frac{1+\gamma}{1-\gamma}|b_1|\right]r^2 \\ &\le (1+|b_1|)r + \frac{1}{\sigma_2(\alpha_1)}\left(\frac{1-\gamma}{2-\gamma} - \frac{1+\gamma}{2-\gamma}|b_1|\right)r^2, \end{aligned}$$

which establish the desired inequality.

As consequences of the above theorem and corollary 1, we state the following corollary.

Corollary 2. Let $f = h + \overline{g}$ and of the form (2) be so that $f \in WV_H([\alpha_1],\gamma)$. Then

$$\left\{ w : |w| < \frac{2\sigma_2(\alpha_1) - 1 - [\sigma_2(\alpha_1) - 1]\gamma}{(2-\gamma)\sigma_2(\alpha_1)} - \frac{2\sigma_2(\alpha_1) - 1 - [\sigma_2(\alpha_1) + 1]\gamma}{(2-\gamma)\sigma_2(\alpha_1)} b_1 \right\} \subset f(U).$$

For a compact family, the maximum or minimum of the real part of any continuous linear functional occurs at one of the extreme points of the closed convex hull. Unlike many other classes, characterized by necessary and sufficient coefficient conditions, the family $WV_H([\alpha_1],\gamma)$ is not a convex family. Nevertheless, we may still apply the coefficient characterization of the $WV_H([\alpha_1],\gamma)$ to determine the extreme points.

Theorem 4. The closed convex hull of $WV_H([\alpha_1],\gamma)$ (denoted by $clco\,WV_H([\alpha_1],\gamma)$) is

$$\left\{ f(z) = z + \sum_{m=2}^{\infty}|a_m| z^m + \overline{\sum_{m=1}^{\infty}|b_m| z^m}, \; : \sum_{m=2}^{\infty} m\left[|a_m| + |b_m|\right] < 1 - b_1 \right\}.$$

$$\frac{(1-\gamma) - (1+\gamma)b_1 - \left(\sum_{m=2}^{\infty}(m-\gamma)\sigma_m(\alpha_1)|a_m|r^{m-1} + (m+\gamma)\sigma_m(\alpha_1)|b_m|r^{m-1}\right)}{1 + |b_1| + \left(\sum_{m=2}^{\infty}\sigma_m(\alpha_1)|a_m| + \sum_{m=1}^{\infty}\sigma_m(\alpha_1)|b_m|\right)r^{m-1}} \ge 0. \qquad (18)$$

By setting $\lambda_m = \frac{1-\gamma}{(m-\gamma)\sigma_m(\alpha_1)}$ and $\mu_m = \frac{1-\gamma}{(m+\gamma)\sigma_m(\alpha_1)}$, then for b_1 fixed, the extreme points for $clco WV_H([\alpha_1], \gamma)$ are

$$\left\{z+\lambda_m xz^m+\overline{b_1 z}\right\}\cup\left\{z+\overline{b_1 z+\mu_m xz^m}\right\} \tag{19}$$

where $m \geq 2$ and $|x| = 1-|b_1|$.

Proof. Any function f in $clco WV_H([\alpha_1],\gamma)$ be expressed as

$$f(z) = z+\sum_{m=2}^{\infty}|a_m|e^{i\eta_m}z^m+\overline{b_1 z}+\overline{\sum_{m=2}^{\infty}|b_m|e^{i\delta_m}z^m},$$

where the coefficient satisfy the inequality (15). Set $h_1(z) = z$, $g_1(z) = b_1 z$, $h_m(z) = z+\lambda_m e^{i\eta_m}z^m$, $g_m(z) = b_1 z + \mu_m e^{i\mu_m}z^m$, for m = 2, 3,… Writing $X_m = \frac{|a_m|}{\lambda_m}$, $Y_m = \frac{|b_m|}{\mu_m}$ m = 2, 3... and $X_1 = 1-\sum_{m=2}^{\infty}X_m$; $Y_1 = 1-\sum_{m=2}^{\infty}Y_m$; we get

$$f(z) = \sum_{m=1}^{\infty}[X_m h_m(z)+Y_m g_m(z)].$$

In particular, putting

$$f_1(z) = z+\overline{b_1 z}$$

and

$$f_m(z) = z+\lambda_m xz^m+\overline{b_1 z}+\overline{\mu_m yz^m}, \quad (m\geq 2,\ |x|+|y| = 1-|b_1|)$$

We see that extreme points of functions in $clco WV_H \cdot ([\alpha_1],\gamma) \subset \{f_m(z)\}$. To see that f_m is not an extreme point if both $|x| \neq 0$ and $|y| \neq 0$, we will show that it can then also be expressed as a convex linear combinations of functions in $clco WV_H([\alpha_1],\gamma)$. Without loss of generality, assume $|x| \geq |y|$. Choose $\in > 0$ small enough so that $\in < \frac{|x|}{|y|}$. Set $A = 1+\in$ and $B = 1-\left|\frac{\in x}{y}\right|$. We then see that both

$$t_1(z) = z+\lambda_m Axz^m+\overline{b_1 z+\mu_m Byz^m}$$

and

$$t_2(z) = z+\lambda_m(2-A)xz^m+\overline{b_1 z+\mu_m(2-B)yz^m}$$

are in $clco WV_H([\alpha_1],\gamma)$, and that $f_m(z) = \frac{1}{2}\{t_1(z)+t_2(z)\}$. The extremal coefficient bounds show that functions of the form (19) are the extreme points for $clco WV_H([\alpha_1],\gamma)$, and so the proof is complete.

4. Inclusion Relation

Following Avici and Zlotkiewicz [9] (see also Ruscheweyh [14]), we refer to the δ-neighborhood of the function $f(z)$ defined by (2) to be the set of functions F for which

$$N_\delta(f) := \left\{F(z) = z+\sum_{m=2}^{\infty}A_m z^m+\sum_{m=2}^{\infty}\overline{B_m z^m},\right.$$
$$\left.\sum_{m=2}^{\infty}m\left(|a_m-A_m|+|b_m-B_m|\right)+|b_1-B_1| \leq \delta\right\}. \tag{20}$$

In our case, let us define the generalized δ–neighborhood of f to be the set

$$N_\delta(f) := \left\{F : \sum_{m=2}^{\infty}\sigma_m(\alpha_1)[(m-\gamma)|a_m-A_m|\right.$$
$$\left.+(m+\gamma)|b_m-B_m|]+(1-\gamma)|b_1-B_1| \leq (1-\gamma)\delta\right\}. \tag{21}$$

Theorem 5. Let f be given by (2). If f satisfies the conditions

$$\sum_{m=2}^{\infty}m(m-\gamma)|a_m|\sigma_m(\alpha_1)$$
$$+\sum_{m=1}^{\infty}m(m+\gamma)|b_m|\sigma_m(\alpha_1) \leq 1-\gamma, \tag{21}$$

$0 \leq \gamma < 1$ and $0 \leq \gamma < 1$, then $N_\delta(f) \subset WS_H([\alpha_1],\gamma)$.

Proof. Let f satisfy (22) and $F(z)$ be given by

$$F(z) = z+\sum_{m=2}^{\infty}A_m z^m+\sum_{m=2}^{\infty}\overline{B_m z^m},$$

which belongs to $N(f)$. We obtain

$$(1+\gamma)|B_1|+\sum_{m=2}^{\infty}(m-\gamma)|A_m|+(m-\gamma)|B_m|\sigma_m(\alpha_1)$$
$$\leq (1+\gamma)|B_1-b_1|+(1+\gamma)|b_1|$$
$$+\sum_{m=2}^{\infty}\sigma_m(\alpha_1)(m-\gamma)|A_m-a_m|$$
$$+(m+\gamma)|B_m-b_m|$$
$$+\sum_{m=2}^{\infty}\sigma_m(\alpha_1)\left[(m-\gamma)|a_m|+(m+\gamma)|b_m|\right]$$
$$\leq (1-\gamma)\delta+(1+\gamma)|b_1|$$
$$+\frac{1}{2-\gamma}\sum_{m=2}^{\infty}m\sigma_m(\alpha_1)\left((m-\gamma)|a_m|+(m+\gamma)|b_m|\right)$$

$$\le (1-\gamma)\delta + (1+\gamma)\,|\,b_1\,| + \frac{1}{2-\gamma}\Big((1-\gamma)-(1+\gamma)\big|b_1\big|\Big) \le 1-\gamma.$$

Hence for $\delta = \frac{1-\gamma}{2-\gamma}\left(1-\frac{1+\gamma}{1-\gamma}|\,b_1\,|\right)$, we infer that $WS_H([\alpha_1],\gamma)$ which concludes the proof of Theorem 5.

Now, we will examine the closure properties of the class $WV_H([\alpha_1],\gamma)$ under the generalized Bernardi-Libera-Livingston integral operator $L_c(f)$ which is defined by

$$L_c(f) = \frac{c+1}{z^c}\int_0^z t^{c-1} f(t)dt,\ c > -1.$$

Theorem 6. Let $f \in WV_H([\alpha_1],\gamma)$. Then $L_c(f) \in WV_H([\alpha_1],\gamma)$.

Proof. From the representation of $L_c(f)$, it follows that

$$L_c(f) = \frac{c+1}{z^c}\int_0^z t^{c-1}\Big[h(t)+\overline{g(t)}\Big]dt$$

$$= \frac{c+1}{z^c}\left(\int_0^z t^{c-1}\left(t-\sum_{m=2}^{\infty}a_m t^m\right)dt + \overline{\int_0^z t^{c-1}\left(\sum_{m=1}^{\infty}b_m t^m\right)dt}\right)$$

$$= z - \sum_{m=2}^{\infty}A_m z^m + \sum_{m=1}^{\infty}B_m z^m\ ,$$

where

$$A_m = \frac{c+1}{c+m}a_m\ ;\quad B_m = \frac{c+1}{c+m}b_m\ .$$

Therefore

$$\sum_{m=1}^{\infty}\left(\frac{m-\gamma}{1-\gamma}\frac{c+1}{c+m}|\,a_m\,| + \frac{m+\gamma}{1-\gamma}\frac{c+1}{c+m}|\,b_m\,|\right)\sigma_m(\alpha_1)$$

$$\le \sum_{m=1}^{\infty}\left(\frac{m-\gamma}{1-\gamma}|\,a_m\,| + \frac{m+\gamma}{1-\gamma}|\,b_m\,|\right)\sigma_m(\alpha_1) \le 2(1-\gamma).$$

Since $f \in WV_H([\alpha_1],\gamma)$, therefore by Theorem 2, $L_c(f) \in WV_H([\alpha_1],\gamma)$.

Theorem 7. For $0 \le \delta \le \gamma < 1$, let $f \in WV_H([\alpha_1],\gamma)$ and $F \in WV_H([\alpha_1],\delta)$. Then $(f*F) \in WV_H([\alpha_1],\gamma) \subset WV_H([\alpha_1],\delta)$.

Proof. Let

$$f(z) = z - \sum_{m=2}^{\infty}a_m\, z^m + \sum_{m=1}^{\infty}\overline{b}_m\, \overline{z}^m \in WV_H([\alpha_1],\gamma)$$

and

$$F(z) = z - \sum_{m=2}^{\infty}A_m\, z^m + \sum_{m=1}^{\infty}\overline{B}_m\, \overline{z}^m \in WV_H([\alpha_1],\delta)$$

Then

$$f(z)*F(z) = z - \sum_{m=2}^{\infty}A_m a_m\, z^m + \sum_{m=1}^{\infty}\overline{B}_m\overline{b}_m\, \overline{z}^m$$

For $(f*F) \in WV_H([\alpha_1],\delta)$ we note that $\left|A_m\right| \le 1$ and $\left|B_m\right| \le 1$. Now by Theorem 2, we have

$$\sum_{m=2}^{\infty}\frac{(m-\delta)\sigma_m(\alpha_1)}{1-\delta}|\,a_m\,\|\,A_m\,| + \sum_{m=1}^{\infty}\frac{(m+\delta)\sigma_m(\alpha_1)}{1-\delta}|\,b_m\,\|\,B_m\,|$$

$$\le \sum_{m=2}^{\infty}\frac{(m-\delta)\sigma_m(\alpha_1)}{1-\delta}|\,a_m\,| + \sum_{m=1}^{\infty}\frac{(m+\delta)\sigma_m(\alpha_1)}{1-\delta}|\,b_m\,|$$

$$\le \sum_{m=2}^{\infty}\frac{(m-\gamma)\sigma_m(\alpha_1)}{1-\gamma}|\,a_m\,| + \sum_{m=1}^{\infty}\frac{(m+\gamma)\sigma_m(\alpha_1)}{1-\gamma}|\,b_m\,| \le 1.$$

Therefore $(f*F) \in WV_H([\alpha_1],\gamma) \subset WV_H([\alpha_1],\delta)$ and since the above inequality bounded by $2(1-\gamma)$ while $2(1-\gamma) \le 2(1-\delta)$.

5. Concluding Remarks

The various results presented in this paper would provide interesting extensions and generalizations of those considered earlier for simpler harmonic function classes (see [10,12,13]). The details involved in the derivations of such specializations of the results presented in this paper are fairly straight-forward.

6. References

[1] J. Clunie and T. Sheil-Small, "Harmonic Univalent Functions," *Annales Academiae Scientiarum Fennicae, Series A I, Mathematica*, Vol. 9, 1984, pp. 3-25.

[2] E. M. Wright, "The Asymptotic Expansion of the Generalized Hypergeometric Function," *Proceedings of the London Mathematical Society*, Vol. 46, 1946, pp. 389-408.

[3] J. Dziok and H. M. Srivastava, "Certain Subclasses of Analytic Functions Associated with the Generalized Hypergeometric Function," *Integral Transforms and Special Functions*, Vol. 14, No. 1, 2003, pp. 7-18.

[4] J. Dziok and R. K. Raina, "Families of Analytic Functions Associated with the Wright Generalized Hypergeometric Function," *Demonstratio Mathematica*, Vol. 37, No. 3, 2004, pp. 533-542.

[5] J. M. Jahangiri, "Harmonic Functions Starlike in the Unit Disc," *Journal of Mathematical Analysis and Applications*, Vol. 235, No. 2, 1999, pp. 470-477.

[6] B. C. Carlson and D. B. Shaffer, "Starlike and Prestarlike Hypergeometric Functions," *SIAM Journal on Mathematical Analysis*, Vol. 15, No. 4, 1984, pp. 737-745.

[7] S. Ruscheweyh, "New Criteria for Univalent Functions," *Proceedings of the American Mathematical Society*, Vol. 49, No. 1, 1975, pp. 109-115.

[8] H. M. Srivastava and S. Owa, "Some Characterization and Distortion Theorems Involving Fractional Calculus, Generalized Hypergeometric Functions, Hadamard Products, Linear Operators and Certain Subclasses of Analytic Functions," *Nagoya Mathematics Journal*, Vol. 106, 1987, pp. 1-28.

[9] Y. Avici and E. Zlotkiewicz, "On Harmonic Univalent Mappings," *Annales Universitatis Mariae Curie-Skłodowska, Sectio A*, Vol. 44, 1990, pp. 1-7.

[10] J. M. Jahangiri and H. Silverman, "Harmonic Univalent Functions with Varying Arguments," *International Journal of Applied Mathematics*, Vol. 8, No. 3, 2002, pp. 267-275.

[11] J. M. Jahangiri, G. Murugusundaramoorthy and K. Vijaya, "Starlikeness of Rucheweyh Type Harmonic Univalent Functions," *Journal of the Indian Academy of Mathematics*, Vol. 26, No. 1, 2004, pp. 191-200.

[12] G. Murugusundaramoorthy, "A Class of Ruscheweyh-Type Harmonic Univalent Functions with Varying Arguments," *Southwest Journal of Pure and Applied Mathematics*, No. 2, 2003, pp. 90-95.

[13] K. Vijaya, "Studies on Certain Subclasses of Harmonic Functions," Ph.D. Thesis, Vellore Institute of Technology University, Vellore, September 2006.

[14] S. Ruscheweyh, "Neighborhoods of Univalent Functions," *Proceedings of the American Mathematical Society*, Vol. 81, No. 4, 1981, pp. 521-528.

Applied Mathematics, 2010, 1, 94-100
doi:10.4236/am.2010.12012 Published Online July 2010 (http://www. SciRP.org/journal/am)

Liouville-Type Theorems for Some Integral Systems

Zhengce Zhang
College of Science, Xi'an Jiaotong University, Xi'an, China
E-mail: zhangzc@mail.xjtu.edu.cn
Received March 20, 2010; *revised May* 21, 2010; *accepted May* 27, 2010

Abstract

In this paper, Liouville-type theorems of nonnegative solutions for some elliptic integral systems are considered. We use a new type of moving plane method introduced by Chen-Li-Ou. Our new ingredient is the use of Stein-Weiss inequality instead of Maximum Principle.

Keywords: Liouville Theorem, Integral System, Moving Plane Method

1. Introduction

In this paper we consider the nonnegative solutions of the systems of integral equations in $\mathbb{R}^N (N \geq 2)$, $0 < \mu < N$,

$$\begin{cases} u(x) = \int_{\mathbb{R}^N} \dfrac{u(y)^{q_1} + v(y)^{q_2}}{|x-y|^{N-\mu}} dy \\ v(x) = \int_{\mathbb{R}^N} \dfrac{v(y)^{p_1} + u(y)^{p_2}}{|x-y|^{N-\mu}} dy \end{cases} \tag{1}$$

and

$$\begin{cases} u(x) = \int_{\mathbb{R}^N} \dfrac{u(y)^{q_1} v(y)^{q_2}}{|x-y|^{N-\mu}} dy \\ v(x) = \int_{\mathbb{R}^N} \dfrac{v(y)^{p_1} u(y)^{p_2}}{|x-y|^{N-\mu}} dy \end{cases} \tag{2}$$

The integral systems are closely related to the following systems of differential equations in $\mathbb{R}^N$

$$\begin{cases} (-\Delta)^{\mu/2} u = u^{q_1} + v^{q_2} \\ (-\Delta)^{\mu/2} v = v^{p_1} + u^{p_2} \end{cases} \tag{3}$$

and

$$\begin{cases} (-\Delta)^{\mu/2} u = u^{q_1} v^{q_2} \\ (-\Delta)^{\mu/2} v = v^{p_1} u^{p_2} \end{cases} \tag{4}$$

In fact, every positive smooth solution of PDE (3)(or (4)) multiplied by a constant satisfies (1) (or (2)) respectively. This equivalence between integral and PDE systems can be verified as in the proof of Theorem 1 in [1]. For single equations, we refer to [2]. Here, in (3) and (4), we have used the following definition:

$$(-\Delta)^{\mu/2} u = (|\xi|^{\mu} u^{\wedge})^{\vee}$$

where $\wedge$ is the Fourier transformation and $\vee$ its inverse.

The question is to determine for which values of the exponents p_i and q_i the only nonnegative solution (u, v) of (1) and (2) is trivial, *i.e.*, $(u; v) = (0, 0)$. When $\mu = 2$, is the case of the Emden-Fowler equation

$$\Delta u + u^k = 0, \quad u \geq 0 \quad \text{in} \quad \mathbb{R}^N \tag{5}$$

When $1 \leq k < (N+2)/(N-2) (N > 3)$, it has been proved in [3,4] that the only solutions of (5) is $u = 0$. In dimension $N = 2$, a similar conclusion holds for $0 \leq k < \infty$. It is also well known that in the critical case, $k = (N+2)/(N-2)$, problem (5) has a two-parameter family of solutions given by

$$u(x) = \left(\frac{c}{d + |x - \bar{x}|^2}\right)^{\frac{N-2}{2}}, \tag{6}$$

where $c = [N(N-2)d]^{\frac{1}{2}}$ with $d > 0$ and $\bar{x} \in \mathbb{R}^N$. If $p_1, q_1 > 1$, $p_2, q_2 \geq 0$ and $\min\{p_1 + 2p_2, q_1 + 2q_2\} \leq (N+2)/(N-2)$, using Pokhozhaev's second identity, Chen and Lu [5] have proved that the problem (4) has no positive radial solutions with $u(x) = u(|x|)$. Suppose that p_1, p_2, q_1 and q_2 satisfy $0 \leq p_1, q_1 \leq 1$, $p_2, q_2 > 1$ and other related conditions, using the method of integral relations, Mitidieri [6] has proved that the problem (4) has no positive solutions of $C^2(\mathbb{R}^N)$. In the present paper, we study Problem (1) and Problem (2) by virtue of the moving plane method and obtain the following theorems of nonexistence of positive solutions in the weaker regularity.

Theorem 1.1: Let (u, v) be a nonnegative solution of Problem (1) and $\frac{N}{N-\mu} < p_1, p_2, q_1, q_2 < \frac{N+\mu}{N-\mu}$ but not equal to $(N+\mu)/(N-\mu)$ at the same time. Suppose that $u \in L^{\beta_1}_{loc}(\mathbb{R}^N) \bigcap L^{\alpha_2}_{loc}(\mathbb{R}^N)$ and $v \in L^{\beta_2}_{loc}(\mathbb{R}^N) \bigcap L^{\alpha_1}_{loc}(\mathbb{R}^N)$ with $\beta_1 = \frac{q_1 - 1}{\frac{N-\mu}{N} q_1 - 1}$, $\beta_2 = \frac{q_2 - 1}{\frac{N-\mu}{N} q_2 - 1}$, $\alpha_1 = \frac{p_1 - 1}{\frac{N-\mu}{N} p_1 - 1}$ and $\alpha_2 = \frac{p_2 - 1}{\frac{N-\mu}{N} p_2 - 1}$. Then both u and v are trivial.

Theorem 1.2: Let (u, v) be a nonnegative solution of Problem (2) and $\frac{N}{N-\mu} < p_1 + p_2, q_1 + q_2 < \frac{N+\mu}{N-\mu}$ but not both equal to $(N+\mu)/(N-\mu)$. Suppose that $u, v \in L^{\beta}(\mathbb{R}^N) \bigcap L^{\alpha}(\mathbb{R}^N)$ with $\beta = \frac{q_1 + q_2 - 1}{\frac{N-\mu}{N}(q_1+q_2) - 1}$ and $\alpha = \frac{p_1 + p_2 - 1}{\frac{N-\mu}{N}(p_1+p_2) - 1}$. Then both u and v are trivial.

Remark 1.1: In the proof of Theorem 1.1 or Theorem 1.2, we only treat the case $\frac{N}{N-\mu} < p_1, p_2, q_1, q_2 < \frac{N+\mu}{N-\mu}$ or $\frac{N}{N-\mu} < p_1 + p_2, q_1 + q_2 < \frac{N+\mu}{N-\mu}$ respectively. The remaining cases can be handled in the same way. We leave this to the interested reader.

We shall need the following doubly weighted Hardy-Littlewood-Sololev inequality of Stein and Weiss (see, for example, [7])

$$\left\| \int_{\mathbb{R}^N} V(x,y) f(y)\, dy \right\|_{L^q(\mathbb{R}^N)} \le \Lambda_{\gamma,\tau,\lambda,p,N} \| f \|_{L^p(\mathbb{R}^N)} \tag{7}$$

where $V(x,y) = |x|^{-\tau} |x-y|^{-\lambda} |y|^{-\gamma}$, $0 \le \gamma < N/p'$, $0 \le \tau < N/q$, $1/p + 1/p' = 1$ and $1/p + (\gamma + \tau + \lambda)/N = 1 + 1/q$.

There are some related works about this paper. For $\mu = 2$, $p_1 = q_1 = 0$ and $1 < p_2$, $q_2 \le (N+2)/(N-2)$ (but p_2 and q_2 are not both equal to $(N+2)/(N-2)$), Figueiredo and Felmer (see [8]) proved the similar Liouville-type theorems to Theorem 1.1 and Theorem 1.2 on nonnegative positive of $C^2(\mathbb{R}^N)$ using the moving plane method and Maximum Principle. Busca and Manásevich obtained a new result (see [9]) using the same method as in [8]. It allows p_2 and q_2 to reach regions where one of the two exponents is supercritical. In [10], Zhang, Wang and Li first introduced the Kelvin transforms and gave a different proof using the method of moving spheres. This approach was suggested in [11], while Li and Zhang had made significant simplifications in the proof of some Liouville theorems for a single equation in [12]. In this paper, by virtue of Hardy-Littlewood-Sololev inequality instead of Maximum Principle, we consider the integral systems (1) and (2) with $0 < \mu < N$ and the general nonlinearities. Therefore, it is a generalization of Liouville-type theorems in [5,6,8,9,13-15].

Let us emphasize that considerable attention has been drawn to Liouville-type results and existence of positive solutions for general nonlinear elliptic equations and systems, and that numerous related works are devoted to some of its variants, such as more general quasilinear operators, and domains. We refer the interested reader to [16-24], and some of the references therein.

In the following, we shall use C to denote different constants which depend only on N, μ, q_i, p_i $(i = 1,2)$ and the solutions u and v in varying places.

2. Kelvin-Type Transform and Proof of Theorem 1.1

To prove Theorem 1.1, we shall use the method of moving planes. We first introduce the Kelvin-type transforms u and v as follows,

$$\bar{u}(x) = |x|^{\mu-N} u\left(\frac{x}{|x|^2}\right) \quad \text{and} \quad \bar{v}(x) = |x|^{\mu-N} v\left(\frac{x}{|x|^2}\right)$$

which are defined for $x \in \mathbb{R}^N \setminus \{0\}$. Then by elementary calculations, one verifies that (1) and (2) are transformed into the following form:

$$\begin{cases} \bar{u}(x) = \int_{\mathbb{R}^N} |x-y|^{\mu-N} \left(|y|^{-s_1} \bar{u}(y)^{q_1} + |y|^{-s_2} \bar{v}(y)^{q_2} \right) dy \\ \bar{v}(x) = \int_{\mathbb{R}^N} |x-y|^{\mu-N} \left(|y|^{-r_1} \bar{v}(y)^{p_1} + |y|^{-r_2} \bar{u}(y)^{p_2} \right) dy \end{cases} \tag{8}$$

and

$$\begin{cases} (-\Delta)^{\mu/2} \bar{u} = |x|^{-s_1} \bar{u}^{q_1} + |x|^{-s_2} \bar{v}^{q_2} \\ (-\Delta)^{\mu/2} \bar{v} = |x|^{-r_1} \bar{v}^{p_1} + |x|^{-r_2} \bar{u}^{p_2} \end{cases} \tag{9}$$

with $s_i = (N+\mu) - (N-\mu) q_i > 0$, $r_i = (N+\mu) - (N-\mu) p_i > 0$ $(i = 1,2)$, and

$$\begin{cases} \bar{u}(x) = \int_{\mathbb{R}^N} |x-y|^{\mu-N} |y|^{-s} \bar{u}(y)^{q_1} \bar{v}(y)^{q_2} dy \\ \bar{v}(x) = \int_{\mathbb{R}^N} |x-y|^{\mu-N} |y|^{-r} \bar{v}(y)^{p_1} \bar{u}(y)^{p_2} dy \end{cases} \tag{10}$$

and

$$\begin{cases}(-\Delta)^{\mu/2}\bar{u}=|x|^{-s}\,\bar{u}^{q_1}\bar{v}^{q_2}\\(-\Delta)^{\mu/2}\bar{v}=|x|^{-r}\,\bar{v}^{p_1}\bar{u}^{p_2}\end{cases}\tag{11}$$

where $s=(N+\mu)-(N-\mu)(q_1+q_2)>0$ and $r=(N+\mu)-(N-\mu)(p_1+p_2)>0$. Obviously, both $\bar{u}(x)$ and $\bar{v}(x)$ have singularities at origin. Since u is locally $L^{\beta_1}\cap L^{\alpha_2}$ and v is locally $L^{\beta_2}\cap L^{\alpha_1}$ (in Theorem 1.1), it is easy to see that $\bar{u}(x)$ and $\bar{v}(x)$ have no singularity at infinity, *i.e.*, for any domain Ω that is a positive distance away from the origin,

$$\int_\Omega \bar{u}^{\beta_1}(y)dy<\infty \quad \text{and} \quad \int_\Omega \bar{u}^{\alpha_2}(y)dy<\infty. \tag{12}$$

$$\int_\Omega \bar{v}^{\beta_2}(y)dy<\infty \quad \text{and} \quad \int_\Omega \bar{v}^{\alpha_1}(y)dy<\infty. \tag{13}$$

For $\lambda\in\mathbb{R}$, define

$$\sum\nolimits_\lambda=\left\{x=(x_1,x_2\cdots,x_N)\,\middle|\,x_1\geq\lambda\right\}.$$

Let $x^\lambda=\{2\lambda-x_1,x_2,\cdots x_N\}$ and define

$$\bar{u}_\lambda(x)=\bar{u}(x^\lambda) \quad \text{and} \quad \bar{v}_\lambda(x)=\bar{v}(x^\lambda)$$

Lemma 2.1: For any solution ($\bar{u}$, $\bar{v}$) of (8), we have

$$\begin{aligned}\bar{u}_\lambda(x)-\bar{u}(x)&=\int_{\Sigma_\lambda}\Big(\frac{1}{|x-y|^{N-\mu}}-\frac{1}{|x^\lambda-y|^{N-\mu}}\Big)\\&\cdot\Big(\frac{1}{|y^\lambda|^{s_1}}\bar{u}_\lambda^{q_1}-\frac{1}{|y|^{s_1}}\bar{u}^{q_1}\Big)dy+\int_{\Sigma_\lambda}\Big(\frac{1}{|x-y|^{N-\mu}}\\&-\frac{1}{|x^\lambda-y|^{N-\mu}}\Big)\Big(\frac{1}{|y^\lambda|^{s_2}}\bar{v}_\lambda^{q_2}-\frac{1}{|y|^{s_2}}\bar{v}^{q_2}\Big)dy\end{aligned}\tag{14}$$

and

$$\begin{aligned}\bar{v}_\lambda(x)-\bar{v}(x)&=\int_{\Sigma_\lambda}\Big(\frac{1}{|x-y|^{N-\mu}}-\frac{1}{|x^\lambda-y|^{N-\mu}}\Big)\\&\cdot\Big(\frac{1}{|y^\lambda|^{r_1}}\bar{v}_\lambda^{p_1}-\frac{1}{|y|^{r_1}}\bar{v}^{p_1}\Big)dy+\int_{\Sigma_\lambda}\Big(\frac{1}{|x-y|^{N-\mu}}\\&-\frac{1}{|x^\lambda-y|^{N-\mu}}\Big)\Big(\frac{1}{|y^\lambda|^{r_2}}\bar{u}_\lambda^{p_2}-\frac{1}{|y|^{r_2}}\bar{u}^{p_2}\Big)dy\end{aligned}\tag{15}$$

Proof. Let $\sum_\lambda^c=\{x=(x_1,\cdots x_N)\,|\,x_1<\lambda\}$. Then it is easy to see that

$$\begin{aligned}\bar{u}(x)&=\int_{\Sigma_\lambda}\frac{1}{|x-y|^{N-\mu}}\frac{1}{|y|^{s_1}}\bar{u}(y)^{q_1}dy\\&+\int_{\Sigma_\lambda}\frac{1}{|x-y|^{N-\mu}}\frac{1}{|y|^{s_2}}\bar{v}(y)^{q_2}dy\\&+\int_{\Sigma_\lambda^c}\frac{1}{|x-y|^{N-\mu}}\frac{1}{|y|^{s_1}}\bar{u}(y)^{q_1}dy\\&+\int_{\Sigma_\lambda^c}\frac{1}{|x-y|^{N-\mu}}\frac{1}{|y|^{s_2}}\bar{v}(y)^{q_2}\\&=\int_{\Sigma_\lambda}\frac{1}{|x-y|^{N-\mu}}\frac{1}{|y|^{s_1}}\bar{u}(y)^{q_1}dy\\&+\int_{\Sigma_\lambda}\frac{1}{|x-y|^{N-\mu}}\frac{1}{|y|^{s_2}}\bar{v}(y)^{q_2}dy\\&+\int_{\Sigma_\lambda}\frac{1}{|x-y^\lambda|^{N-\mu}}\frac{1}{|y^\lambda|^{s_1}}\bar{u}(y^\lambda)^{q_1}dy\\&+\int_{\Sigma_\lambda}\frac{1}{|x-y^\lambda|^{N-\mu}}\frac{1}{|y^\lambda|^{s_2}}\bar{v}(y^\lambda)^{q_2}\\&=\int_{\Sigma_\lambda}\frac{1}{|x-y|^{N-\mu}}\frac{1}{|y|^{s_1}}\bar{u}(y)^{q_1}dy\\&+\int_{\Sigma_\lambda}\frac{1}{|x-y|^{N-\mu}}\frac{1}{|y|^{s_2}}\bar{v}(y)^{q_2}dy\\&+\int_{\Sigma_\lambda}\frac{1}{|x^\lambda-y|^{N-\mu}}\frac{1}{|y^\lambda|^{s_1}}\bar{u}_\lambda(y)^{q_1}dy\\&+\int_{\Sigma_\lambda}\frac{1}{|x^\lambda-y|^{N-\mu}}\frac{1}{|y^\lambda|^{s_2}}\bar{v}_\lambda(y)^{q_2}\end{aligned}$$

Here we have used the fact that $|x-y^\lambda|=|x^\lambda-y|$. Substituting x by x^λ, we get

$$\begin{aligned}\bar{u}(x^\lambda)&=\int_{\Sigma_\lambda}\frac{1}{|x^\lambda-y|^{N-\mu}}\frac{1}{|y|^{s_1}}\bar{u}(y)^{q_1}dy\\&+\int_{\Sigma_\lambda}\frac{1}{|x^\lambda-y|^{N-\mu}}\frac{1}{|y|^{s_2}}\bar{v}(y)^{q_2}dy\\&+\int_{\Sigma_\lambda}\frac{1}{|x-y|^{N-\mu}}\frac{1}{|y^\lambda|^{s_1}}\bar{u}_\lambda(y)^{q_1}dy\\&+\int_{\Sigma_\lambda}\frac{1}{|x-y|^{N-\mu}}\frac{1}{|y^\lambda|^{s_2}}\bar{v}_\lambda(y)^{q_2}\end{aligned}$$

Thus

$$\begin{aligned}\bar{u}_\lambda(x)-\bar{u}(x)&=\int_{\Sigma_\lambda}\Big(\frac{1}{|x-y|^{N-\mu}}-\frac{1}{|x^\lambda-y|^{N-\mu}}\Big)\\&\cdot\Big(\frac{1}{|y^\lambda|^{s_1}}\bar{u}_\lambda^{q_1}-\frac{1}{|y|^{s_1}}\bar{u}^{q_1}\Big)dy+\int_{\Sigma_\lambda}\Big(\frac{1}{|x-y|^{N-\mu}}\\&-\frac{1}{|x^\lambda-y|^{N-\mu}}\Big)\Big(\frac{1}{|y^\lambda|^{s_2}}\bar{v}_\lambda^{q_2}-\frac{1}{|y|^{s_2}}\bar{v}^{q_2}\Big)dy\end{aligned}$$

This implies (14). Similarly, we can get (15). So Lemma 2.1 is proved.

Proof of Theorem 1.1.

Outline: Let x_1 and x_2 be any two points in $\mathbb{R}^N$. We shall show that

$$u(x_1) = u(x_2) \text{ and } v(x_1) = v(x_2)$$

and therefore u and v must be constants. This is impossible unless $u = v = 0$. To obtain this, we show that u and v are symmetric about the midpoint $(x_1 + x_2)/2$. Since the integral equations are invariant under translation, we may assume that the midpoint is at the origin. Let $\bar{u}$ and $\bar{v}$ be the Kelvin-type transformations of u and v respectively. Then what left to prove is that u and v are symmetric about the origin. We shall carry this out in the following three steps.

Step 1. Define

$$\sum{}_\lambda^{\bar{u}} = \{x \mid x \in \sum{}_\lambda,\ \bar{u}(x) < \bar{u}_\lambda(x)\}$$

and

$$\sum{}_\lambda^{\bar{v}} = \{x \mid x \in \sum{}_\lambda,\ \bar{v}(x) < \bar{v}_\lambda(x)\}$$

We want to show that for sufficiently negative values of λ, both $\sum_\lambda^{\bar{u}}$ and $\sum_\lambda^{\bar{v}}$, must be empty. We note that $|x-y| \le |x^\lambda - y|$, $\forall x,\ y \in \sum_\lambda$. Moreover, since $\lambda < 0$, $|y^\lambda| \ge |y|$ for any $y \in \sum_\lambda$. Then by (14), for any $x \in \sum_\lambda^{\bar{u}}$,

$$\begin{aligned}
&\bar{u}_\lambda(x) - \bar{u}(x) \\
&\le \int_{\sum_\lambda} (|x-y|^{\mu-N} - |x^\lambda - y|^{\mu-N}) \\
&\quad \cdot |y|^{-s_1} (\bar{u}_\lambda(y)^{q_1} - \bar{u}(y)^{q_1}) dy \\
&\quad + \int_{\sum_\lambda} (|x-y|^{\mu-N} - |x^\lambda - y|^{\mu-N}) \\
&\quad \cdot |y|^{-s_2} (\bar{v}_\lambda(y)^{q_2} - \bar{v}(y)^{q_2}) dy \\
&\le \int_{\sum_\lambda^{\bar{u}}} |x-y|^{\mu-N} |y|^{-s_1} (\bar{u}_\lambda(y)^{q_1} - \bar{u}(y)^{q_1}) dy \\
&\quad + \int_{\sum_\lambda^{\bar{v}}} |x-y|^{\mu-N} |y|^{-s_2} (\bar{v}_\lambda(y)^{q_2} - \bar{v}(y)^{q_2}) dy \\
&\le q_1 \int_{\sum_\lambda^{\bar{u}}} |x-y|^{\mu-N} |y|^{-s_1} [\bar{u}_\lambda^{q_1-1}(\bar{u}_\lambda - \bar{u})](y) dy \\
&\quad + q_2 \int_{\sum_\lambda^{\bar{v}}} |x-y|^{\mu-N} |y|^{-s_2} [\bar{v}_\lambda^{q_2-1}(\bar{v}_\lambda - \bar{v})](y) dy
\end{aligned}$$

It follows from (7) and then the Hölder inequality that, for any $\gamma > \max\{N/(N+s_1-\mu), N/(N+s_2-\mu)\}$,

$$\begin{aligned}
&\|\bar{u}_\lambda - \bar{u}\|_{L^\gamma(\sum_\lambda^{\bar{u}})} \\
&\le C\Big(\Big\| \int_{\sum_\lambda^{\bar{u}}} |x-y|^{\mu-N} |y|^{-s_1} \\
&\quad \cdot [\bar{u}_\lambda^{q_1-1}(\bar{u}_\lambda - \bar{u})](y) dy \Big\|_{L^\gamma(\sum_\lambda^{\bar{u}})} \\
&\quad + \Big\| \int_{\sum_\lambda^{\bar{v}}} |x-y|^{\mu-N} |y|^{-s_2} \\
&\quad \cdot [\bar{v}_\lambda^{q_2-1}(\bar{v}_\lambda - \bar{v})](y) dy \Big\|_{L^\gamma(\sum_\lambda^{\bar{u}})} \Big) \\
&\le C\Big(\|\bar{u}_\lambda\|_{L^{\beta_1}(\sum_\lambda^{\bar{u}})}^{q_1-1} \|\bar{u}_\lambda - \bar{u}\|_{L^\gamma(\sum_\lambda^{\bar{u}})} \\
&\quad + \|\bar{v}_\lambda\|_{L^{\beta_2}(\sum_\lambda^{\bar{v}})}^{q_2-1} \|\bar{v}_\lambda - \bar{v}\|_{L^\gamma(\sum_\lambda^{\bar{v}})} \Big)
\end{aligned} \tag{16}$$

where $\beta_1 = \dfrac{q_1 - 1}{\frac{N-\mu}{N} q_1 - 1}$ and $\beta_2 = \dfrac{q_2 - 1}{\frac{N-\mu}{N} q_2 - 1}$.

Similarly, one can show that

$$\begin{aligned}
&\|\bar{v}_\lambda - \bar{v}\|_{L^\gamma(\sum_\lambda^{\bar{v}})} \\
&\le C\Big(\|\bar{v}_\lambda\|_{L^{\alpha_1}(\sum_\lambda^{\bar{v}})}^{p_1-1} \|\bar{v}_\lambda - \bar{v}\|_{L^\gamma(\sum_\lambda^{\bar{v}})} \\
&\quad + \|\bar{u}_\lambda\|_{L^{\alpha_2}(\sum_\lambda^{\bar{u}})}^{p_2-1} \|\bar{u}_\lambda - \bar{u}\|_{L^\gamma(\sum_\lambda^{\bar{u}})} \Big)
\end{aligned} \tag{17}$$

where $\alpha_1 = \dfrac{p_1 - 1}{\frac{N-\mu}{N} p_1 - 1}$ and $\alpha_2 = \dfrac{p_2 - 1}{\frac{N-\mu}{N} p_2 - 1}$.

Combining (16) and (17), we have

$$\begin{aligned}
&\|\bar{u}_\lambda - \bar{u}\|_{L^\gamma(\sum_\lambda^{\bar{u}})} \\
&\le C\Big[\Big(1 - C\|\bar{u}_\lambda\|_{L^{\beta_1}(\sum_\lambda^{\bar{u}})}^{q_1-1}\Big) \Big]^{-1} \|\bar{u}_\lambda\|_{L^{\alpha_2}(\sum_\lambda^{\bar{u}})}^{p_2-1} \\
&\quad \cdot \Big[\Big(1 - C\|\bar{v}_\lambda\|_{L^{\alpha_1}(\sum_\lambda^{\bar{v}})}^{p_1-1}\Big) \Big]^{-1} \|\bar{v}_\lambda\|_{L^{\beta_2}(\sum_\lambda^{\bar{v}})}^{q_2-1} \\
&\quad \cdot \|\bar{u}_\lambda - \bar{u}\|_{L^\gamma(\sum_\lambda^{\bar{u}})}
\end{aligned} \tag{18}$$

By conditions (12) and (13), we can choose N sufficiently large, such that for $\lambda \le -N$, we have

$$\begin{aligned}
&C\Big[\Big(1 - C\|\bar{u}_\lambda\|_{L^{\beta_1}(\sum_\lambda^{\bar{u}})}^{q_1-1}\Big) \Big]^{-1} \|\bar{u}_\lambda\|_{L^{\alpha_2}(\sum_\lambda^{\bar{u}})}^{p_2-1} \\
&\cdot \Big[\Big(1 - C\|\bar{v}_\lambda\|_{L^{\alpha_1}(\sum_\lambda^{\bar{v}})}^{p_1-1}\Big) \Big]^{-1} \|\bar{v}_\lambda\|_{L^{\beta_2}(\sum_\lambda^{\bar{v}})}^{q_2-1} \le \frac{1}{2} .
\end{aligned}$$

Then (18) implies that

$$\|\bar{u}_\lambda - \bar{u}\|_{L^\gamma(\sum_\lambda^{\bar{u}})} = 0,$$

and therefore $\sum_\lambda^{\bar{u}}$ must be measure zero, and hence empty. Similarly, one can show that $\sum_\lambda^{\bar{v}}$ is empty.

Step 2. Now we have that for $\lambda \le -N$,

$$\bar{u}(x) \ge \bar{u}_\lambda(x) \text{ and } \bar{v}(x) \ge \bar{v}_\lambda(x) \quad \forall x \in \sum{}_\lambda . \tag{19}$$

So the plane can start moving continuously from $\lambda \le -N$ to the right as long as (19) holds. Suppose that there exists $\lambda_0 < 0$ such that, on $\sum_{\lambda_0}$,

$$\bar{u}(x) \ge \bar{u}_{\lambda_0}(x) \text{ and } \bar{v}(x) \ge \bar{v}_{\lambda_0}(x),$$

but meas $\left\{x\in\sum_{\lambda_0}\left|\bar{u}(x)>\bar{u}_{\lambda_0}(x)\right.\right\}>0$ or meas $\left\{x\in\sum_{\lambda_0}\left|\bar{v}(x)>\bar{v}_{\lambda_0}(x)\right.\right\}>0$.

We shall show that the plane can move further to the right, *i.e.*, there exists an ε depending on N, p_i, q_i (i = 1, 2), and the solutions ($\bar{u},\bar{v}$) such that (19) holds for all $\lambda\in[\lambda_0,\lambda_0+\varepsilon)$.

Once either meas $\left\{x\in\sum_{\lambda_0}\left|\bar{u}(x)>\bar{u}_{\lambda_0}(x)\right.\right\}>0$ or meas $\left\{x\in\sum_{\lambda_0}\left|\bar{v}(x)>\bar{v}_{\lambda_0}(x)\right.\right\}>0$ holds, we see by (14) that in $\bar{u}(x)>\bar{u}_{\lambda_0}(x)$ the interior of $\sum_{\lambda_0}$. Let

$$\widetilde{\sum}{}^{\bar{u}}_{\lambda_0}=\left\{x\left|x\in\sum{}_{\lambda_0},\ \bar{u}(x)\le\bar{u}_{\lambda_0}(x)\right.\right\}$$

and

$$\widetilde{\sum}{}^{\bar{v}}_{\lambda_0}=\left\{x\left|x\in\sum{}_{\lambda_0},\ \bar{v}(x)\le\bar{v}_{\lambda_0}(x)\right.\right\}.$$

It is easy to see that $\widetilde{\sum}{}^{\bar{u}}_{\lambda_0}$ has measure zero, and $\lim_{\lambda\to\lambda_0}\sum{}^{\bar{u}}_{\lambda_0}\subset\widetilde{\sum}{}^{\bar{u}}_{\lambda_0}$. The similar results also hold for v. Let Ω^* be the reflection of the set Ω about the plane $x_1=\lambda$. From (16) and (17), we deduce

$$\begin{aligned}&\left\|\bar{u}_\lambda-\bar{u}\right\|_{L^\gamma(\sum^{\bar{u}}_\lambda)}\\&\le C\left[(1-C\left\|\bar{u}_\lambda\right\|^{q_1-1}_{L^{\beta_1}((\sum^{\bar{u}}_\lambda)^*)})\right]^{-1}\left\|\bar{u}_\lambda\right\|^{p_2-1}_{L^{\alpha_2}((\sum^{\bar{u}}_\lambda)^*)}\\&\cdot\left[(1-C\left\|\bar{v}_\lambda\right\|^{p_1-1}_{L^{\alpha_1}((\sum^{\bar{v}}_\lambda)^*)})\right]^{-1}\left\|\bar{v}_\lambda\right\|^{q_2-1}_{L^{\beta_2}((\sum^{\bar{v}}_\lambda)^*)}\\&\cdot\left\|\bar{u}_\lambda-\bar{u}\right\|_{L^\gamma(\sum^{\bar{u}}_\lambda)}\end{aligned}\tag{20}$$

Again conditions (12) and (13) ensure that one can choose ε small enough such that, for all $\lambda\in[\lambda_0,\lambda_0+\varepsilon)$,

$$\begin{aligned}&C\left[(1-C\left\|\bar{u}_\lambda\right\|^{q_1-1}_{L^{\beta_1}((\sum^{\bar{u}}_\lambda)^*)})\right]^{-1}\left\|\bar{u}_\lambda\right\|^{p_2-1}_{L^{\alpha_2}((\sum^{\bar{u}}_\lambda)^*)}\\&\cdot\left[(1-C\left\|\bar{v}_\lambda\right\|^{p_1-1}_{L^{\alpha_1}((\sum^{\bar{v}}_\lambda)^*)})\right]^{-1}\left\|\bar{v}_\lambda\right\|^{q_2-1}_{L^{\beta_2}((\sum^{\bar{v}}_\lambda)^*)}\le\frac{1}{2}\ .\end{aligned}$$

Now by (20), we have

$$\left\|\bar{u}_\lambda-\bar{u}\right\|_{L^\gamma(\sum^{\bar{u}}_\lambda)}=0$$

and therefore $\sum^{\bar{u}}_\lambda$ must be empty. Similarly, $\sum^{\bar{v}}_\lambda$ must be empty, too.

Step 3. If the plane stops at $\lambda_0<0$, then $\bar{u}(x)$ and $\bar{v}(x)$ must be symmetric and monotone about the plane $x_1=\lambda_0$. This implies that $\bar{u}(x)$ and $\bar{v}(x)$ have no singularity at the origin. But Equation (8) tells us that this is impossible if $\bar{u}(x)$ and $\bar{v}(x)$ are nontrivial. Hence we can move the plane to $x_1 = 0$. Then $\bar{u}(x)$ and $\bar{v}(x)$ must be symmetric about the origin. Thus $u = v = 0$. This completes the proof.

3. Proof of Theorem 1.2

In this section we establish Theorem 1.2. The proof is along the same line of the proof of Theorem 1.1. First establishing Lemma 3.1 which is similar to Lemma 2.1, we omit its proof.

Lemma 3.1: For any solution ($\bar{u},\bar{v}$) of (10), we have

$$\begin{aligned}\bar{u}_\lambda(x)-\bar{u}(x)&=\int_{\sum_\lambda}\Big(\frac{1}{\left|x-y\right|^{N-\mu}}-\frac{1}{\left|x^\lambda-y\right|^{N-\mu}}\Big)\\&\cdot\Big(\frac{1}{\left|y^\lambda\right|^s}\bar{u}^{q_1}_\lambda\bar{v}^{q_2}_\lambda-\frac{1}{\left|y\right|^s}\bar{u}^{q_1}\bar{v}^{q_2}\Big)dy\end{aligned}\tag{21}$$

and

$$\begin{aligned}\bar{v}_\lambda(x)-\bar{v}(x)&=\int_{\sum_\lambda}\Big(\frac{1}{\left|x-y\right|^{N-\mu}}-\frac{1}{\left|x^\lambda-y\right|^{N-\mu}}\Big)\\&\cdot\Big(\frac{1}{\left|y^\lambda\right|^r}\bar{v}^{p_1}_\lambda\bar{u}^{p_2}_\lambda-\frac{1}{\left|y\right|^r}\bar{v}^{p_1}\bar{u}^{p_2}\Big)dy\end{aligned}\tag{22}$$

Proof of Theorem 1.2.

Here we only provide necessary changes in Step 1, the rest is same as the proof of Theorem 1.1. $\sum^{\bar{u}}_\lambda$ and $\sum^{\bar{v}}_\lambda$ are defined as above. We want to show that for sufficiently negative values of λ, both $\sum^{\bar{u}}_\lambda$ and $\sum^{\bar{v}}_\lambda$ must be empty. We note that $\left|x-y\right|\le\left|x^\lambda-y\right|$ $\forall x,\ y\in\sum_\lambda$. Moreover, since $\lambda<0$, $\left|y^\lambda\right|\ge\left|y\right|$ for any $y\in\sum_\lambda$. Then by (21), for any $x\in\sum^{\bar{u}}_\lambda$,

$$\begin{aligned}&\bar{u}_\lambda(x)-\bar{u}(x)\\&\le\int_{\sum_\lambda}(\left|x-y\right|^{\mu-N}-\left|x^\lambda-y\right|^{\mu-N})\left|y\right|^{-s}\\&\quad\cdot\left[\bar{u}_\lambda(y)^{q_1}\bar{v}_\lambda(y)^{q_2}-\bar{u}(y)^{q_1}\bar{v}(y)^{q_2}\right]dy\\&\le\int_{\sum^{\bar{u}}_\lambda}\left|x-y\right|^{\mu-N}\left|y\right|^{-s}\bar{v}(y)^{q_2}[\bar{u}_\lambda(y)^{q_1}-\bar{u}(y)^{q_1}]dy\\&\quad+\int_{\sum^{\bar{v}}_\lambda}\left|x-y\right|^{\mu-N}\left|y\right|^{-s}\bar{u}_\lambda(y)^{q_1}[\bar{v}_\lambda(y)^{q_2}-\bar{v}(y)^{q_2}]dy\\&\le q_1\int_{\sum^{\bar{u}}_\lambda}\left|x-y\right|^{\mu-N}\left|y\right|^{-s}[\bar{u}^{q_1-1}_\lambda\bar{v}^{q_2}(\bar{u}_\lambda-\bar{u})](y)dy\\&\quad+q_2\int_{\sum^{\bar{v}}_\lambda}\left|x-y\right|^{\mu-N}\left|y\right|^{-s}[\bar{v}^{q_2-1}_\lambda\bar{u}^{q_1}_\lambda(\bar{v}_\lambda-\bar{v})](y)dy.\end{aligned}$$

It follows from (7) and then the Hölder inequality that, for any $\gamma>N/(N+s-\mu)$,

$$\|\bar{u}_\lambda - \bar{u}\|_{L^\gamma(\Sigma_\lambda^{\bar{u}})}$$
$$\le C\Big(\Big\|\int_{\Sigma_\lambda^{\bar{u}}} |x-y|^{\mu-N}|y|^{-s}$$
$$\cdot [\bar{u}_\lambda^{q_1-1}\bar{v}^{q_2}(\bar{u}_\lambda - \bar{u})](y)dy\Big\|_{L^\gamma(\Sigma_\lambda^{\bar{u}})}$$
$$+ \Big\|\int_{\Sigma_\lambda^{\bar{v}}} |x-y|^{\mu-N}|y|^{-s}$$
$$\cdot [\bar{v}_\lambda^{q_2-1}\bar{u}_\lambda^{q_1}(\bar{v}_\lambda - \bar{v})](y)dy\Big\|_{L^\gamma(\Sigma_\lambda^{\bar{u}})}\Big)$$
$$\le C\Big(\|\bar{u}_\lambda\|^{q_1-1}_{L^\beta(\Sigma_\lambda^{\bar{u}})}\|\bar{v}\|^{q_2}_{L^\beta(\Sigma_\lambda^{\bar{u}})}\|\bar{u}_\lambda-\bar{u}\|_{L^\gamma(\Sigma_\lambda^{\bar{u}})}$$
$$+\|\bar{u}_\lambda\|^{q_1}_{L^\beta(\Sigma_\lambda^{\bar{v}})}\|\bar{v}_\lambda\|^{q_2-1}_{L^\beta(\Sigma_\lambda^{\bar{u}})}\|\bar{v}_\lambda-\bar{v}\|_{L^\gamma(\Sigma_\lambda^{\bar{v}})}\Big) \tag{23}$$

Similarly, one can show that

$$\|\bar{v}_\lambda - \bar{v}\|_{L^\gamma(\Sigma_\lambda^{\bar{v}})}$$
$$\le C\Big(\|\bar{v}_\lambda\|^{p_1-1}_{L^\alpha(\Sigma_\lambda^{\bar{u}})}\|\bar{u}_\lambda\|^{p_2-1}_{L^\alpha(\Sigma_\lambda^{\bar{u}})}\|\bar{u}_\lambda-\bar{u}\|_{L^\gamma(\Sigma_\lambda^{\bar{u}})}$$
$$+\|\bar{v}_\lambda\|^{p_1-1}_{L^\alpha(\Sigma_\lambda^{\bar{v}})}\|\bar{u}\|^{p_2}_{L^\alpha(\Sigma_\lambda^{\bar{v}})}\|\bar{v}_\lambda-\bar{v}\|_{L^\gamma(\Sigma_\lambda^{\bar{v}})}\Big) \tag{24}$$

where $\alpha = \dfrac{p_1+p_2-1}{\frac{N-\mu}{N}(p_1+p_2)-1}$ and $\beta = \dfrac{q_1+q_2-1}{\frac{N-\mu}{N}(q_1+q_2)-1}$.

Combining (23) and (24), we have

$$\|\bar{u}_\lambda - \bar{u}\|_{L^\gamma(\Sigma_\lambda^{\bar{u}})}$$
$$\le C\Big[(1-C\|\bar{u}_\lambda\|^{q_1-1}_{L^\beta(\Sigma_\lambda^{\bar{u}})}\|\bar{v}\|^{q_2}_{L^\beta(\Sigma_\lambda^{\bar{u}})}\Big]^{-1}$$
$$\cdot\|\bar{u}_\lambda\|^{q_1}_{L^\beta(\Sigma_\lambda^{\bar{v}})}\|\bar{v}_\lambda\|^{q_2-1}_{L^\beta(\Sigma_\lambda^{\bar{v}})}$$
$$\cdot\Big[(1-C\|\bar{v}_\lambda\|^{p_1-1}_{L^\alpha(\Sigma_\lambda^{\bar{v}})}\|\bar{u}\|^{p_2}_{L^\alpha(\Sigma_\lambda^{\bar{v}})}\Big]^{-1}$$
$$\cdot\|\bar{v}_\lambda\|^{p_1}_{L^\alpha(\Sigma_\lambda^{\bar{u}})}\|\bar{u}_\lambda\|^{p_2-1}_{L^\alpha(\Sigma_\lambda^{\bar{u}})}\cdot\|\bar{u}_\lambda-\bar{u}\|_{L^\gamma(\Sigma_\lambda^{\bar{u}})} \tag{25}$$

By the hypotheses in Theorem 1.2, we can choose N sufficiently large, such that for $\lambda \le -N$,

$$C\Big[(1-C\|\bar{u}_\lambda\|^{q_1-1}_{L^\beta(\Sigma_\lambda^{\bar{u}})}\|\bar{v}\|^{q_2}_{L^\beta(\Sigma_\lambda^{\bar{u}})}\Big]^{-1}$$
$$\cdot\|\bar{u}_\lambda\|^{q_1}_{L^\beta(\Sigma_\lambda^{\bar{v}})}\|\bar{v}_\lambda\|^{q_2-1}_{L^\beta(\Sigma_\lambda^{\bar{v}})}$$
$$\cdot\Big[(1-C\|\bar{v}_\lambda\|^{p_1-1}_{L^\alpha(\Sigma_\lambda^{\bar{v}})}\|\bar{u}\|^{p_2}_{L^\alpha(\Sigma_\lambda^{\bar{v}})}\Big]^{-1}$$
$$\cdot\|\bar{v}_\lambda\|^{p_1}_{L^\alpha(\Sigma_\lambda^{\bar{u}})}\|\bar{u}_\lambda\|^{p_2-1}_{L^\alpha(\Sigma_\lambda^{\bar{u}})} \le \frac{1}{2}.$$

Then (25) implies that

$$\|\bar{u}_\lambda - \bar{u}\|_{L^\gamma(\Sigma_\lambda^{\bar{u}})} = 0,$$

and therefore $\sum_\lambda^{\bar{u}}$ must be measure zero, and hence empty. Similarly $\sum_\lambda^{\bar{v}}$ is also empty.

4. Acknowledgements

This work is supported by Youth Foundation of NSFC (No. 10701061), and it was completed while the author was visiting University of Notre Dame.

5. References

[1] W. X. Chen and C. M. Li, “Classification of Positive Solutions for Nonlinear Differential and Integral Systems with Critical Exponents,” *Acta Mathematica Scientia*, in press.

[2] W. X. Chen, C. M. Li and B. Ou, “Classification of Solutions for an Integral Equation,” *Communications on Pure and Applied Mathematics*, Vol. 59, No. 3, 2006, pp. 330-343.

[3] L. Caffarelli, B. Gidas and J. Spruck, “Asymptotic Symmetry and Local Behavior of Semilinear Elliptic Equations with Critical Sobolev Growth,” *Communications on Pure and Applied Mathematics*, Vol. 42, No. 3, 1989, pp. 271-297.

[4] B. Gidas and J. Spruck, “Global and Local Behaviour of Positive Solutions of Nonlinear Elliptic Equations,” *Communications on Pure and Applied Mathematics*, Vol. 34, No. 6, 1981, pp. 525-598.

[5] S. H. Chen and G. Z. Lu, “Existence and Nonexistence of Positive Radial Solutions for a Class of Semilinear Elliptic System,” *Nonlinear Analysis*, Vol. 38, No. 7, 1999, pp. 919-932.

[6] E. Mitidieri, “Nonexistence of Positive Solutions of Semilinear Elliptic Systems in $\mathbb{R}^N$,” *Differential and Integral Equations*, Vol. 9, No. 3, 1996, pp. 465-479.

[7] E. Lieb, “Sharp Constants in the Hardy-Littlewood-Sobolev and Related Inequalities,” *Annals of Mathematics*, Vol. 118, 1983, pp. 349-374.

[8] D. G. de Figueiredo and P. L. Felmer, “A Liouville-Type Theorem for Elliptic Systems,” *Annali della Scuola Normale Superiore di Pisa XXI*, Vol. 21, No. 3, 1994, pp. 387-397.

[9] J. Busca and R. Manásevich, “A Liouville-Type Theorem for Lane-Emden Systems,” *Indiana University Mathematics Journal*, Vol. 51, No. 1, 2002, pp. 37-51.

[10] Z. C. Zhang, W. M. Wang and K. T. Li, “Liouville-Type Theorems for Semilinear Elliptic Systems,” *Journal of Partial Differential Equations*, Vol. 18, No. 4, 2005, pp. 304-310.

[11] Y. Y. Li and M. Zhu, “Uniqueness Theorems through the Method of Moving Spheres,” *Duke Mathematical Journal*, Vol. 80, No. 2, 1995, pp. 383-417.

[12] Y. Y. Li and L. Zhang, “Liouville-Type Theorems and Harnack-Type Inequalities for Semilinear Elliptic Equations,” *Journal d’Analyse Mathematique*, Vol. 90, 2003, pp. 27-87.

[13] W. X. Chen, C. M. Li and B. Ou, "Classification of Solutions for a System of Integral Equations," *Communications in Partial Differential Equations*, Vol. 30, No. 1-2, 2005, pp. 59-65.

[14] W. X. Chen, C. M. Li and B. Ou, "Qualitative Properties of Solutions for an Integral Equation," *Discrete and Continuous Dynamical Systems*, Vol. 12, No. 2, 2005, pp. 347-354.

[15] L. Ma and D. Z. Chen, "A Liouville Type Theorem for an Integral System," *Communications on Pure and Applied Analysis*, Vol. 5, No. 4, 2006, pp. 855-859.

[16] C. S. Lin, "A Classification of Solutions of a Conformally Invariant Fourth Order Equation in $\mathbb{R}^N$," *Commentarii Mathematici Helvetici*, Vol. 73, No. 2, 1998, pp. 206-231.

[17] L. A. Peletier and R. C. A. M. van der Vorst, "Existence and Non-Existence of Positive Solutions of Non-Linear Elliptic Systems and the Biharmonic Equation," *Differential and Integral Equations*, Vol. 5, No. 4, 1992, pp. 747-767.

[18] J. Serrin and H. Zou, "The Existence of Positive Entire Solutions of Elliptic Hamitonian Systems," *Communications in Partial Differential Equations*, Vol. 23, No. 3-4, 1998, pp. 577-599.

[19] M. A. Souto, "A Priori Estimates and Existence of Positive Solutions of Semilinear Elliptic Systems," *Differential and Integral Equations*, Vol. 8, No. 5, 1995, pp. 1245-1258.

[20] E. M. Stein, "Singular Integral and Differentiability Properties of Functions," Princeton University Press, Princeton, 1970.

[21] Z. C. Zhang and Z. M. Guo, "Structure of Nontrivial Nonnegative Solutions of Singularly Perturbed Quasilinear Dirichlet Problems," *Mathematische Nachrichten*, Vol. 280, No. 13-14, 2007, pp. 1620-1639.

[22] Z. C. Zhang and K. T. Li, "Spike-Layered Solutions of Singularly Perturbed Quasilinear Dirichlet Problems," *Journal of Mathematical Analysis and Applications*, Vol. 283, No. 2, 2003, pp. 667-680.

[23] Z. C. Zhang and K. T. Li, "Spike-Layered Solutions with Compact Support to Some Singularly Perturbed Quasilinear Elliptic Problems in General Smooth Domains," *Journal of Computational and Applied Mathematics*, Vol. 162, No. 2, 2004, pp. 327-340.

[24] L. P. Zhu, Z. C. Zhang and W. M. Wang, "On the Positive Solutions for a Class of Semilinear Elliptic Systems," *Mathematical Applications*, Vol. 19, No. 2, 2006, pp. 440-445.

Applied Mathematics, **2010, 1, 101-103**
doi:10.4236/am.2010.12013 Published Online July 2010 (http://www. SciRP.org/journal/am)

Bondage Number of 1-Planar Graph*

Qiaoling Ma, Sumei Zhang, Jihui Wang†
School of Science, University of Jinan, Jinan, China
E-mail: *wangjh@ujn.edu.cn*
Received May 8, 2010; *revised June* 1, 2010; *accepted June* 11, 2010

Abstract

The bondage number $b(G)$ of a nonempty graph *G* is the cardinality of a smallest set of edges whose removal from *G* results in a graph a domination number greater than the domination number of *G*. In this paper, we prove that $b(G) \le 12$ for a 1-planar graph *G*.

Keywords: Domination Number, Bondage number, 1-Planar Graph, Combinatorial Problem

1. Introduction

Throughout this paper, we consider connected graphs without loops or multiple edges. A 1-planar graph is a graph which can be drawn on the plane so that every edge crosses at most one other edge. For a graph *G*, $V(G)$ and $E(G)$ are used to denote the vertex set and edge set of *G*, respectively. The degree of a vertex *u* in *G* is denoted by $d(u)$. For a vertex subset $S \subseteq V(G)$, define $N(S) = \{x \in V(G) \setminus S \mid$ there is a $y \in S$ such that $xy \in E(G)\}$. When $S = \{v\}$, we write $N(v) = N(S)$ for short. The minimum degree of vertices in *G* is denoted by $\delta(G)$ and the maximum degree by $\Delta(G)$. The distance between two vertices *u* and *v* in *G* is denoted by $d(u,v)$. For a subset $X \subseteq V(G)$, $G[X]$ denotes the subgraph of *G* induced by *X*.

A subset *D* of $V(G)$ is called a dominating set, if $D \cup N(D) = V(G)$. The domination number of *G*, denoted by $\gamma(G)$, is the minimum cardinality of a dominating set. The bondage number $b(G)$ of a nonempty graph *G* is the cardinality of a smallest set of edges whose removal from *G* results in a graph with domination number greater than $\gamma(G)$.

The bondage number was first introduced by Bauer *et al*. [1] in 1983. The following two main outstanding conjectures on bondage number were formulated by Teschner [2].

Conjecture 1.1 If *G* is a planar graph, then $b(G) \le \Delta(G) + 1$.

Conjecture 1.2 For any graph *G*, $b(G) \le \frac{3}{2}\Delta(G)$.

In 2000, Kang and Yuan [3] proved that $b(G) \le \min\{8, \Delta(G) + 2\}$ for any planar graph. That is, conjecture 1.1 is showed for planar graph with $\Delta(G) \ge 7$. Up to now, conjecture 1.1 is still open for planar graph *G* with $\Delta(G) \le 6$. Conjecture 1.2 is still open. In this paper, we prove that $b(G) \le 12$ for a 1-planar graph *G*.

2. Preliminary Results

First of all, we recall some useful results that we will need

Lemma 2.1 [4] If *G* is a graph, then for every pair of adjacent vertices *u* and *v* in *G*, then $b(G) \le d(u) + d(v) - 1 - |N(u) \cap N(v)|$.

Lemma 2.2 [5,6] If *u* and *v* are two vertices of *G* with $d(u,v) \le 2$, then $b(G) \le d(u) + d(v) - 1$.

Lemma 2.3 [7] Let *G* be a 1-planar graph, then $\delta(G) \le 7$.

Lemma 2.4 [7] Let *G* be a 1-planar graph on *n* vertices and *m* edges, then $m \le 4n - 8$.

Lemma 2.5 Let *G* be a bipartite 1-planar graph on *n* vertices and *m* edges, then $m \le 3n - 6$.

Proof. Without loss of generality, let *G* be a maximal bipartite 1-planar graph on *n* vertices and *X*, *Y* is a bipartition of graph *G*. Form a 1-planar graph G' from *G* as follows: add some edges to join vertices in *X*, and add some edges to join the vertices in *Y*, such that G' is a maximal 1-planar graph with $G \subseteq G'$. By the maximal-

*This work was supported by NSFC (10901097) and the Nature Science Foundation of Shandong Province (Y2008A20), also was supported by the Scientific Research and Development Project of Shandong Provincial Education Department (TJY0706) and the Science and Technology Foundation of University of Jinan (XKY0705).

ity of G', the subgraph $G'[X]$ and $G'[Y]$ must be connected. Then we have

$$|E(G'[X])| \geq |X| - 1, \quad |E(G'[Y])| \geq |Y| - 1 .$$

By lemma 2.4, $|E(G')| \leq 4n - 8$. So

$$|E(G)| = |E(G')| - |E(G'[X])| - |E(G'[Y])|$$

$$\leq 4n - 8 - |X| + 1 - |Y| + 1 = 3n - 6 .$$

This completes the prove of lemma 2.5.

3. Bondage Number of 1-Planar Graph

Theorem 3.1 If G is a 1-planar graph, then $b(G) \leq 12$.

Proof. Suppose to the contrary that G is a 1-planar graph with $b(G) \geq 13$. Then we have

Claim 1. For two distinct vertices x, y of G, if $\max\{d(x), d(y)\} \leq 7$, and $\min\{d(x), d(y)\} \leq 6$, then it must be the case that $d(x, y) \geq 3$.

Otherwise, $d(x, y) \leq 2$. But then, by lemma 2.2, $b(G) \leq d(x) + d(y) - 1 \leq 12$, a contradiction.

Claim 2. If there is some $x \in V(G)$ such that $d(x) \leq 5$ then $d(y) \geq 9$ for all $y \in N(x)$.

Otherwise, $b(G) \leq d(x) + d(y) - 1 \leq 5 + 8 - 1 = 12$, a contradiction.

Now, we define

$$V_1 = \{x \in V(G) \mid d(x) \leq 5\},$$

$$V_2 = \{x \in V(G) \mid d(x) = 6\},$$

$$V_3 = \{x \in V(G) \mid d(x) = 7\}.$$

Let $A \subseteq V_3$ be the maximum and such that A is independent of G. By Claim 1 and the maximality of A, we have also

Claim 3. $N(V_2) \bigcap N(A) = \phi$ and $V_3 \subseteq A \bigcup N(A)$,

Let $V_2 \bigcup A = \{x_1, x_2 \cdots x_k\}$, and $H = G - V_1$. Define

$$H_0 = H ,$$

$$H_i = H_{i-1} + F_i, \quad 1 \leq i \leq k.$$

where $F_i \subseteq E_{x_i} = \{xy \mid x, y \in N(x_i), x \neq y, xy \notin E(H_{i-1})\}$ such that $H_{i-1} + F_i = H_i$ is still a 1-planar graph and such that $H_i[N(x_i)]$ is 2-connected. It is easy to see that $H_k[N(x_i)]$ is still 2-connected for $1 \leq i \leq k$.

Claim 4. If $V_2 \neq \phi$, then for each vertex $v \in N(V_2)$, v is of degree at least 9 in H_k .

In fact, let $x \in V_2$ and $v \in N(x)$. If $N(v) \bigcap N(x) = \varphi$ in G, then by lemma 2.2, $d(v) + d(x) - 1 \geq 13$, and $d(v) \geq 14 - d(x) = 8$, by the 2-connectivity of $H_k[N(x)]$, v is of degree at least 10 in H_k . If $N(v) \bigcap N(x) \neq \phi$, then by lemma 2.1, $d(v) + d(x) - 2 \geq 13$. Then $d(v) \geq 9$.

Analogously, we have

Claim 5. If $A \neq \phi$, then for each vertex $v \in N(A)$, v is of degree at least 9 in H_k .

Now, $G^* = H_k - V_2$ is a 1-planar graph, satisfying

(a) The minimum degree of G^* is 7,

(b) $A = \{v \in V(G^*) \mid d_{G^*}(v) = 7\}$,

(c) A is independent of G^*,

(d) For every vertex $v \in N_{G^*}(A) = N(A)$, $d_{G^*}(v) \geq 9$.

Let $\partial(A) = \{xy \in E(G^*) \mid x \in A, y \in N(A)\}$. Then $(A, N(A); \partial(A))$ is a bipartite 1-planar graph with $7|A|$ edges. By lemma 2.5,

$$7|A| \leq 3|A| + 3|N(A)| - 6 .$$

Hence

$$|N(A)| \geq \frac{4}{3}|A| + 2 .$$

Then we have

$$|E(G^*)| = \frac{1}{2}\sum_{v \in V(G^*)} d_{G^*}(v)$$

$$\geq \frac{1}{2}(7|A| + 9|N(A)| + 8(|V(G^*)| - |A| - |N(A)|))$$

$$= 4|V(G^*)| + \frac{1}{2}|N(A)| - \frac{1}{2}|A|$$

$$\geq 4|V(G^*)| + \frac{1}{6}|A| + 1$$

$$> 4|V(G^*)| - 8 .$$

A contradiction.

This completes the proof of the theorem.

Theorem 3.2 If G is a 1-planar graph and there is no degree seven vertex, then $b(G) \leq 11$.

Proof. Suppose to the contrary that $b(G) \geq 12$.

Let $X = \{v \in V(G) \mid d(v) \leq 6\}$, and suppose that $X = \{x_1, x_2 \cdots x_k\}$

By lemma 2.2, for any two distinct vertices $x, y \in X$, $d(x, y) \geq 3$.

Define

$$H_0 = G ,$$

$$H_i = H_{i-1} + F_i, \quad 1 \leq i \leq k .$$

where $F_i \subseteq E_{x_i} = \{xy \mid x, y \in N(x_i), x \neq y, xy \notin E(H_{i-1})\}$ such that $H_{i-1} + F_i = H_i$ is still a 1-planar graph and such that $H_i[N(x_i)]$ is 2-connected when $d(x_i) \geq 3$.

Now, by lemma 2.1 and 2.2, for any $x \in X, y \in N(y)$, if $d(x) \leq 2$ then $d(y) \geq 11$ and so y is of degree at least 11 in H_k; If $d(x) \geq 3$ and $|N(x) \cap N(y)| \leq 1$, then $d(y) \geq 8$ and so y is of degree at least 9 in H_k; If $d(x) \geq 3$ and $|N(x) \cap N(y)| \geq 2$, then $d(y) \geq 9$ and So y is of degree at least 9 in H_k.

By the construction of H_k, we know that H_k is a 1-planar graph. But $H_k - X$ is a 1-planar graph with a minimum degree of at least 8. It contradicts with lemma 2.3, and the proof is completed.

4. References

[1] D. Bauer. F. Harry, J. Nieminen and C. L. Suffel, "Domination Alteration Sets in Graphs," *Discrete Mathematics*, Vol. 47, 1983, pp. 153-161.

[2] U. Teschner, "A New Upper Bound for the Bondage Number of Graphs with Small Domination Number," *Australasian Journal of Combinatorics*, Vol. 12, 1995, pp. 27-35.

[3] L. Kang and J. Yuan, "Bondage Number of Planar Graphs," *Discrete Mathematics*, Vol. 222, No. 1-3, 2000, pp. 191-198.

[4] B. L. Hartnell and D. F. Rall, "Bounds on the Bondage Number of a Graph," *Discrete Mathematics*, Vol. 128, No. 1-3, 1994, pp. 173-177.

[5] B. L. Hartnell and D. F. Rall, "A Bound on the Size of a Graph with Given Order and Bondage Number," *Discrete Mathematics*, Vol. 197/198, 1999, pp. 409-413.

[6] U. Teschner, "New Results about the Bondage Number of a Graph," *Discrete Mathematics*, Vol. 171, No. 1-3, 1997, pp. 249-259.

[7] I. Fabrici, "The Structure of 1-Planar Graphs," *Discrete Mathematics*, Vol. 307, No. 1, 2007, pp. 854-865.

Applied Mathematics, 2010, 1, 104-117
doi:10.4236/am.2010.12014 Published Online July 2010 (http://www.SciRP.org/journal/am)

Numerical Solution of the Rotating Shallow Water Flows with Topography Using the Fractional Steps Method

Hossam S. Hassan[1], Khaled T. Ramadan[1], Sarwat N. Hanna[2]
[1]*Department of Basic and Applied Science, Arab Academy for Science, Technology and Maritime Transport, Alexandria, Egypt*
[2]*Department of Engineering Mathematics and Physics, Faculty of Engineering, Alexandria University, Alexandria, Egypt*
E-mail: *hossams@aast.edu*
Received April 16, 2010; *revised June* 2, 2010; *accepted June* 12, 2010

Abstract

The two-dimensional nonlinear shallow water equations in the presence of Coriolis force and bottom topography are solved numerically using the fractional steps method. The fractional steps method consists of splitting the multi-dimensional matrix inversion problem into an equivalent one dimensional problem which is successively integrated in every direction along the characteristics using the Riemann invariant associated with the cubic spline interpolation. The height and the velocity field of the shallow water equations over irregular bottom are discretized on a fixed Eulerian grid and time-stepped using the fractional steps method. Effects of the Coriolis force and the bottom topography for particular initial flows on the velocity components and the free surface elevation have been studied and the results are plotted.

Keywords: Shallow Water Equations, Fractional Steps Method, Riemann Invariants, Bottom Topography, Cubic Spline Interpolation

1. Introduction

Shallow water equations form a set of hyperbolic partial differential equations that describe the flow below the pressure surface in the fluid, sometimes, but not necessarily, a free surface. The equations are derived from depth-integrating the Navier-Stokes equations, in the case where the horizontal length scale is much greater than the vertical length scale. They can be used to model Rossby and Kelvin waves in the atmosphere, rivers, lakes and oceans in a large domain as well as gravity waves. The rotating shallow water equations including topographic effects are a leading order model to study coastal hydrodynamics on several scales including intermediate scale rotational waves and breaking waves on beaches. Also, they are used with Coriolis forces in atmospheric and oceanic modeling, as a simplification of the primitive equations of atmospheric flow.

Due to the nonlinearity of the model as well as the complexity of the geometries encountered in real-life applications such as flow of pollutants, tsunamis, avalanches, dam break, flooding, potential vorticity field…etc, much effort has been made in recent years to develop numerical methods to solve the equations approximately.

Bottom topography plays a major role in determining the flow field in the oceans, rivers, shores, coastal sea and so on. One of the most important applications of the shallow water waves is the tsunami waves [1], usually generated by underwater earthquakes which cause an irregular topography of increasing or decreasing water depth. In particular, the main problem in solving the shallow water equations is the presence of the source terms modeling the bottom topography and the Coriolis forces included in the system.

The shallow water equations used in geophysical fluid dynamics are based on the assumption H/L << 1, where H and L are the characteristic values for the vertical and horizontal length scales of motion respectively. These equations are a two-dimensional hyperbolic system modeling the depth and the depth-averaged horizontal velocities for an incompressible fluid.

Perhaps, rotation is the most important factor that distinguishes geophysical fluid dynamics from classical fluid dynamics. If latitudinal varying Coriolis forces are included in the shallow water equations, the resulting system can support both Rossby and gravity waves. On the other hand, by neglecting the Coriolis forces in the shallow water system, there is no Rossby-wave solution for the system.

The Coriolis force is proportional in magnitude to the flow speed and directed perpendicular to the direction of the flow. It acts to the left of the flow in the southern hemisphere and to the right in the northern hemisphere. A somewhat inaccurate but helpful way to see why the direction is different in the two hemispheres is related to the principle of conservation of angular momentum. For a given horizontal motion, the strongest horizontal deflection is at the poles and there is no horizontal deflection at the equator; for vertical motion the opposite is true. The magnitude of the Coriolis force proportionally depends upon the latitude and the wind speed. The direction of the Coriolis force always acts at right angles to the direction of movement, which is to the right in the Northern Hemisphere and to the left in the Southern Hemisphere [2].

Many authors have used different numerical techniques to solve the shallow water equations such as finite volume method, finite element method and fractional steps method.

Lukácová-Medvid'ová *et al*. [3] presented a new well-balanced finite volume method within the framework of the finite volume evolution Galerkin (FVEG) schemes for the shallow water equations with source terms modeling the bottom topography and the Coriolis forces.

Gallouët *et al*. [4] studied the computation of the shallow water equations with topography by finite volume method, in a one-dimensional framework. In their paper, they considered approximate Riemann solvers. Several single step methods are derived from this formulation and numerical results are compared with the fractional steps method.

Dellar and Salmon [5] derived an extended set of shallow water equations that describe a thin inviscid fluid layer above fixed topography in a frame rotating about an arbitrary axis.

Karelsky *et al*. [6] executed the generalization of classical shallow water theory to the case of flows over an irregular bottom. They showed that the simple self-similar solutions that are characteristic for the classical problem exist only if the underlying surface has a uniform slope.

George [7] presented a class of augmented approximate Riemann solvers for the one-dimensional shallow water equations in the presence of an irregular bottom, neglecting the effect of Coriolis force. These methods belong to the class of finite volume Godunov type methods that use a set of propagation jump discontinuities, or waves, to approximate the true Riemann solution.

Shoucri [8] applied the fractional steps technique for the numerical solution of the shallow water equations with flat bottom in the presence of the Coriolis force. The method of fractional steps that he presented in his paper has the great advantage of solving the shallow water equations without the iterative steps involved in the multi-dimensional interpolation, and without the iteration associated with the intermediate step of solving the Helmholtz equation [9].

Abd-el-Malek and Helal [10] developed a mathematical simulation to determine the water velocity in the Lake Mariut, taking into consideration its concentration and the distribution of the temperature along it, by applying the fractional steps method for the numerical solution of the shallow water equations.

Shoucri [11] applied the fractional steps technique for the numerical solution of the shallow water equations to study the evolution of the vorticity field. The method is Eulerian [8], and the different variables are discretized on a fixed grid.

Yohsuke *et al.* [12] presented two efficient explicit schemes with no iterative process for the two-dimensional shallow-water equations of a hydrostatic weather forecast model. One is the directional-splitting fractional-step method, which uses a treatment based on the characteristics approach (Shoucri [8,11]).The other is the interpolated differential operator (IDO) scheme (Aoki [13]), which is one of the multimoment Eulerian schemes. They compared the forecast geopotential heights obtained from the fractional-step method and the IDO scheme after 48 h for various resolutions with those of the referenced scheme by Temperton and Staniforth [14].

Rotating shallow water equations including topographic terms are numerically dealt with the fractional steps method. In most real applications there is variable bottom topography that adds a source term to the shallow water equations. There are several works, where both the Coriolis forces as well as the bottom topography are taken into account, see [3,15-17]. A standard and easy way to deal with these source terms is to treat them independently by using the fractional steps method. It has the great advantage of solving the equations without the iterative steps involved in the multidimensional interpolation problems.

In this work, we apply the fractional steps method to solve the two-dimensional shallow water equations with source terms (including the Coriolis force and bottom topography) for different initial flows observed in the real-life such as the tsunami propagation wave and the dam break wave. The objective of the present work is to simulate the influence of different profiles of the irregular bottom in case of neglecting and including the effect of the Coriolis force on the velocity component in the x-and y-directions, water depth and the free surface elevation for different time. The results are illustrated graphically for particular initial flows.

2. Mathematical Formulation of the Problem

The shallow water equations (Saint-Venant equations) describe the free surface flow of incompressible water in response to gravitational and rotational accelerations (Coriolis accelerations), where the vertical depth of water is much less than the horizontal wavelength of the disturbance of the free surface [wave motion]. These equations are often used as a mathematical model when numerical methods for solving weather or climate prediction problems are tested. **Figure 1** illustrates the shallow water model where, "*h*" denotes the water height above the non-flat bottom, "*H*" is the undisturbed free surface level, $\zeta = \zeta(x, y)$ denotes the bottom topography, "*h**" is the water height above the flat bottom and $\eta = h^* - H$ denotes the free surface elevation.

The Continuity equation and the momentum equations for the two-dimensional shallow water equations system taking into account the effects of topography and the Earth's rotation are formulated by Pedlosky [2] as

Continuity equation:

$$\frac{\partial h}{\partial t} + \frac{\partial (u h)}{\partial x} + \frac{\partial (v h)}{\partial y} = 0 \tag{1}$$

Momentum equations:

$$\frac{\partial (h u)}{\partial t} + \frac{\partial (h u^2)}{\partial x} + \frac{\partial (h u v)}{\partial y} + \frac{g}{2}\frac{\partial (h^2)}{\partial x} = -g h \frac{\partial \zeta}{\partial x} + f h v, \tag{2}$$

$$\frac{\partial (h v)}{\partial t} + \frac{\partial (h u v)}{\partial x} + \frac{\partial (h v^2)}{\partial y} + \frac{g}{2}\frac{\partial (h^2)}{\partial y} = -g h \frac{\partial \zeta}{\partial y} - f h u. \tag{3}$$

The model is run over a rectangular domain centered at the earth origin, such that the x-axis is taken eastward and the y-axis is taken northward, with *u* and *v* the corresponding velocity components, respectively, g stands for the gravitational constant, $f = 2\Omega \sin\phi$ is the Coriolis parameter, Ω is the angular velocity of the earth rotation, ϕ is the geographical latitude of the earth origin coordinate and $(fv, -fu)$ represents the Coriolis acceleration which is produced by the effect of rotation.

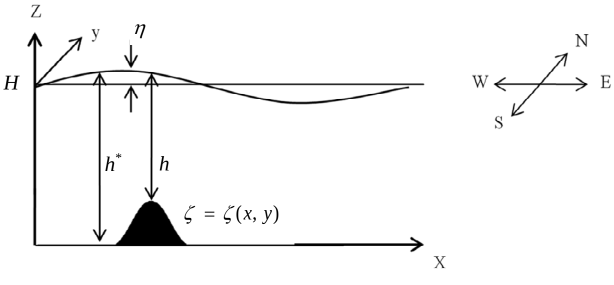

Figure 1. Geometry of the shallow water model.

Let the geopotential height be

$$\Phi = g\, h \tag{4}$$

Substitution (4) into (1)-(3), yields

$$\frac{\partial \Phi}{\partial t} + u \frac{\partial \Phi}{\partial x} + \Phi \frac{\partial u}{\partial x} + v \frac{\partial \Phi}{\partial y} + \Phi \frac{\partial v}{\partial y} = 0 \tag{5}$$

$$\frac{\partial u}{\partial t} + u \frac{\partial u}{\partial x} + v \frac{\partial u}{\partial y} + \frac{\partial \Phi}{\partial x} = -g \frac{\partial \zeta}{\partial x} + f v \tag{6}$$

$$\frac{\partial v}{\partial t} + u \frac{\partial v}{\partial x} + v \frac{\partial v}{\partial y} + \frac{\partial \Phi}{\partial y} = -g \frac{\partial \zeta}{\partial y} - f u \tag{7}$$

We concern ourselves to approximate the two dimensional shallow water Equations (5)-(7) with source terms modelling the bottom topography and the Coriolis forces for different initial flows observed in the real-life such as the tsunami propagation wave and the dam break wave.

3. Solution of the Problem

Our solution is based on applying the fractional steps method which was first proposed by Yanenko [18], to the system of non-linear partial differential Equations (5)-(7) by splitting the equations into two one-dimensional problems that are solved alternately in x- and y-directions [19].

3.1. Fractional Steps Method

Step 1. *Solve for* $\Delta t / 2$ *in the x– direction* (*without the source terms*):

Equations (5)-(7) will be

$$\frac{\partial \Phi}{\partial t} + u \frac{\partial \Phi}{\partial x} + \Phi \frac{\partial u}{\partial x} = 0, \tag{8}$$

$$\frac{\partial u}{\partial t} + u \frac{\partial u}{\partial x} + \frac{\partial \Phi}{\partial x} = 0, \tag{9}$$

$$\frac{\partial v}{\partial t} + u \frac{\partial v}{\partial x} = 0. \tag{10}$$

Equations (8) and (9) can be written as

$$\frac{\partial R_{x\pm}}{\partial t} + (u \pm \sqrt{\Phi}) \frac{\partial R_{x\pm}}{\partial x} = 0 \tag{11}$$

where $R_{x\pm} = u \pm 2\sqrt{\Phi}$ are the Riemann invariants.

By applying the classical finite difference scheme to (11), which is a first-order equation in time and space, we get

$$\left[R_{x\pm}(x,y,t+\Delta t/2)-R_{x\pm}(x,y,t)\right] + (u\pm\sqrt{\Phi})\Delta t/(2\Delta x) \left[R_{x\pm}(x+\Delta x,y,t)-R_{x\pm}(x,y,t)\right]=0. \quad (12)$$

The CFL stability condition is given by $\left|(u\pm\sqrt{\Phi})\Delta t/(2\Delta x)\right|\le 1$. Let $\Delta x = -(u\pm\sqrt{\Phi})\Delta t/2$, so, (12) will be

$$R_{x\pm}\left(x,y,t+\Delta t/2\right) = R_{x\pm}\left(x-(u\pm\sqrt{\Phi})\Delta t/2,y,t\right) \quad (13)$$

The right-hand side of (13) is the value of the function at time $t = n\Delta t$ at the departure points of the characteristics. The value of the function at $t+\Delta t/2$ at the arrival grid points is obtained using cubic spline interpolation from the values of the function at the grid points at $t = n\Delta t$, (*i.e.* the value $R_{x\pm}$ after the time $\Delta t/2$ from time t is the same value of $R_{x\pm}$ at that same time but after the distance *x* is shifted by Δx).

Similarly, the solution of (10) for v at $t+\Delta t/2$ is written as

$$v\left(x,y,t+\Delta t/2\right) = v\left(x-u\Delta t/2,y,t\right), \quad (14)$$

where $\Delta x = -u\Delta t/2$, *i.e.* the solution of Equations (8)-(10) can be written after time $(n+1/2)\Delta t$, n = 1,2,3…as the equality

$$\begin{pmatrix} R_{x\pm} \\ v \end{pmatrix}_{(x,y,(n+1/2)\Delta t)} = \begin{pmatrix} R_{x\pm} \\ v \end{pmatrix}_{(x_\pm,y,n\Delta t)}$$

where $x_\pm = x-(u\pm\sqrt{\Phi})\Delta t/2$ for the first row and $x_\pm = x-u\,\Delta t/2$ for the second row. Hence the CFL stability condition will be satisfied automatically at any time evolution $(n+1/2)\Delta t$.

So, The solutions of $R_{x\pm}$, give the values of h and u after time $(n+1/2)\Delta t$ in the $x-$direction. So, the interpolated values in (13) and (14) are calculated using the cubic spline interpolation, where no iteration is implied in this calculation.

Step 2. *Solve for* $\Delta t/2$ *in the* $y-$*direction* (*without the source terms*):

Equations (5)-(7) will be

$$\frac{\partial\Phi}{\partial t}+v\frac{\partial\Phi}{\partial y}+\Phi\frac{\partial v}{\partial y}=0 \quad (15)$$

$$\frac{\partial u}{\partial t}+v\frac{\partial u}{\partial y}=0 \quad (16)$$

$$\frac{\partial v}{\partial t}+v\frac{\partial v}{\partial y}+\frac{\partial\Phi}{\partial y}=0 \quad (17)$$

Use the results obtained at the end of Step 1, to solve (15)-(17) for $\Delta t/2$.

Equations (15) and (17) can be rewritten as

$$\frac{\partial R_{y\pm}}{\partial t}+(v\pm\sqrt{\Phi})\frac{\partial R_{y\pm}}{\partial y}=0, \quad (18)$$

where $R_{y\pm} = v \pm 2\sqrt{\Phi}$ are the Riemann invariants.

The solutions of (16) and (18) at $t+\Delta t/2$ are

$$u\left(x,y,t+\Delta t/2\right)=u\left(x,y-v\Delta t/2,t\right), \quad (19)$$

and

$$R_{y\pm}\left(x,y,t+\Delta t/2\right) = R_{y\pm}\left(x,y-(v\pm\sqrt{\Phi})\Delta t/2,t\right), \quad (20)$$

i.e. after time $(n+1/2)\Delta t$ we rewrite Equations (19) and (20) as

$$\begin{pmatrix} R_{y\pm} \\ u \end{pmatrix}_{(x,y,(n+1/2)\Delta t)} = \begin{pmatrix} R_{y\pm} \\ u \end{pmatrix}_{(x,y_\pm,n\Delta t)}$$

where $y_\pm = y-(v\pm\sqrt{\Phi})\Delta t/2$ for the first row and $y_\pm = y-v\,\Delta t/2$ for the second row.

Again, the solutions of $R_{y\pm}$, give the values of *h* and *v* after $\Delta t/2$ in the y-direction.

Step 3. *Solve for* Δt (*for the source terms*):

Equations (5)-(7) will be

$$\frac{\partial u}{\partial t} = -g\frac{\partial\zeta}{\partial x}+f\,v \quad (21)$$

$$\frac{\partial v}{\partial t} = -g\frac{\partial\zeta}{\partial y}-f\,u \quad (22)$$

Use the results obtained at the end of Step 2, to solve (21) and (22) for Δt.

Solutions of (21) and (22) are calculated at Δt

$$u\left(x,y,(n+1)\,\Delta t\right) = U_0-(g\,\Delta t/\Delta x)[\zeta(x,y,nt) - \zeta(x-\Delta x,y,nt)]+f\,V_0 \quad (23)$$

$$v\left(x,y,(n+1)\,\Delta t\right) = V_0-(g\,\Delta t/\Delta y)[\zeta(x,y,nt) - \zeta(x,y-\Delta y,nt)]-f\,U_0 \quad (24)$$

where U_0 and V_0 are the values of *u* and *v* at the beginning of Step 3.

Step 4. *Repeat Step* 2:

The results obtained at the end of Step 3 are used to solve for $\Delta t/2$ the equations in the y-direction as in Step 2.

$$i.e. \quad \begin{pmatrix} R_{y\pm} \\ u \end{pmatrix}_{(x,y,(n+1)\Delta t)} = \begin{pmatrix} R_{y\pm} \\ u \end{pmatrix}_{(x,y_\pm,(n+1/2)\Delta t)}$$

Step 5. *Repeat Step* 1:

The results obtained at the end of Step 4 are used to solve for $\Delta t/2$ the equations in the x- direction as in Step 1.

$$i.e. \quad \begin{pmatrix} R_{x\pm} \\ v \end{pmatrix}_{(x,y,(n+1)\Delta t)} = \begin{pmatrix} R_{x\pm} \\ v \end{pmatrix}_{(x_\pm,y,(n+1/2)\Delta t)}$$

Shoucri [11] applied the fractional steps method for the numerical solution of the shallow water equations over flat bottom. He used the calculated variables (the height and the velocity field) in studying the evolution of the potential vorticity field.

Abd-el-Malek and Helal [10] developed a mathematical simulation to determine the water velocity in the Lake Mariut, taking into consideration its concentration and the distribution of the temperature over it, by applying the fractional steps method for the numerical solution of the shallow water equations. The application they presented over flat bottom requires the variables at two time-levels Δt and $\Delta t/2$ according to Strang method [20] which is more accurate in time, since it has a second-order accurate. They proved the convergence of the fractional steps method and verified that the order of convergence is of the first order.

In this problem, we use the same trend as done by Abd-el-Malek and Helal [10] and Shoucri [11] in solving numerically the two-dimensional nonlinear shallow water equations in the presence of Coriolis force and bottom topography using the fractional steps method. We study the effects of the Coriolis force and the bottom topography for particular initial flows on the velocity components and the free surface elevation.

3.2. Cubic Spline Interpolation

To approximate the arbitrary functions on closed intervals by the aid of the polynomials, we used the most common piecewise polynomial approximation using cubic polynomials between each successive pairs of nodes which is called cubic spline interpolation. A general cubic polynomial involves four constants, so, there is a sufficient flexibility in the cubic spline procedure to ensure that the interpolant is not only continuously differentiable on the interval, but also it has a continuous second derivative on the interval, [21].

4. Results and Discussion

We apply the numerical scheme presented in Section 3 to solve the problem at different values of time for different initial flows describing the dam break wave and the tsunami propagation wave over two main profiles of the non-flat bottom in cases of neglecting and including the Coriolis force. We represent the bottom with two different shapes which are a hump and rising hill topography respectively, as follows.

***Hump topography*:** (25)

***Rising up hill topography*:** (26)

The two forms of $\zeta(x)$ are defined for $y \in [0,100]$. We present the bottom topographies considered by a hump with maximum height 250 m and rising hill topography up to 1850 m, **Figures 2** and **3**. The problem is solved for $g = 9.806\ m/s^2$ and maximum depth $H = 2$ km. The scale is based with length $x = 500$ km, and width $y = 100$ km. The horizontal grid cell length is $\Delta x = \Delta y = 1$ km resulting in 500×100 grid cells at time step $\Delta t = 1\ s$. We assume the initial velocities $u(x, y, 0) = v(x, y, 0) = 0$.

The initial flows describing the tsunami propagation wave and the dam break wave are illustrated as follows:

$$\zeta(x) = \begin{cases} 0.125\,[1 + \cos(\frac{\pi}{25}(x - 375))], & 350 \le x \le 400 \\ 0 & otherwise \end{cases} \tag{25}$$

$$\zeta(x) = \begin{cases} 0.925\,(1 + \cos(\frac{\pi}{200}(x - 400))), & 200 \le x \le 400 \\ 1.850, & 400 \le x \\ 0 & otherwise \end{cases} \tag{26}$$

***Tsunami propagation wave*:**

Tsunamis are long waves generated by submarine earthquakes. Once they reach the open ocean and travel through deep water tsunamis which have extremely small amplitudes but travel fast. Tsunami propagation velocity can be estimated by using the wave speed equation $C = \sqrt{gH}$. For 2000 m water depth, the speed will be about 504 km/hour. The most difficult phase of the dynamics of tsunami waves deals with their breaking as they approach the shore. This phase depends greatly on the bottom bathymetry. As a model of this initial tsunami displacement, we consider the wave presented by George [7] which is given by (27).

***Dam break wave*:**

The dam-break problem is an environmental problem involving unsteady flows in waterways. The study of flooding after the dam break is very important because of the risk to life and property in the potentially inundated area below the dam. The initial dam break model assumed is given by (28).

Figures 4 and **5** represent the tsunami propagation and dam break waves, respectively, as initial flows. In case of the dam break problem, the water is assumed to be at rest on both sides of the dam initially. At $t = 0$ the dam is suddenly destroyed, causing a shock wave (bore) travelling downstream with $\eta = -10$ on x > 250 and a rarefaction wave (depression wave) traveling upstream with $\eta = 10$ on x < 250. The water pushing down from above acts somewhat like a piston being pushed downstream with acceleration.

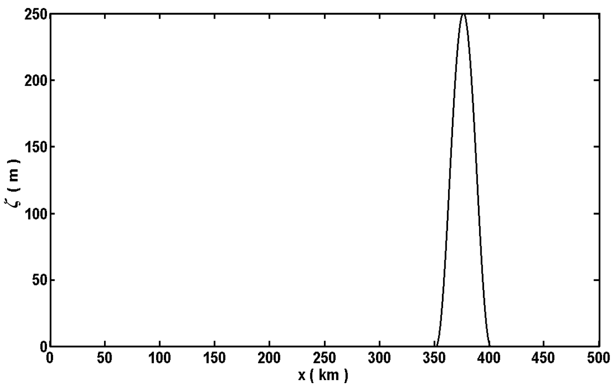

Figure 2. Profile of hump topography.

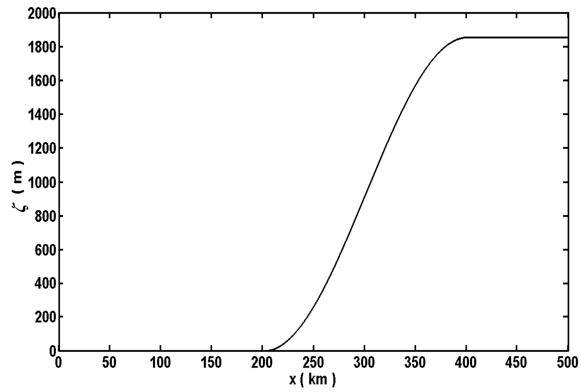

Figure 3. Profile of rising up hill topography.

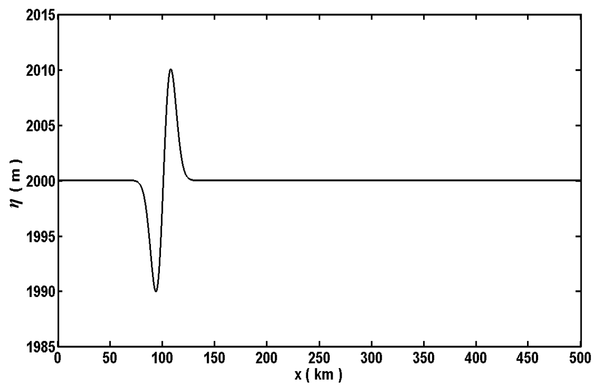

Figure 4. Tsunami propagation initial wave.

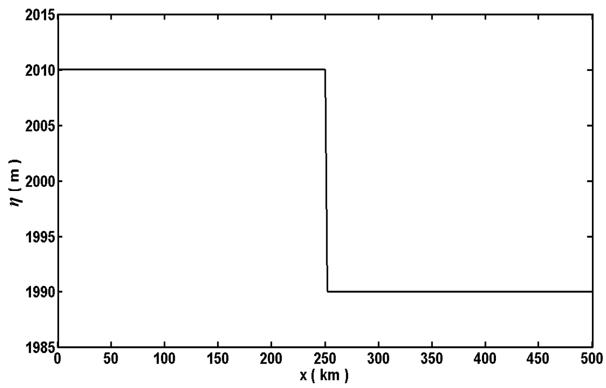

Figure 5. Dam break initial wave.

$$h^*(x,y,0) = \begin{cases} 0.00235(x-100)e^{-\left(\frac{x-100}{10}\right)^2} + H, & 50 \le x \le 150 \\ \text{H}, & \text{otherwise} \end{cases} \tag{27}$$

$$h^*(x,y,0) = \begin{cases} (H + 0.01)\,\mathrm{sgn}\,(x - 250) & \mathit{for} \quad 0 \le x \le 250 \\ (H - 0.01)\,\mathrm{sgn}\,(x - 250) & \mathit{for} \quad 250 \le x \le 500 \end{cases} \tag{28}$$

From the geophysical fluid dynamics point of view, as a first step toward understanding the role of bottom topography, consider the flow in a periodic zonal channel with solid boundaries to the North and the South with idealized topography. Here $f = 0.01$ is chosen such that the domain is resides in the northern hemisphere of the earth. Sea surface velocities and water height over the bottom topography at various time and different initial conditions are illustrated in the cases of neglecting and including the Coriolis force

Equations (1)-(3) contain the most fundamental balances of shallow water flows, see [22,23]. The convective part on the left-hand side is a hyperbolic system of conservation laws and the source term on the right-hand side is due to gravitational acceleration and rotation of the earth (Coriolis force). The steady state results from a balance between the advection and decay processes [24].

This suggests that we may have difficulties with a fractional-step method in order to balance between the advection terms and the source terms, where we first solve the advection equation ignoring the reactions and then solve the reaction equation ignoring the advection [24]. Even if we start with the exact steady-state solution, each of these steps can be expected to make a change in the solution. In principle the two effects should exactly cancel out, but numerically they typically will not, since different numerical techniques are used in each step [24].

4.1. The Velocity Component in the x-Direction

Figures 6 and **7** illustrate the behavior of the velocity u over the topography $\zeta(x)$ represented by a hump given by (25) for an initial flow represented by the dam break wave given by (28), in case of neglecting and including the Coriolis force at $t = 400$, 1200 and 1800 sec respectively. By neglecting the effect of earth rotation (*i.e.* no Coriolis force), the coupling between Equations (2) and (3) due to Coriolis force does no longer exists. Consequently, it is expected that the velocity vector is in the direction of wave propagation and that minor oscillations will appear in the results when the wave propagates

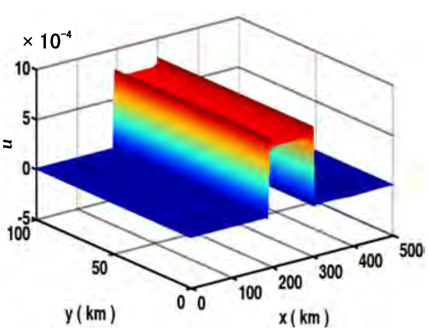

t = 400 sec

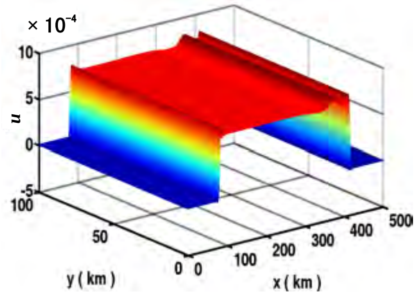

t = 1200 sec

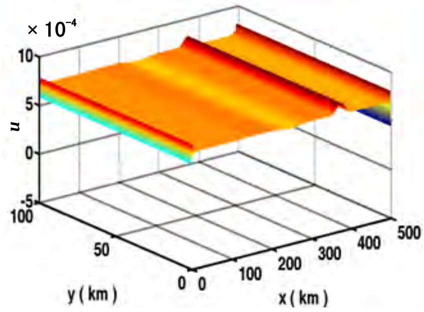

t = 1800 sec

Figure 6. Behavior of u with hump topography and dam break initial flow without the effect of the Coriolis force at t = 400, 1200 and 1800 sec.

over topography. This is in good agreement with the result shown in **Figure 6**. In fact, since the water at $x = 250$ km seems likely to acquire instantaneously, a velocity different from zero, **Figure 6**.

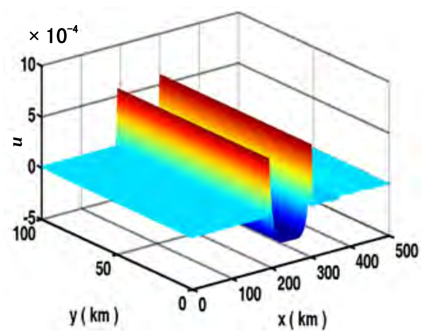

t = 400 sec

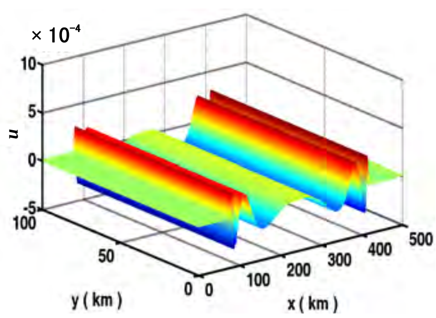

t = 1200 sec

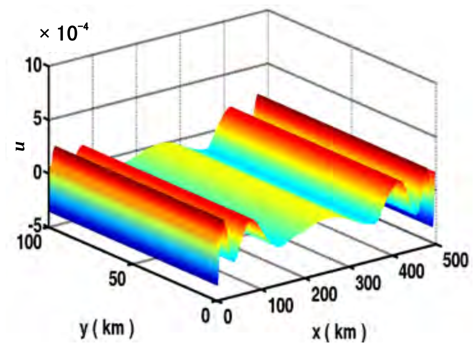

t = 1800 sec

Figure 7. Behavior of *u* with hump topography and dam break initial flow with the effect the Coriolis force at *t* = 400, 1200 and 1800 sec.

Figures 8 and **9** illustrate the behavior of the velocity u over the topography $\zeta(x)$ representing a rising up function given by (26) for an initial flow representing the tsunami propagation wave given by (27), in case of neglecting and including the Coriolis force at t = 400, 1200 and 3000 sec respectively. As mentioned before, in case of neglecting the Coriolis force, the velocity vector is in the direction of the wave propagation and minor oscillations will appear in the results when the wave propagates over the topography, **Figure 8**.

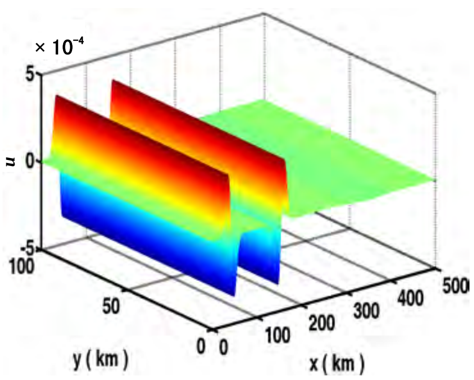

t = 400 sec

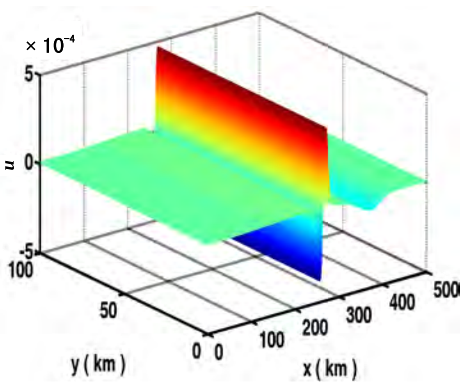

t = 1200 sec

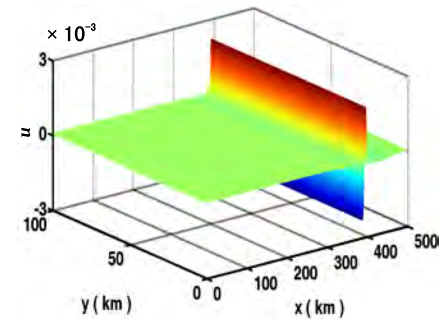

t = 3000 sec

Figure 8. Behavior of *u* with rising up topography and tsunami propagation initial flow without the effect of the Coriolis force at *t* = 400, 1200 and 3000 sec.

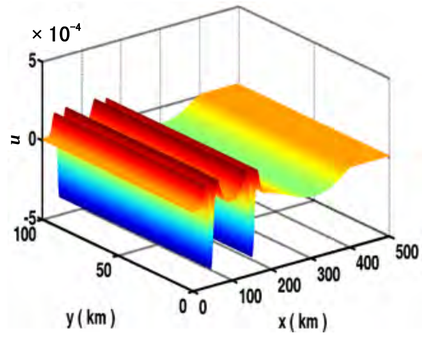

t = 400 sec

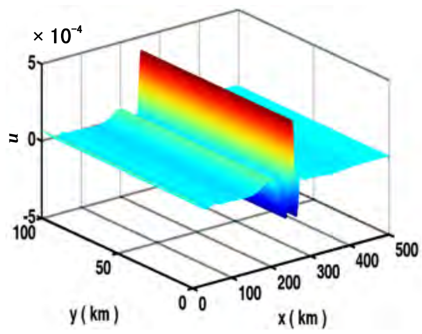

t = 1200 sec

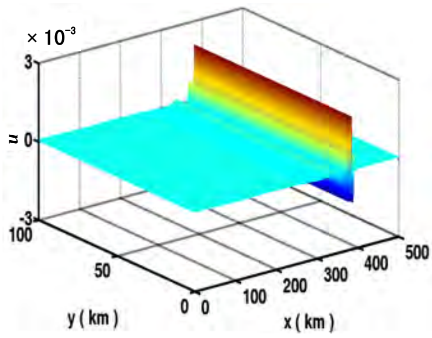

t = 3000 sec

Figure 9. Behavior of *u* with rising up topography and tsunami propagation initial flow with the effect the Coriolis force at *t* = 400, 1200 and 3000 sec.

4.2. The Velocity Component in the y-Direction

Figures 10 and **11** illustrate the behavior of the velocity v over the topography $\zeta(x)$ representing a hump given by (25) for an initial flow representing the dam break wave give n by (28) and a rising up function given by (26) for an initial flow representing the tsunami propagation wave given by (27) with the effect of Coriolis force.

4.3. The Water Height h^*

Figures 12 and **13** illustrate the behavior of the water height h^* over the topography $\zeta(x)$ representing by a hump given by (25) for an initial flow representing by the dam break wave given by (28) in case of neglecting and including the Coriolis force at t = 400, 1200 and 1800 sec respectively at y = 0.

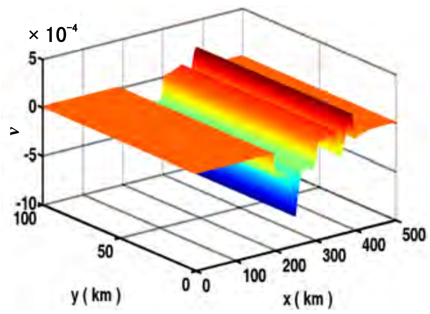

t = 400 sec

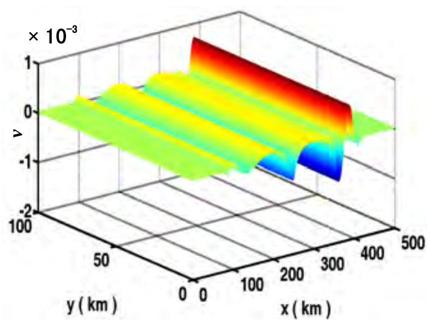

t = 1200 sec

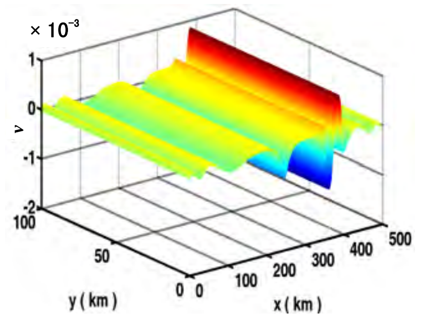

t = 1800 sec

Figure 10. Behavior of *v* with hump topography and dam break initial flow with the effect of the Coriolis force at *t* = 400, 1200 and 1800 sec.

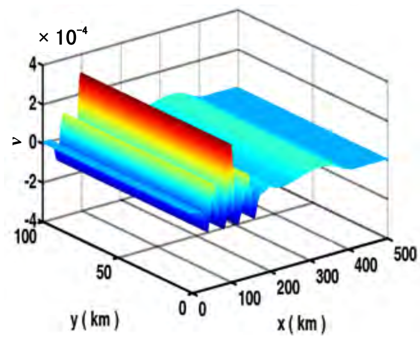

t = 400 sec

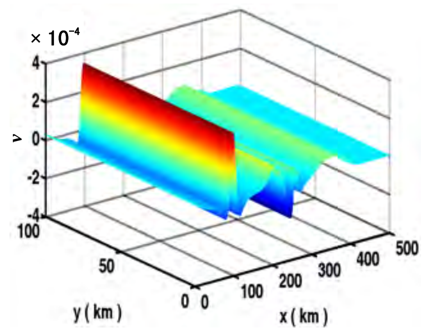

t = 1200 sec

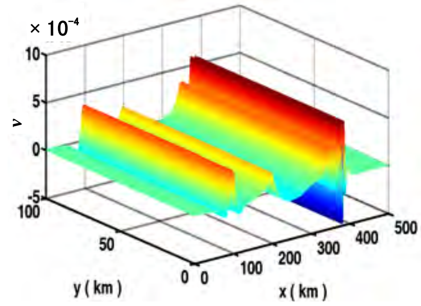

t = 3000 sec

Figure 11. Behavior of *v* with rising up topography and tsunami propagation initial flow with the effect the Coriolis force at *t* = 400, 1200 and 3000 sec.

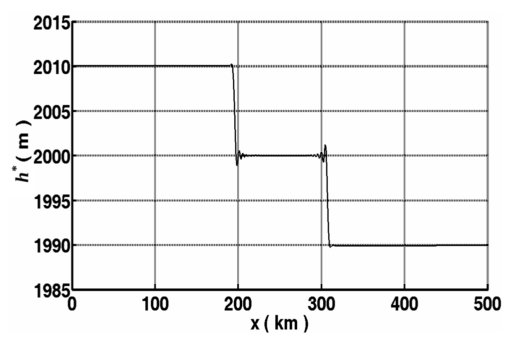

t = 400 sec

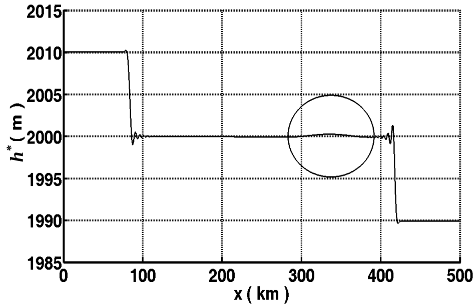

t = 1200 sec

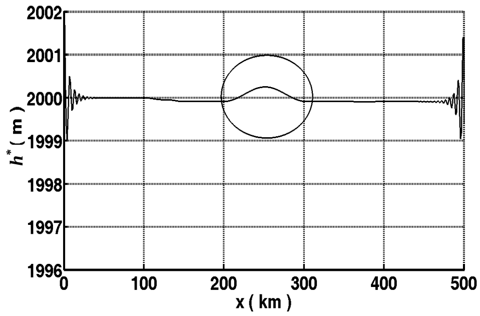

t = 1800 sec

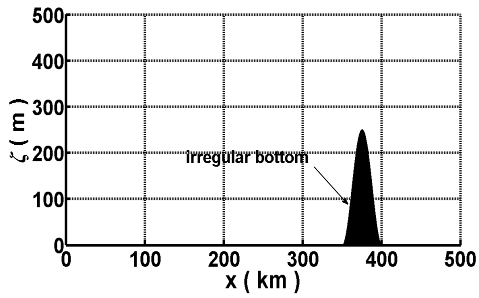

Figure 12. Behavior of *h with hump topography and dam break initial flow without the effect of the Coriolis force at *t* = 400, 1200 and 1800 sec.**

Figures 14 and **15** illustrate the behavior of the water height h^* over the topography $\zeta(x)$ representing a rising up function given by (26) for an initial flow representing by the tsunami propagation wave given by (27) in case of neglecting and including the Coriolis force at t = 400, 1200 and 3000 sec respectively at y = 0.

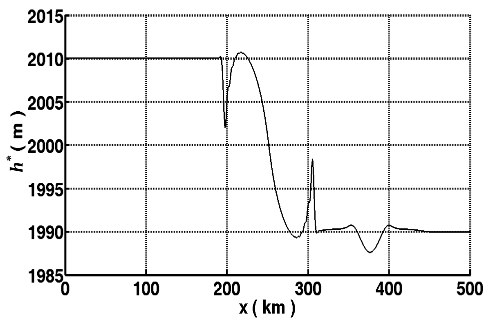

t = 400 sec

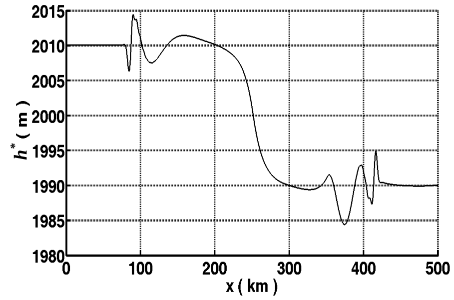

t = 1200 sec

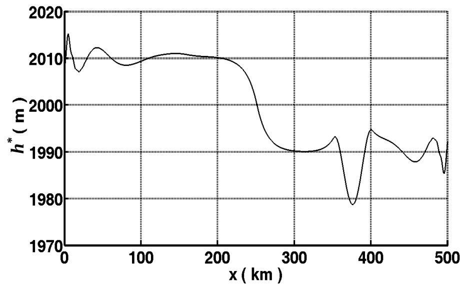

t = 1800 sec

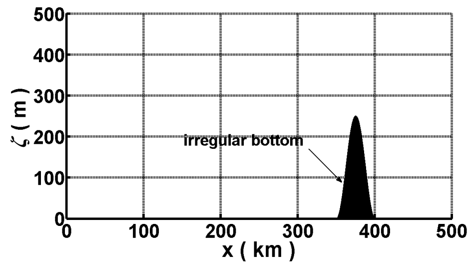

Figure 13. Behavior of *h with hump topography and dam break initial flow with the effect the Coriolis force at *t* = 400, 1200 and 1800 sec.**

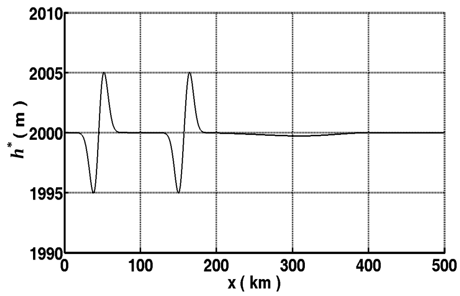

t = 400 sec

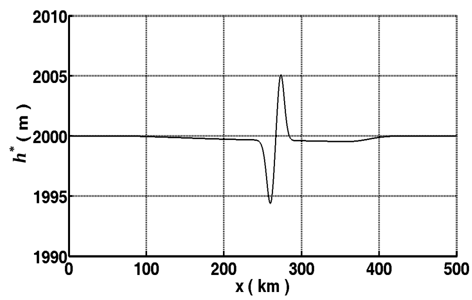

t = 1200 sec

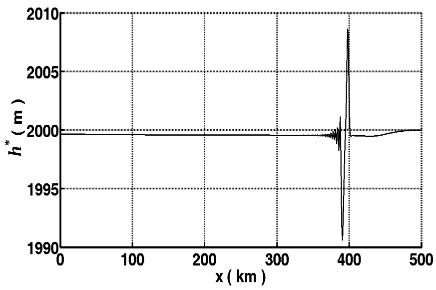

t = 3000 sec

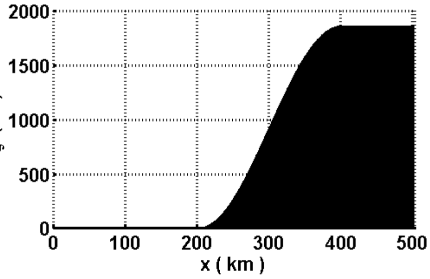

Figure 14. Behavior of *h with rising up topography and tsunami propagation initial flow without the effect of the Coriolis force at *t* = 400, 1200 and 3000 sec.**

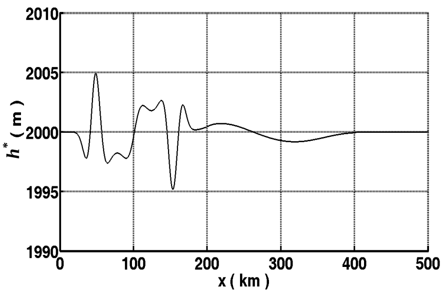

t = 400 sec

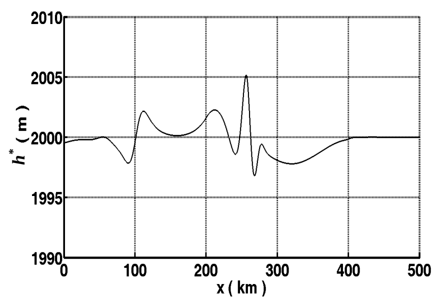

t = 1200 sec

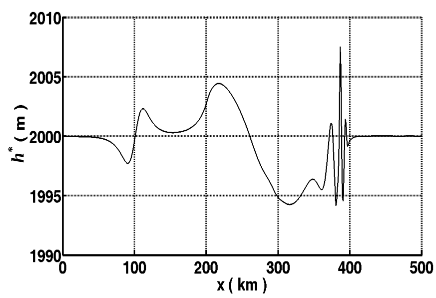

t = 3000 sec

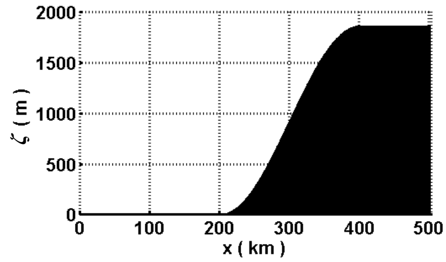

Figure 15. Behavior of *h with rising up topography and tsunami propagation initial flow with the effect the Coriolis force at *t* = 400, 1200 and 3000 sec.**

Since the water at $x = 250$ km seems likely to acquire instantaneously, it is plausible that a shock would be created instantly on the upstream side and a relatively small propagated wave in the negative X-direction due to bottom topography as shown in the circle in **Figure 12**.

By taking the Coriolis force $(fv, -fu)$ into consideration, it becomes responsible for the oscillatory motion according to the solutions of Equations (23) and (24) obtained in Step 3 in the fractional steps method. The coupling between the velocity components u and v causes the deflection of fluid parcels which are oscillating back and forth in the direction of wave motion and causes gravity waves to disperse as shown in **Figures 13** and **15**. The magnitude of this deflection proved to be independent of the absolute depth and depends only on the slope of the bottom, as demonstrated in the momentum Equations (2) and (3).

In case of the tsunami wave, the initial waves split into two similar waves, one propagates in the positive x-direction and the other in the negative x-direction. The height above mean sea level of the two oppositely traveling tsunamis is approximately half that of the original tsunami, as shown in **Figure 14**. This happened because the potential energy that results from pushing water above mean sea level is transferred to horizontal propagation of the tsunami wave (kinetic energy) (*i.e.* the tsunami converts potential energy into kinetic energy). It is well known when the local tsunami travels over the continental topography, that the wave amplitude increases and the wavelength and velocity decreases, which results in steepening of the leading wave, see **Figure 14**.

In case of the dam break problem, the effect of the Coriolis force on the water height at a sequence of times after the breakage of a dam causes a wave travelling downstream and a wave travelling upstream as shown in **Figure 13**. The rarefaction wave that developed in **Figure 13** is overtaken by dispersive wave which should form shocks on both sides of propagation.

In case of the tsunami waves, they propagate in coherent wave packets, with little loss of amplitude over very long distances as shown in **Figure 15**. As the water depth decreases, the wave amplitude increases and the wavelength and velocity decreases, resulting in steepening of the dispersed wave.

4.4. The Free Surface Elevation (η)

Figures 16 and **17** illustrate the effect of the Coriolis force on the free surface elevation η when travelling over the topography $\zeta(x)$ representing a hump given by (25) and a rising up function given by (26) for an initial flow representing the dam break wave given by (28) at $t = 1200$ sec.

The 500 kilometers long dam wall, which runs parallel to the y-axis is 10 meters wide and is centered at x = 250 kilometers. Along the boundaries, at x = 0 kilometers and x = 500 kilometers and η is fixed at the upstream and downstream water depth respectively. All other boundaries are considered as reflective boundary conditions. In case of neglecting the Coriolis force, a shock front always exists as shown in **Figure 16**, while the free surface elevation η under the effect of the Coriolis force has no shock travelling downstream and hence travelled in the direction of propagation over the topography $\zeta(x)$ as seen in **Figure 17**.

As seen in **Figure 16**, the jump at the generated shock first decreases and then it increases as the shock approaches the bottom topography. It is observed that the increasing in the shock wave when travelling over the rising up hill topography is greater than when travelling over hump topography.

It can be observed that the free surface elevation η in **Figure 17** clearly differs from that in **Figure 16** due to the effect of the Coriolis force which is responsible for the oscillatory motion in the direction of wave motion which causes gravity waves to disperse.

Figures 18 and **19** illustrate the effect of the Coriolis force on the free surface elevation η when travelling over the topography $\zeta(x)$ representing a hump given by (25) and a rising up function given by (26) for an initial flow representing the tsunami propagation wave given by (27), at $t = 2400$ sec.

The effect of the Coriolis force on the tsunami propagation wave is responsible for some part of the energy, which is transmitted to the ocean with the seismic bottom motions, to accumulate in the region of the disturbance. This leads to a reduction of the barotropic wave energy and tsunami amplitude. The direction of the tsunami radiation varies and the energy flow transferred by the waves is redistributed.

The effect of Coriolis force on transoceanic tsunami with and without Coriolis terms shows differences in wave height but not much difference in arrival time as observed in **Figure 18** and **Figure 19**.

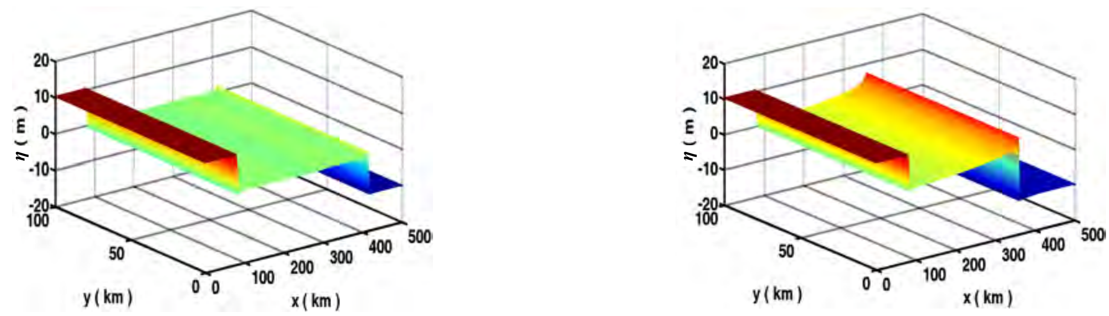

(a) (b)

Figure 16. Behavior of η for the dam break initial flow without the effect of the Coriolis force at *t* = 1200 sec over: (a) Hump topography; (b) Rising up hill topography.

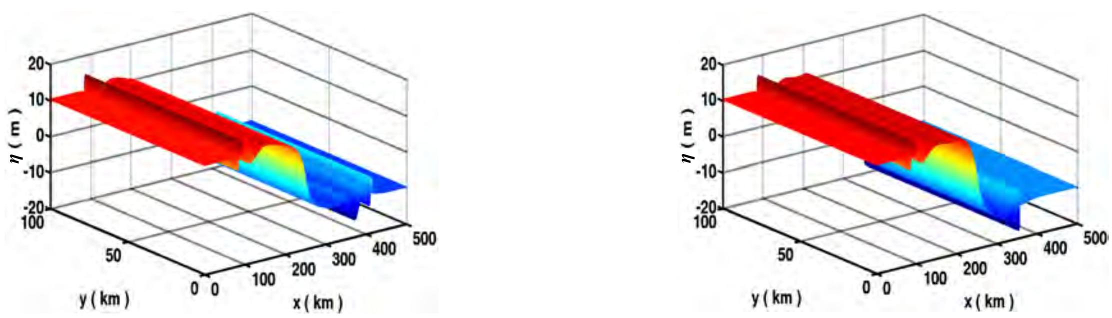

(a) (b)

Figure 17. Behavior of η for the dam break initial flow with the effect of the Coriolis force at *t* = 1200 sec over: (a) Hump topography; (b) Rising up hill topography.

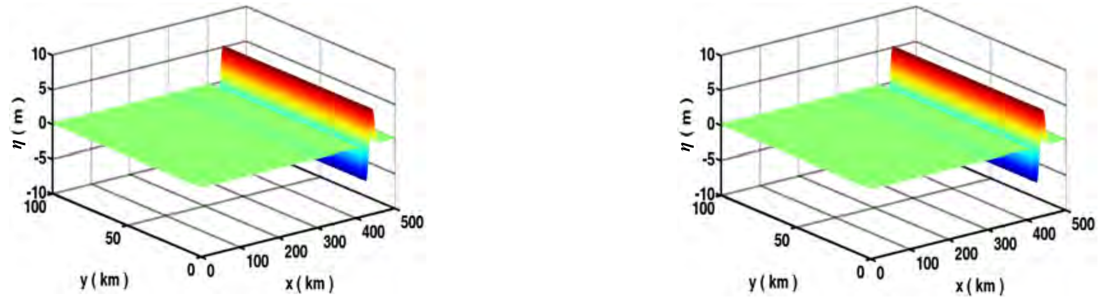

(a) (b)

Figure 18. Behavior of η for the tsunami propagation initial flow without the effect of the Coriolis force at t = 2400 sec over: (a) Hump topography; (b) Rising up hill topography.

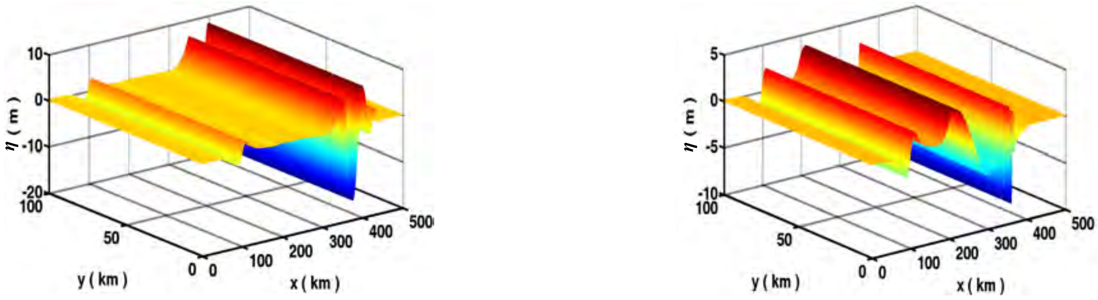

(a) (b)

Figure 19. Behavior of η for the tsunami propagation initial flow with the effect of the Coriolis force at t = 2400 sec over: (a) Hump topography; (b) Rising up hill topography.

Therefore the dispersion effects become more significant as the wave energy is more spatially spread out and scattered. The variability of the bathymetry is also quite variable being an important parameter of wave dispersion as it controlled in the speed and the height of the tsunami wave when there was a sudden change in the depth of water as seen in **Figure 18** and **Figure 19**.

As seen from **Figures 16-19**, the wave propagated faster when travelling over the hump topography than travelling over the increasing hill topography. This was expected due to the wave speed equation $C = \sqrt{gH}$ which is proportional to the water depth and inversely proportional to the bottom bathymetry.

5. Conclusions

The fractional steps method for the numerical solution of the shallow water equations is applied to study the evolution of the height and the velocity field of the flow under the effect of Coriolis force and bottom topography. The method consists of splitting the equations and successively integrating in the x-and y-directions along the characteristics using the Riemann invariants, associated with the cubic spline interpolation. In this work, we applied the fractional steps method to solve the two-dimensional shallow water equations with source terms (including the Coriolis force and bottom topography) for two different initial flows namely dam break wave and tsunami wave. The presence of the Coriolis force in the shallow water equations causes the deflection of fluid parcels in the direction of wave motion and causes gravity waves to disperse. As water depth decreases due to bottom topography, the wave amplitude increases, the wavelength and wave speed decreases resulting in steepening of the wave. The effect of the Coriolis force is responsible for the oscillatory motion in the direction of wave motion which causes gravity waves to disperse. The overall performance of the fractional steps method in solving the shallow water equations with source terms is particularly attractive, simple, efficient and highly accurate as our results verified the reality about the nature of the dam break problem and the tsunami propagation wave. In future, we shall apply the fractional steps method to the shallow water equations with the source term including Coriolis force and a movable topography as it appears in oceanographic modeling as well as in the river flow modeling is underway and compare the results analytically using Lie-group method, [25-29].

6. Acknowledgements

The authors would like to express their sincere thank the reviewers for suggesting certain changes in the original manuscript, for their valuable comments which improved the paper and for their great interest in that work.

7. References

[1] D. G. Dritschel, L. M. Polvani and A. R. Mohebalhojeh, "The Contour-Advective Semi-Lagrangian Algorithm for the Shallow Water Equations," *Monthly Weather Review*, Vol. 127, No. 7, 1999, pp. 1551-1564.

[2] J. Pedlosky, "Geophysical Fluid Dynamics," Springer, New York, 1987.

[3] M. Lukácová-Medvid'ová, S. Noelle and M. Kraft, "Well-Balanced Finite Volume Evolution Galerkin Methods for the Shallow Water Equations," *Journal of Computational Physics*, Vol. 221, No. 1, 2007, pp. 122-147.

[4] T. Gallouët, J. M. Hérard and N. Seguin, "Some Approximate Godunov Schemes to Compute Shallow-Water Equations with Topography," *Computers* & *Fluids*, Vol. 32, No. 4, 2003, pp. 479-513.

[5] P. J. Dellar and R. Salmon, "Shallow Water Equations with a Complete Coriolis Force and Topography," *Physics of Fluids*, Vol. 17, No. 10, 2005, pp. 106601-106619.

[6] K. V. Karelsky, V. V.Papkov, A. S. Petrosyan and D. V. Tsygankov, "Particular Solution of the Shallow-Water Equations over a Non-Flat Surface," *Physics Letters A*, Vol. 271, No. 5-6, 2000, pp. 341-348.

[7] D. L. George, "Augmented Riemann Solvers for the Shallow Water Equations over Variable Topography with Steady States and Inundation," *Journal of Computational Physics*, Vol. 227, No. 6, 2008, pp. 3089-3113.

[8] M. Shoucri, "The Application of a Fractional Steps Method for the Numerical Solution of the Shallow Water Equations," *Computer Physics Communications*, Vol. 164, No. 1-3, 2004, pp. 396-401.

[9] A. Stainiforth and C. Temperton, "Semi-Implicit Semi-Lagrangian Integration Scheme for a Baratropic Finite-Element Regional Model," *Monthly Weather Review*, Vol. 114, No. 11, 1986, pp. 2078-2090.

[10] M. B. Abd-el-Malek and M. H. Helal, "Application of the Fractional Steps Method for the Numerical Solution of the Two-Dimensional Modeling of the Lake Mariut," *Applied Mathematical Modeling*, Vol. 33, No. 2, 2009, pp. 822-834.

[11] M. Shoucri, "Numerical Solution of the Shallow Water Equations with a Fractional Step Method," *Computer Physics Communications*, Vol. 176, No. 1, 2007, pp. 23-32.

[12] I. Yohsuke, A. Takayuki and M. Shoucri, "Comparison of Efficient Explicit Schemes for Shallow-Water Equations-Characteristics-Based Fractional-Step Method and Multimoment Eulerian Scheme," *Journal of Applied Meteorology and Climatology*, Vol. 46, No. 3, 2007, pp. 388-395.

[13] A. Takayuki, "Interpolated Differential Operator (IDO) Scheme for Solving Partial Differential Equations," *Computer Physics Communications*, Vol. 102, No. 1-3, 1997, pp. 132-146.

[14] C. Temperton and A. Stainiforth, "An Efficient Two-Time-Level Semi-Lagrangian Semi-Implicit Integration Scheme," *Quarterly Journal of the Royal Meteorological Society*, Vol. 113, No. 477, 1987, pp. 1025-1039.

[15] E. Audusse, F. Bouchut, M. Bristeau, R. Klein and B. Perthame, "A Fast and Stable Well-Balanced Scheme with Hydrostatic Reconstruction for Shallow Water Flows," *SIAM Journal on Scientific Computing*, Vol. 25, No. 6, 2004, pp. 2050-2065.

[16] M. E. Talibi and M. H. Tber, "On a Problem of Shallow Water Type," *Electronic Journal of Differential Equations*, Vol. 11, 2004, pp. 109-116.

[17] V. R. Ambati and O. Bokhove, "Space-Time Discontinuous Galerkin Discretization of Rotating Shallow Water Equations," *Journal of Computational Physics*, Vol. 225, No. 2, 2007, pp. 1233-1261.

[18] N. N. Yanenko, "The Method of Fractional Steps, the Solution of Problems of Mathematical Physics in Several Variables," Springer-Verlag, Berlin, 1971.

[19] D. R. Durran, "Numerical Methods for Wave Equations in Geophysics Fluid Dynamics," Springer-Verlag, New York, 1999.

[20] G. Strang, "On the Construction and Comparison of Finite Difference Schemes," *Society for Industrial and Applied Mathematics*, *Journal for Numerical Analysis*, Vol. 5, No. 3, 1968, pp. 506-517.

[21] R. L. Burden and J. D. Faires, "Numerical Analysis," PWS Publishing Company, Boston, 1993.

[22] S. Noelle, N. Pankratz, G. Puppo and J. R. Natvig, "Well-Balanced Finite Volume Schemes of Arbitrary Order of Accuracy for Shallow Water Flows," *Journal of Computational Physics*, Vol. 213, No. 2, 2006, pp. 474-499.

[23] S. Noelle, Y. Xing and C. Shu, "High-Order Well-Balanced Finite Volume WENO Schemes for Shallow Water Equation with Moving Water," *Journal of Computational Physics*, Vol. 226, No. 1, 2007, pp. 29-58.

[24] R. LeVeque, "Finite Volume Methods for Hyperbolic Problems," Cambridge University Press, Cambridge, 2004.

[25] Y. Z. Boutros, M. B. Abd-el-Malek, N. A. Badran and H. S. Hassan, "Lie-Group Method for Unsteady Flows in a Semi-infinite Expanding or Contracting Pipe with Injection or Suction through a Porous Wall," *Journal of Computational and Applied Mathematics*, Vol. 197, No. 2, 2006, pp. 465-494.

[26] Y. Z. Boutros, M. B. Abd-el-Malek, N. A. Badran and H. S. Hassan, "Lie-Group Method Solution for Two-dimensional Viscous Flow between Slowly Expanding or Contracting Walls with Weak Permeability," *Applied Mathematical Modelling*, Vol. 31, No. 6, 2007, pp. 1092-1108.

[27] Y. Z. Boutros, M. B. Abd-el-Malek, N. A. Badran and H. S. Hassan, "Lie-Group Method of Solution for Steady Two-Dimensional Boundary-Layer Stagnation-Point Flow Towards a Heated Stretching Sheet Placed in a Porous Medium," *Meccanica*, Vol. 41, No. 6, 2007, pp. 681-691.

[28] M. B. Abd-el-Malek, N. A. Badran and H. S. Hassan, "Lie-Group Method for Predicting Water Content for Immiscible Flow of Two Fluids in a Porous Medium," *Applied Mathematical Sciences*, Vol. 1, No. 24, 2007, pp. 1169-1180.

[29] M. B. Abd-el-Malek and H. S. Hassan, "Symmetry Analysis for Solving Problem of Rivlin-Ericksen Fluid of Second Grade Subject to Suction," submitted for publication.

Applied Mathematics, **2010, 1, 118-123**
doi:10.4236/am.2010.12015 Published Online July 2010 (http://www.SciRP.org/journal/am)

On Stable Reconstruction of the Impact in the System of Ordinary Differential Equations

Andrei Y. Vdovin, Svetlana S. Rubleva
The Ural State Forest-Engineering University, Ekaterinburg, Russia
E-mail: *rublevas@mail.ru*
Received February 18, 2010; *revised May* 27, 2010; *accepted June* 8, 2010

Abstract

Approach to expansion of an opportunity of the reception the guaranteed estimation for a problem of reconstruction the impact within the limits of the dynamical algorithm is considered in the article.

Keywords: Dynamical Algorithm, The Reconstruction of the Impact, The Estimation of Accuracy of the Algorithm

1. Problem Statement

Consider the problem of reconstruction of entrance impact $u(\cdot)$ in the dynamical system

$$x'(t) = p(t, x(t)) + f(t, x(t))u(t),\ x(a) = x_a,\ t \in [a,b], \quad (1)$$

according to inexact measurements $x_h(\cdot)$ of states $x(\cdot)$ of the system (1) in knots of splitting [a,b]: $a = t_0 < t_1 < \ldots < t_n = b : |x_h(t_i) - x(t_i)| \leqslant h$.

Here $p(\cdot)$, $f(\cdot)$ are mappings from [a,b] × R^m into R^m (with Euclidean norm $|\cdot|$) and into $R^{m\times q}$ — the matrix space of dimension $m \times q$ (with spectral norm $\|\cdot\|$), respectively; values of the impact $u(\cdot)$ belong to compactum $Q \subset R^q$, and values of the $x(t)$ belong to compactum $X \subset R^m$.

The problem in such statement has been widely covered in the literature. For its decision we will adhere to the approach, considered in [1]. It was offered to restore the impact $u_*(\cdot)$ with the minimum norm in L_2[a,b] among all impacts $u(\cdot)$ generating observable movement $x(\cdot)$ for stability of algorithm.

Essence of method consists in the following: let $\alpha(\cdot)$, $\Delta(\cdot)$: (0, ∞) → (0, ∞), $\langle\cdot,\cdot\rangle$ – scalar product, compactum Q is convex, and index T is denote transposing.

In each partition interval $[t_i, t_{i+1})$ are formed:

1) the value at the point t_{i+1} of the system of the model functioning according to the rule

$$w_h(t) = w_h(t_i) + (p(t_i, x_h(t_i)) + f(t_i, x_h(t_i))u_i)(t - t_i),$$

2) the value of u_i, being the result of projection on Q of the vector

$$\frac{1}{\alpha(h)} f^T(t_i, x_h(t_i))(x_h(t_i) - w_h(t_i)).$$

So, the considered algorithm (further D_h) puts in conformity to measurement $x_h(\cdot)$ the piecewise constant approximation $u_h(\cdot)$ of the impact $u_*(\cdot)$, where $u_h(t) = u_i$, $t \in [t_i, t_{i+1})$.

Suppose that $\rho_F(h) = \sup_{x_h(\cdot)} \|u_h(\cdot) - u_*(\cdot)\|_{F[a,b]}$, where $F[a,b]$ – some functional space. If $\lim_{h\to 0} \rho_F(h) = 0$, then algorithm is called $F[a,b]$ – regularizing.

Statement 1: [1] Suppose that $x(t)$ at $t \in [a,b]$ belong to compactum X from R^m; functions $p(t,x)$, $f(t, x)$ at $(t, x(t)) \in [a,b] \times X$ are Lipschitz with respect to all the variables with common constant L; parameters $\alpha(h)$, $\Delta(h)$ are vanishing together with h so that $\lim_{h\to 0} \dfrac{h + \Delta(h)}{\alpha(h)} = 0$.

Then D_h — L_2[a,b] – regularizing.

The question on estimations of accuracy of algorithm is essential at its use. Let's enter the following concepts:

Definition. *A function* $v_1(h)(v_2(h)) : [0, h_*) \to [0,\infty)$ *is called a lower (upper) estimate of the accuracy of the algorithm* D_h *in a space* $F[a,b]$, *if for all* $h \in (0, h_*]$ *inequalities* $v_1(h) \leqslant \rho_F(h) \leqslant v_2(h)$ *hold, and* $\gamma(h) : [0, h_*) \to [0,\infty)$ *is called the order of the accuracy of the algorithm* D_h *in* $F[a,b]$, *if there exist positive constant* $C_i, i = 1,2$ *such that* $C_1 h^{\gamma(h)} \leqslant \rho_F(h) \leqslant C_2 h^{\gamma(h)}$.

The number γ_0 *is called asymptotic order of accuracy of the algorithm* D_h *in* $F[a,b]$, *if* $\lim\limits_{h\to 0}\gamma(h)=\gamma_0$ *exists*.

The estimations of the accuracy for the discontinuous impact in space $L_1[a,b]$ for the described algorithm are received, for example [2,3]. The purpose of the article is construction of modification D_h [4] and indication the additional assumptions at which receipting of asymptotic order in $C[a,b]$ is possible. For this purpose we will adhere to the approach offered in [2], therefore we will omit common proves of lemmas.

Note, that on first step of work of the algorithm as approximation of $u_*(\cdot)$ we select projection of zero on Q. The last make receipt of estimation with condition $\lim\limits_{h\to 0}v_2(h)=0$ is impossible. If the initial condition $u(a)$ is known (we fix left end of interval), then system (1) can be led to the kind:

$$x'(t)=g(t,x(t))+f(t,x(t))v(t),\ x(a)=x_a,\ v(a)=0 \quad (2)$$

where $v(t)=u(t)-u(a)$, $g(t,x(t))=p(t,x(t))+f(t,x(t))u(a)$, $t\in[a,b]$.

Consider the problem of reconstruction of impact $v_*(\cdot)$ in new system (2).

In what follows, we assume of performance of the following set of conditions:

Condition (*)**.** In additional to the assertions of statement 1 we suppose that for all $t\in[a,b]$ 1) rank $(f(t,x(t)))$ is equal r, 2) $v_*(\cdot)$ is satisfied to condition of Lipschitz with constant L_v; 3) the infima with respect to t of distances between the boundaries of compactumes Q and X and $v_*(t)$ and $x(t)$, respectively, are positive; 4) the value $v(a)$ is known with some error: $|v(a)-v_\sigma(a)|\leqslant\sigma(h)$.

Remark. Condition (*) involves the existence of positive constants M_f, M_g, M_v such that $\|f(\cdot)\|\leqslant M_f$, $|g(\cdot)|\leqslant M_g$, $|v(\cdot)|\leqslant M_v$.

In the modification $D_h^{(1)}$ of the algorithm D_h besides transformation of the kind of system we refuse from procedure of projection on compactum Q. The last decrease of arithmetical operations executed at each step, in which case the approximation for $v_h(\cdot)$, where $t\in[t_i,t_{i+1})$, is given by the formula:

$$v_i=f^T(t_i,x_h(t_i))\frac{x_h(t_i)-w_h(t_i)}{\alpha(h)}.$$

Let us fix $\alpha(h)$. The vector

$$v_0(t)=\frac{1}{\alpha(h)}f^T(t,x(t))(x(t)-w_0(t))$$

and the system - model

$$w_0'(t)=g(t,x(t))+A(t,x(t))\frac{x(t)-w_0(t)}{\alpha(h)},\ w_0(a)=x_a, \quad (3)$$

where

$$A(t,x(t))=f(t,x(t))f^T(t,x(t)) \quad (4)$$

we'll name the ideal.

In practice, it is impossible to construct $v_0(\cdot)$ on the basis of measurement of $x_h(\cdot)$, but, in what follows, we shall only need estimates of $|v_0(t)-v_*(t)|$ and the norms of difference between $v_0(\cdot)$ and $v_h(\cdot)$, which allow us to obtain the asymptotic order of accuracy of $D_h^{(1)}$.

2. Estimation of Norm of a Difference $v_0(\cdot)$ and $v_*(\cdot)$

Let's consider some important statements.

Statement 2: [5,6] If H – arbitrary matrix, H^+ is its pseudo-inverse, then equalities $H=HH^T(H^T)^+$, $HH^+=(HH^+)^T$, $(H^T)^+=(H^+)^T$ are valid.

Statement 3: [5,7] If $t\in[a,b]$, and the matrix $A(t,x(t))$ is defined by equality (4), then its eigenvalues $\lambda_k(t), k=\overline{1,m}$ are non-negatives: $\lambda_1(t)\geqslant\ldots\geqslant\lambda_r(t)>0$, $\lambda_{r+1}(t)=\ldots=\lambda_m(t)=0$, and $\|A^+(t,x(t))\|\leqslant\dfrac{1}{\lambda_r(t)}$.

Statement 4: [5] If matrix $H\in R^{m\times m}$ is hermitian, $R_0(H)$ is its kernel, and $R_1(H)$ its image, then $R^m=R_0(H)\oplus R_1(H)$, where $\oplus$ is the sign of the direct sum.

Further, for $k=0$, 1 the projection operator $P_k(H)$ onto subspace $R_k(H)$ is identified with the matrix $P_k(H)$, $k=0$, 1, corresponding to it in a fixed basis in R^m.

Statement 5: If $k=0$, 1, and matrix $P_k(A(t,x(t)))$ is projector on $R_k(A(t,x(t)))$, then:

1) $P_0(A(t,x(t)))+P_1(A(t,x(t)))=E$, ($E$ is unity matrix);

2) projectors $P_0(A(t,x(t)))$, $P_1(A(t,x(t)))$ are orthogonal;

3) $P_k^2(A(t,x(t)))=P_k(A(t,x(t)))$ [6];

4) $P_1(A(t,x(t)))=A(t,x(t))A^+(t,x(t))$ [6].

The solution of the Cauchy problem (3) is of the form

$$\begin{aligned} w_0(t)=\kappa(t,a;A(\cdot))x_a+\int_a^t\kappa(t,\tau;A(\cdot))(g(\tau,x(\tau))\\ +\frac{1}{\alpha(h)}A(\tau,x(\tau))x(\tau))d\tau \end{aligned} \quad (5)$$

here $\kappa(t,\tau;A(\cdot))$ — is a solution of the equation

$$\frac{\partial}{\partial\tau}\big(\kappa(t,\tau;A(\cdot))\big)=\frac{1}{\alpha(h)}\kappa(t,\tau;A(\cdot))A(\tau,x(\tau)) \quad (6)$$

with initial condition $\kappa(t,t;A(\cdot))=E$.

Integration by parts from a to t on the right-hand side of (5), and taking (2) and (6) into account, we obtain

$$\frac{x(t)-w_0(t)}{\alpha(h)} = \frac{1}{\partial(h)}\int_a^t \kappa(t,\tau;A(\cdot))f(\tau,x(\tau)d\tau . \quad (7)$$

Note a few properties of the functions in the right part of (7). According to statement 2 and point 4 of a statement 5 we have

$$\left(x(t)-w_0(t)\right)/\alpha(h) = 1/\alpha(h)\int_a^t \kappa(t,\tau;A(\cdot)) \times P_1(A(\tau,x(\tau)))A(\tau,x(\tau))F(\tau)d\tau, \quad (8)$$

where $F(\tau) = (f^T(\tau,x(\tau)))^+ v(\tau)$.

Both parts of the previous equality are multiplied on $P_1(A(t,x(t)))$:

$$P_1(A(t,x(t)))\frac{x(t)-w_0(t)}{\alpha(h)} = \frac{1}{\alpha(h)}\int_a^t \kappa_1(t,\tau;A(\cdot)) \times P_1(A(\tau,x(\tau)))A(\tau,x(\tau))F(\tau)d\tau, \quad (9)$$

where $\kappa_1(t,\tau;A(\cdot)) = P_1(A(t,x(t)))\kappa(t,\tau;A(\cdot))$ is a solution of the differential equation (6) with initial condition $\kappa_1(t,t;A(\cdot)) = P_1(A(t,x(t)))$.

Statement 6: [2] Suppose that assertions of statement 1 hold and for all $t\in[a,b]$ 1) rank $(f(t,x(t)))$ is equal r, 2) the infima with respect to t of distances between the boundaries of compactumes Q and X and $v_*(t)$ and $x(t)$, respectively, are positive. Then there exist positive constants h_1, K_1, K_2 such that, for all $t\in[a,b]$, $\tau\in[a,t]$, $h\in(0,h_1]$ the following estimation holds

$$\left\|\kappa(t,\tau;A(\cdot))P_1(A(\tau,x(\tau)))\right\| \leqslant K_1 e^{-\frac{\lambda(t-\tau)}{4\alpha(h)}} + \alpha(h)K_2,$$

here λ is positive constant such that, for all $t\in[a,b]$ minimal positive eigenvalue $\lambda_r(t)$ of matrix $A(t,x(t))$ satisfies the inequality $\lambda_r(t) \geqslant \lambda > 0$.

Corollary 1 According to (8) and boundedness $F(t)$ such positive constant K_0 exists that for all $t\in[a,b]$ inequality $\left|(x(t)-w_0(t)/\alpha(h)\right| \leqslant K_0$ is valid.

Corollary 2 For all $t\in[a,b]$, $\tau\in[a,t]$, $h\in(0,h_1]$ the following inequality holds:

$$\left\|\kappa_1(t,\tau;A(\cdot))P_1(A(\tau,x(\tau)))\right\| \leqslant K_1 e^{-\frac{\lambda(t-\tau)}{4\alpha(h)}} + \alpha(h)K_2$$

Definition. *Suppose that* $h\in(0,\infty)$, $\Phi h(\cdot): [a,b]\times[a,b]\to R^{m\times m}$, $\varphi(\cdot):[a,b]\to R^m$ *and* $\Phi_h(t,t)\varphi(t) = \varphi(t)$. *Consider the representation* $\int_a^t \Phi_h(t,s)\varphi(s)ds = \varphi(t) + \varepsilon(h)$. *Let's name the integral operator on the left-hand side of this equality is operator of reconstruction of the value of* $\varphi(t)$; $\Phi_h(t,s)$ *— is its kernel, and* $\varepsilon(h)$ *— error of the reconstruction*.

Consider a function

$$\Phi_h^{(1)}(t,\tau) = \frac{\partial}{\partial\tau}\left(\kappa_1(t,\tau;A(\cdot))P_1(A(\tau,x(\tau)))\right).$$

Let us show that

$$\int_a^t \Phi_h^{(1)}(t,\tau)F(\tau)d\tau \quad (10)$$

is the operator of reconstruction of the value of $F(t)$, and let us estimate the error of the reconstruction. It is not difficult to receive the following results.

Lemma 1: If matrix $H(\cdot):\ [a,b]\to R^{m\times m}$, mapping $p(\cdot):\ [a,b]\to R^m$ satisfies of the Lipschitz condition with constant L_p and for all $t\in[a,b]$ the representations $\|H(t)\| \leqslant M_H$, $\left\|\int_a^t H(\tau)d\tau\right\| \leqslant \varepsilon$ are valid, then $\left|\int_a^t H(\tau)\cdot(p(\tau)-p(t))d\tau\right| \leqslant \varepsilon L_p(b-a)$.

Lemma 2: If $t\in[a,b]$, $v(\cdot)$ satisfies of the condition Lipschitz, and the rank of the matrix $f(t,x(t))$ is constant, then for all t_1, $t_2\in[a,b]$ there is constant $L_F = \frac{6}{\lambda}LM_v\cdot(1+M_g+M_fM_v)+\frac{L_v}{\sqrt{\lambda}}$ so that $\left|F(t_1)-F(t_2)\right| \leqslant L_F\left|t_1-t_2\right|$.

The formulated lemmas allow to pass to an estimation the error of the reconstruction operator of the function value:

Lemma 3: Suppose that condition (*) hold; $\delta(h)$, $\frac{\alpha(h)}{\delta(h)}$ tend to zero together with h, $v(t)\equiv 0$ for $t\in[a-\delta(h),a)$ and $k\in\mathbb{N}$. Then there exist positive constants $h_2(k)$, K_3, K_4 such that, for $h\in(0,h_2(k)]$ the error of operator of reconstruction of the value of $F(t)$ with kernel $\Phi_h^{(1)}(t,\tau)$ satisfies the estimation

$$\varepsilon(h) \leqslant (2K_1+K_2)L_F\delta(h)+K_3\left(\frac{4\alpha(h)}{\lambda\delta(h)}\right)^k+\alpha(h)K_4 .$$

Proof. Let's put $\Phi_h^{(1)}(t,\tau)=\Phi_h^{(1)}(t,a)$ when $\tau\in[a-\delta(h),a)$, and define

$$I_1 = \left|\int_{a-\delta(h)}^{t-\delta(h)}\Phi_h^{(1)}(t,\tau)(F(\tau)-F(t))d\tau\right|,$$

$$I_2 = \left|\int_{t-\delta(h)}^{t}\Phi_h^{(1)}(t,\tau)(F(\tau)-F(t))d\tau\right|,$$

$$I_3 = \left|\int_{a-\delta(h)}^{t}\Phi_h^{(1)}(t,\tau)F(t)d\tau-F(t)\right|\cdot$$

Let's estimate each of these quantities. According to lemmas 1, 2, and statements 3, 6 for I_1 are valid:

$$I_1 \leqslant \left(L_F(b-a)+\left|F(t-\delta(h))\right|+\left|F(t)\right|\right)$$
$$\times\left\|\int_{a-\delta(h)}^{t-\delta(h)}\Phi_h^{(1)}(t,\tau)d\tau\right\| \leqslant \left(L_F(b-a)+\frac{2}{\sqrt{\lambda}}M_v\right)$$
$$\times\left\|\kappa_1(t,t-\delta(h);A(\cdot))P_1(A(t-\delta(h),x(t-\delta(h)))\right.$$
$$\left.-\kappa_1(t,a-\delta(h);A(\cdot))P_1(A(a-\delta(h),x(a-\delta(h)))\right\|$$
$$\leqslant \left(L_F(b-a)+\frac{2M_v}{\sqrt{\lambda}}\right)(K_1e^{-\frac{\lambda\delta(h)}{4\alpha(h)}}+K_1e^{-\frac{\lambda(t-a+\delta(h))}{4\alpha(h)}}$$
$$+2\alpha(h)K_2) \leqslant 2(K_1e^{-\frac{\lambda\delta(h)}{4\alpha(h)}}+\alpha(h)K_2)\cdot$$
$$(L_F(b-a)+\frac{2}{\sqrt{\lambda}}M_v);$$

for I_2: $I_2 \leqslant L_F\delta(h)\int_{t-\delta(h)}^{t}\left\|\Phi_h^{(1)}(t,\tau)d\tau\right\| \leqslant (2K_1+K_2)\cdot L_F\,\delta(h)$;

for I_3, according to statements 2 and 6:

$$I_3 \leqslant \left|[\kappa_1(t,t;A(\cdot))P_1(A(t,x(t)))\right.$$
$$-\kappa_1(t,a-\delta(h);A(\cdot))P_1(A(a-\delta(h),x(a-\delta(h)))$$
$$\left.-P_1(A(t,x(t)))]F(t)\right| \leqslant (K_1e^{-\frac{\lambda\delta(h)}{4\alpha(h)}}+2\alpha(h)K_2)\frac{M_v}{\sqrt{\lambda}}$$

The error of the operator of reconstruction defined by (10) satisfies the inequality

$$\varepsilon(h)=\left|\int_a^t\Phi_h^{(1)}(t,\tau)F(\tau)d\tau-F(t)\right|$$
$$\leqslant \left|\int_{a-\delta(h)}^{t-\delta(h)}\Phi_h^{(1)}(t,\tau)(F(\tau)-F(t))d\tau\right|$$
$$+\left|\int_{t-\delta(h)}^{t}\Phi_h^{(1)}(t,\tau)(F(\tau)-F(t))d\tau\right|$$
$$+\left|\int_{a-\delta(h)}^{t}\Phi_h^{(1)}(t,\tau)F(\tau)d\tau-F(t)\right|.$$

The last, taking into account the estimations for I_j at $K_3=K_1(2L_F(b-a)+\frac{5M_v}{\sqrt{\lambda}})$, $K_4=2K_2(L_F(b-a)+\frac{3M_v}{\sqrt{\lambda}})$, implies relation $\varepsilon(h) \leqslant (2K_1+K_2)L_F\delta(h)+K_3e^{-\frac{\lambda\delta(h)}{4\alpha(h)}}+\alpha(h)K_4$.

Note that, for any $k\in\mathbb{N}$ we can indicate such $h_2(k)>0$ that, for all $h\in(0,h_2(k)]$ inequality $e^{-\frac{\lambda\delta(h)}{4\alpha(h)}} \leqslant \left(\frac{4\alpha(h)}{\lambda\delta(h)}\right)^k$ is valid.

This fact implies the assertion of the lemma.

Let's pass from the integral on the right-hand side of (9) to the operator of reconstruction of value $F(t)$ with kernel $\Phi_h^{(1)}(t,\tau)$, $t\in[a,b]$, $\tau\in[a,t]$.

According to (6), $\kappa_1(t,\tau;A(\cdot))P_1(A(\tau,x(\tau)))$ is a solution the problem of Cauchy

$$\frac{\partial}{\partial\tau}\left(\kappa_1(t,\tau;A(\cdot))P_1(A(\tau,x(\tau)))\right)=\frac{\kappa_1(t,\tau;A(\cdot))}{\alpha(h)}$$
$$\times P_1(A(\tau,x(\tau)))A(\tau,x(\tau))+\kappa_1(t,\tau;A(\cdot))$$
$$\times\frac{d}{d\tau}\left(P_1(A(\tau,x(\tau))\right),$$
$$\kappa_1(t,t;A(\cdot))P_1(A(t,x(t)))=P_1(A(t,x(t))),$$

which implies that (9) takes the form:

$$P_1(A(t,x(t)))\frac{x(t)-w_0(t)}{\alpha(h)}=\int_a^t\Phi_h^{(1)}(t,\tau)F(\tau)d\tau$$
$$-\int_a^t\kappa_1(t,\tau;A(\cdot))\frac{d}{d\tau}\left(P_1(A(\tau,x(\tau)))\right)F(\tau)d\tau$$

In [2] the following result has been received:

Lemma 4: If conditions of statement 6 are satisfied, then there are such positive constant K_4 and h_3 that for all $t\in[a,b]$, $\tau\in[a,t]$, $h\in(0,h_3]$

$$\left\|\kappa_1(t,\tau;A(\cdot))P_0(A(\tau,x(\tau)))\right\| \leqslant \alpha(h)K_4$$

According to the approach offered in [2], it is not difficult to receive the following result.

Lemma 5: Suppose that the assumptions of lemma 3 hold. Then there exist positive constants K_5, K_6, K_7 such that, for all $t\in[a,b]$ the following estimate is valid.

$$\left|v_0(t)-v_*(t)\right| \leqslant K_7\delta(h)+K_8\left(\frac{4\alpha(h)}{\lambda\delta(h)}\right)^k+K_9\alpha(h).$$

3. Estimate of the Norm of Difference between $v_0(\cdot)$ and $v_h(\cdot)$

To derive this estimate, we need, first, to estimate $\left|w_h(t)-w_0(t)\right|$. Note that the rule

$$w_h(t)=w_h(t_i)+(g(t_i,x(t_i))+f(t_i,x(t_i))v_i)\times(t\text{-}t_i),\quad t\in[t_i,t_{i+1}),\quad v_0=v_\sigma(a) \tag{11}$$

can be regarded as the implementation of the Euler method for solving problem (3) with an inexact calculated right-hand side. In view of the specific character of our equation, we cannot use familiar results. For obtaining of a required estimation we will adhere to the approach offered in [2]. For simplicity we assume in what follows that $\frac{b-a}{\Delta(h)}\in\mathbb{N}$.

Consider the Euler method for the differential equation (3) with exactly calculated right-hand side: for $t \in [t_i, t_{i+1})$

$$w_e(t) = w_e(t_i) + \left(g(t_i, x(t_i)) + \frac{1}{\alpha(h)} A(t_i, x(t_i)) \right. \\ \left. \times (x(t_i) - w_e(t_i)) \right)(t - t_i), \quad w_e(a) = w_0(a). \tag{12}$$

In [2] the following result has been received:

Lemma 6: Let condition (*) hold. Then there exist positive constants h_4, K_{10} such that for all $h \in (0, h_4]$ and $t \in [a,b]$ the following estimate holds:

$$|w_0(t) - w_e(t)| \leqslant \frac{\Delta(h)}{\alpha(h)} K_{10}$$

Lemma 7: Let condition (*) hold. Then there exist positive constants h_5, K_{12}, K_{13} such that for all $h \in (0, h_5]$ and $t \in [a,b]$ the following estimate holds:

$$|w_h(t) - w_e(t)| \leqslant \frac{h}{\alpha(h)} K_{12} + \sigma(h) K_{13}.$$

Proof. According to (11) and (12), the following relation holds

$$w_h(t_{i+1}) - w_e(t_{i+1}) = (E - A(t_i, x_h(t_i))\frac{\Delta(h)}{\alpha(h)} \\ \times (w_h(t_i) - w_e(t_i)) + A(t_i, x_h(t_i))\frac{x_h(t_i) - x(t_i)}{\alpha(h)} \\ \times \Delta(h) + \left(A(t_i, x_h(t_i)) - A(t_i, x(t_i))\right) \\ \times \left(\frac{x(t_i) - w_0(t_i)}{\alpha(h)} + \frac{w_0(t_i) - w_e(t_i)}{\alpha(h)} \right) \Delta(h) \\ + (g(t_i, x_h(t_i)) - g(t_i, x(t_i)))\Delta(h),$$

Taking into account (*), corollary 1 from statement 6 and lemma 6 the following estimations hold:

$$|x_h(t) - x(t_i)| \leqslant h; \quad \left| \frac{x(t_i) - w_0(t_i)}{\alpha(h)} \right| \leqslant K_0;$$

$$\|A(t_i, x_h(t_i)) - A(t_i, x(t_i))\| \leqslant 2LM_f h;$$

$$|w_0(t_i) - w_e(t_i)| \leqslant \frac{\Delta(h)}{\alpha(h)} K_{11};$$

$$|g(t_i, x_h(t_i)) - g(t_i, x(t_i))| \leqslant h(L + LM_v) + \sigma M_f,$$

hence there exist positive constant h_5, $K_{11} = M_f^2 + 2LM_f K_0 + 4LM_f M_{10} + L(1 + M_v)$ such that, for all $h \in (0, h_5]$

$$|w_h(t_{i+1}) - w_e(t_{i+1})| \leqslant |w_h(t_i) - w_e(t_i)| \\ + \frac{h\Delta(h)}{\alpha(h)} K_{11} + \sigma(h)\Delta(h) M_f \tag{13}$$

Since, in this case, $|w_h(t_0) - w_e(t_0)| \leqslant h$, it follows from the (13) that, for any $i = 1,n$:

$$|w_h(t_i) - w_e(t_i)| \leqslant h + n(\frac{h\Delta(h)}{\alpha(h)} K_{11} + \sigma(h)\Delta(h) M_f) \\ = h + \frac{b-a}{\Delta(h)} \left(\frac{\Delta(h) h}{\alpha(h)} K_{11} + \sigma(h)\Delta(h) M_f \right) \\ \leqslant \frac{h}{\alpha(h)} K_{12} + \sigma(h) K_{13},$$

$K_{12} = (b-a)K_{12} + 1$, $K_{13} = (b-a)M_f$. The lemma is proved.

Using lemmas 6, 7, we obtain the following result.

Lemma 8: Let the assumption of lemma 6 hold, $\Delta(h) = h$. Then there exist positive constant K_{14}, K_{15} such that, for all $t \in [a,b]$, the following estimate hold:

$$|w_h(t) - w_0(t)| \leqslant \frac{h}{\alpha(h)} K_{14} + \sigma(h) K_{15}.$$

Note that the difference between $v_0(t)$ and $v_h(t)$ for $t \in [t_i, t_{i+1})$ can be expressed as:

$$v_0(t) - v_h(t) = f^T(t, x(t)) \frac{x(t) - x_h(t_i)}{\alpha(h)} \\ + f^T(t, x(t)) \frac{w_h(t_i) - w_h(t)}{\alpha(h)} \\ + f^T(t, x(t)) \frac{w_h(t) - w_0(t)}{\alpha(h)} \\ + (f^T(t, x(t)) - f^T(t_i, x_h(t_i))) \frac{x_h(t_i) - w_h(t_i)}{\alpha(h)} \tag{14}$$

In view of (14) and lemma8 the following result hold:

Lemma 9: Suppose that the assumptions of lemma 8 hold, quantities $\frac{h}{\alpha^2}$, $\frac{\sigma(h)}{\alpha(h)}$ are bounded. Then there exist positive constants K_v, h_6 such that $|v_h(t)| \leqslant K_v$ for all $h \in (0, h_6]$ and $t \in [a,b]$.

According to approach, considered in [2], we can obtain the next result. It is required to obtain a sharper estimate.

Lemma 10: Suppose that assumptions of lemma 9 hold. Then there exist constants K_{16}, K_{17} such that for all $t \in [a,b]$ the following inequality holds:

$$|w_0(t) - w_h(t)| \leqslant hK_{16} + \alpha(h)\sigma(h) K_{17}.$$

Let's now refine the norm of the difference between $v_0(\cdot)$ and $v_h(\cdot)$. From the (14), the condition (*), lemmas 5 and 10 the next result hold.

Lemma 11: Suppose that the assumptions the lemma 8 hold, then there exist constants K_{18}, $K_{19} > 0$ that for all $t \in [a,b]$ the following inequality holds

$$\left|v_0(t) - v_h(t)\right| \leqslant \frac{h}{\alpha(h)} K_{18} + \sigma(h) K_{19}.$$

4. The Upper Estimation, the Asymptotic Order of Accuracy

It is known that there exist constant $K_{20} > 0$ such that the lower estimation of accuracy D_h in $C[a,b]$ is of the form

$$v_1(h) \geqslant K_{20}\sqrt{h}$$

In view of lemmas 5, 11, the following estimate hold:

Theorem 1: (upper bound for the accuracy). Let condition $(*)$ hold and $\delta_1(h) = \frac{\lambda}{4}\delta(h)$. Then the upper bound for the accuracy in $C[a,b]$ is of the form:

$$v_2(h) \leqslant \frac{4K_7}{\lambda}\delta_1(h) + K_8\left(\frac{\alpha(h)}{\delta_1(h)}\right)^k + \alpha(h)K_9 + \frac{h}{\alpha(h)}K_{18} + \sigma(h)K_{19}.$$

Remark 1: Optimal on h the order of upper estimation of accuracy may be realized, at choice $\delta_1(h) = h^{\frac{k}{2k+1}}$, $\alpha(h) = h^{\frac{k+1}{2k+1}}$, $\sigma(h) = \alpha(h)$, hence $\gamma_0 = \frac{1}{2}$.

Remark 2: In our case the unknowing impact $u_*(\cdot)$ can be defined as $u_*(\cdot) = v_*(\cdot) + P_1(A(t,x(t)))u(a)$.

5. References

[1] Y. S. Osipov and A. V. Kryazhimskii, “Inverse Problems for Ordinary Differential Equations: Dynamical Solutions,” Gordon and Breach Science Publishers, London, 1995.

[2] A. Y. Vdovin and S. S. Rubleva, “On the Guaranteed Accuracy of a Dynamical Recovery Procedure for Controls with Bounded Variation in Systems Depending Linearly on the Control,” *Mathematical Notes*, Vol. 87, No. 3, 2010, pp. 316-335.

[3] A. Y. Vdovin, A. V. Kim and S. S. Rubleva, “On Asymptotic Accuracy in L1 of One Dynamical Algorithm for Reconstructing a Disturbance,” *Proceedings of the Steklov Institute of Mathematics*, Vol. 255, 2006, pp. 216-224.

[4] Y. S. Osipov, F. P. Vasilyev and M. M. Potapov, “Bases of the Method Dynamic Regulation,” in Russian, Moscow State University Press, Moscow, 1999.

[5] V. V. Voevodin and Y. A. Kuznetzov, “Matrixes and Calculations,” in Russian, Publishing House “Nauka”, Moscow, 1984.

[6] A. Albert, “Regression and the Moor–Penrose Pseudoinverse,” Academic Press, New York, 1972.

[7] P. A. Wedin, “Pertubation Theory for Pseudoinverces,” *BIT Numerical Mathematics*, Vol. 13, No. 2, 1973, pp. 217-232.

Applied Mathematics, **2010, 1, 124-127**
doi:10.4236/am.2010.12016 Published Online July 2010 (http://www.SciRP.org/journal/am)

Problem of Determining the Two-Dimensional Absorption Coefficient in a Hyperbolic-Type Equation

Durdimurat K. Durdiev
Bukhara State University, Bukhara, Uzbekistan
E-mail: *durdiev65@mail.ru*
Received March 25, 2010; *revised May* 16, 2010; *accepted May* 29, 2010

Abstract

The problem of determining the hyperbolic equation coefficient on two variables is considered. Some additional information is given by the trace of the direct problem solution on the hyperplane $x = 0$. The theorems of local solvability and stability of the solution of the inverse problem are proved.

Keywords: Inverse Problem, Hyperbolic Equation, Delta Function, Local Solvability

1. Statement of the Problem and the Main Results

We consider the generalized Cauchy problem

$$u_{tt} - u_{xx} - b(x, t)u_t = \delta(x, t - s), \quad (x, t) \in R^2, \ s > 0, \qquad u\big|_{t<0} \equiv 0, \tag{1}$$

where $\delta(x,t)$ is the two-dimensional Dirac delta function, $b(x,t)$ is a continuous function, s is a problem parameter, and $u(x,t,s)$. We pose the inverse problem as follows: it is required to find absorption coefficient $b(x,t)$ if the values of the solution for are known, *i.e.*, if the function

$$u(0,t,s) = f(t,s), \ t > 0, \ s > 0. \tag{2}$$

Definition. *A function* $b(x,t)$ *such that the solution of problem* (1) *corresponding to this function satisfies relation* (2) *is called a solution of inverse problem* (1), (2).

The inverse problem posed in this paper is two-dimensional. For the case where $b(x,t) = b(x)$ the solvability problems for different statements of problems close to (1), (2) were studied in [1] (Chapter 2) and [2] (Chapter 1). The solvability problems for multidimensional inverse problems were considered in [2] (Chapter 3), [3,4], where the local existence theorems were proved in the class of functions smooth one of the variables and analytic in the other variables. In [5], the problems of stability and global uniqueness were investigated for inverse problem of determining the nonstationary potential in hyperbolic-type equation. In this paper, we prove the local solvability theorem and stability of the solution of the inverse problem (1), (2).

Let

$$Q_T := \{(t,s) \,|\, 0 \le s \le t \le T\},$$

$$\Omega_T := \{(x,t) \,|\, 0 \le |x| \le t \le T - |x|\}, \ T > 0,$$

$C_t^1(Q_T)$ is the class of function continuous in s, continuously differentiable in t, and defined on Q_T. We let B denote the set of function $b(x,t)$ such that

$$b(x,t) \in C(\Omega_T), \ b(-x,t) = b(x,t).$$

Theorem 1. *If at a* $T > 0$ $f(t,s) \in C^1(Q_T)$ *and the condition*

$$f(s+0,s) = \frac{1}{2} \tag{3}$$

is met, then for all $T \in (0, T\_0)$, $T_0 = (1/40)\alpha_0$, $\alpha_0 = 4\left\| f_t^{'}(t,s) \right\|_{C(Q_T)}$ *the solution to the inverse problems* (1), (2) *in the class of function* $b(x,t) \in B$ *exists and is unique.*

Theorem 2. *Let the conditions in Theorem* 1 *hold for the functions* $f_k(t,s)$, $k = 1, 2,$ *and let* $b_k(x,t)$, $k = 1, 2,$ *be the solutions to the inverse problems with the data* $f_k(t,s)$, $k = 1, 2,$ *respectively. Then the following estimate is valid for* $T \in (0, T_0)$, $((T_0)$ *is defined in the same way as in proof of the Theorem* 1)

$$\left\| b_1(x,t) - b_2(x,t) \right\|_{C(\Omega_T)} \le \frac{4}{1-\rho} \left\| f_1(t,s) - f_2(t,s) \right\|_{C_t^1(Q_T)}, \tag{4}$$

where $\rho = \frac{T}{T_0}$.

2. Construction of a System Integral Equations for Equivalent Inverse Problems

We represent the solution of problem (1) as

$$u(x,t,s) = \frac{1}{2}\theta(t-s-|x|) + v(x,t,s). \quad (5)$$

where $\theta(t) = 1$ for $t \geq 0$, $\theta(t) = 0$, for $t < 0$, $v(x, t, s)$ is a some regular function.

We substitute the Expression (5) in (1), take into account that $\theta(t-s-|x|)/2$ satisfies (in the generalized sense) the equation $u_{tt} - u_{xx} = \delta(x)\delta'(t-s)$, and obtain the problem for the function v:

$$v_{tt} - v_{xx} = b(x,t)\left[\frac{1}{2}\delta(t-s-|x|) + v_t(x,t,s)\right], \quad (x,t) \in R^2, \quad s > 0, \quad v\big|_{t,0} \equiv 0. \quad (6)$$

It follows from the d'Alembert formula that the solution of problem (6) satisfies the integral equation

$$v(x,t,s) = \frac{1}{2}\iint_{\Delta(x,t)} b(\xi,\tau)\left[\frac{1}{2}\delta(\tau-s-|\xi|) + v_t(\xi,\tau,s)\right]\cdot d\xi d\tau, \ (x,t) \in R^2, \quad s > 0, \quad (7)$$

where $\Delta(x,t) = \{(\xi,\tau) | 0 \leq \tau \leq t - |x-\xi|, \ x-t \leq \xi \leq x+t\}$. We use the properties of the δ - function and easily obtain the relation in a different form:

$$v(x,t,s) = \frac{1}{4}\int_{\frac{x+(t-s)}{2}}^{\frac{x-(t-s)}{2}} b(\xi, s+|\xi|)d\xi + \frac{1}{2}\iint_{Y(x,t,s)} b(\xi,\tau)v_t(\xi,\tau,s)d\tau d\xi, \quad t-s \geq |x|, \quad (8)$$

where the domain $Y(x,t,s)$ is defined by

$$Y(x,t,s) = \left\{(\xi,\tau) \middle| |\xi| + s \leq \tau \leq t - |x-\xi|, \frac{x-(t-s)}{2} \leq \xi \leq \frac{x+t-s}{2}, 0 \leq s \leq t, \ s = const\right\}.$$

By differentiating the equality (8), we obtain

$$v_t(x,t,s) = \frac{1}{8}\left[b\left(\frac{x+t-s}{2}, \frac{x+t+s}{2}\right) + b\left(\frac{x-t+s}{2}, \frac{-x+t+s}{2}\right)\right]$$
$$\frac{1}{2}\int_{\frac{x-(t-s)}{2}}^{\frac{x+(t-s)}{2}} b(\xi, t-|x-\xi|)v_t(\xi, t-|x-\xi|, s)d\xi, \ t-s \geq |x|. \quad (9)$$

It is obvious that $f(t,s) = u(0,t,s) = \frac{1}{2} + v(0,t,s)$ for $t \geq 0$. Moreover, the function $f(t,s)$ be must satisfy the condition (9).

We set $x = 0$ in the equality (9), use the fact that the function $b(x,t)$ is even in x, and obtain the relation

$$f_t(t,s) = \frac{1}{4}b\left(\frac{t-s}{2}, \frac{t+s}{2}\right) + \int_{-\frac{t-s}{2}}^{\frac{t-s}{2}} b(\xi, t-\xi)v_t(\xi, t-\xi, s)d\xi, \quad (t,s) \in Q_T.$$

We rewrite this equality, replacing $(t-s)/2$ with $|x|$ and $(t+s)/2$ with t, and solve it for $b(x,t)$. We obtain

$$b(x,t) = 4f_t'(t+|x|, t-|x|) - 4\int_{-|x|}^{|x|} b(\xi, t+|x|-\xi)\cdot v_t(\xi, t+|x|-\xi, t-|x|)d\xi, \quad t \geq |x|. \quad (10)$$

Let

$$Y_T = \{(x,t,s) \| x| + s \leq t \leq T - |x|, 0 \leq s \leq t \leq T\}$$

The domain Y_T in the space of the variables $x, t,$ and s is a pyramid with the base Ω_t and vertex $(0, T, T/2)$. To find the value of the function b at (x,t), it is hence necessary to integrate $b(x,t)$ over the interval with the endpoints $(-|x|, t)$ and $(|x|, t)$ and to integrate the function $v_t(x,t,s)$ over the interval with the endpoints $(-|x|, t, t-|x|)$ and $(|x|, t, t-|x|)$, which belong to the domain Y_T.

One can rewrite the system of Equations (9) and (10) in the nonlinear operator form,

$$\psi = \mathrm{A}\psi, \quad (11)$$

where

$$\psi = \begin{bmatrix} \psi_1(x,t,s) \\ \psi_2(x,t) \end{bmatrix} = \begin{bmatrix} v_t(x,t,s) - \frac{1}{8}\left[b\left(\frac{x+t-s}{2}, \frac{x+t+s}{2}\right) + b\left(\frac{x-t+s}{2}, \frac{-x+t+s}{2}\right)\right] \\ b(x,t) \end{bmatrix}$$

The operator A is defined on the set of functions $\psi \in C[Y_T]$ and, according to (9), (10), has the form

$$A = (A_1,\ A_2),$$

where

$$A_1\psi = \frac{1}{2}\int_{\frac{x-(t-s)}{2}}^{\frac{x+(t-s)}{2}} \psi_2\left(\xi, t-|x-\xi|\right)\{\psi_1(\xi, t-|x-\xi|)$$

$$+\frac{1}{8}\left[\psi_2\left(\frac{\xi+t-|x-\xi|-s}{2}, \frac{\xi+t-|x-\xi|+s}{2}\right)\right.$$

$$\left.+\psi_2\left(\frac{\xi-t+|x-\xi|+s}{2}, \frac{-\xi+t-|x-\xi|+s}{2}\right)\right]\}d\xi,$$

$$A_2\psi = 4f_t'(t+|x|,\ t-|x|) - 4\int_{-|x|}^{|x|} \psi_2(\xi, t+|x|-\xi)\cdot$$

$$\left\{\psi_1(\xi, t+|x|-\xi, t-|x|) + \frac{1}{8}\left[\psi_2\left(|x|, t\right)\right.\right.$$

$$\left.\left.+\psi_2\left(\xi-|x|, t-\xi\right)\right]\right\}\mathrm{d}\xi.$$

At fulfillment of the condition (3) the inverse problem (1), (2) is equivalent to the operator Equation (11).

3. Proofs of the Theorems

Define

$$\|\psi\|_T = \max\left(\|\psi_1\|_{C(Y_T)},\quad \|\psi_2\|_{C(\Omega_T)}\right).$$

Let s be the set of $\psi \in C(Y_T)(\Omega_T \subset Y_T)$ that satisfy the following conditions:

$$\|\psi - \psi^0\|_T \le \|\psi^0\|_T,$$

where $\psi^0 = (\psi_{01},\ \psi_{02}) = (0,\ 4f_t'(t+|x|, t-|x|)$. It is obviously, that $\|\psi^0\|_T \le 4\|f_t'(t,s)\|_{C(Q_T)} = \alpha_0\ (Q_T \subset Y_T)$. Now we can show that if T is small enough, A is a contraction mapping operator in S. The local theorem of existence and uniqueness then follows immediately from the contraction mapping principle. First let us prove that A has the first property of a contraction mapping operator, *i.e.*, if $\psi \in S$, then $A\psi \in S$ when T is small enough. Let $\psi \in S$. It is then easy to see that

$$\|\psi\|_T \le \|\psi - \psi^0\|_T + \|\psi^0\|_T \le 2\alpha_0.$$

Furthermore, one has

$$|A_1\psi - \psi_{01}| \le \frac{1}{2}\int_{\frac{x-(t+s)}{2}}^{\frac{x+(t+s)}{2}} \left|\psi_2\left(\xi, t-|x-\xi|\right)\right|$$

$$\times\left\{\left|\psi\left(\xi, t-|x-\xi|, s\right)\right| + \frac{1}{8}\left[\left|\psi_2\left(\frac{\xi+t-|x-\xi|-s}{2},\right.\right.\right.\right.$$

$$\left.\left.\frac{\xi+t-|x-\xi|+s}{2}\right)\right| + \left|\psi_2\left(\frac{\xi-t+|x-\xi|+s}{2},\right.\right.$$

$$\left.\left.\left.\left.\frac{-\xi+t-|x-\xi|+s}{2}\right)\right|\right]\right\}d\xi \le \frac{5T}{8}\alpha_0\|\psi^0\|_T^2,$$

$$|A_2\psi - \psi_{02}| \le 4\int_{-|x|}^{|x|} \left|\psi_2\left(\xi\textit{б}, t+|x|-\xi\right)\right|$$

$$\times\left\{\left|\psi_1\left(\xi, t+|x|-\xi, t-|x|\right)\right| + \frac{1}{8}\left[\left|\psi_2\left(|x|, t\right)\right|\right.\right.$$

$$\left.\left.+\left|\psi_2\left(\xi-|x|, t-\xi\right)\right|\right]\right\}d\xi \le 10T\alpha_0\|\psi^0\|_T^2.$$

Therefore, if $T^* = 1/10\alpha_0$, then for $T \in (0, T_0)$ the operator A satisfies the condition $A\psi \in S$. Consider next the second property of contraction mapping operator for A *i.e.*, if $\psi^{(1)} \in S$, $\psi^{(2)} \in S$, then $\|A\psi^{(1)} - A\psi^{(1)}\| \le \rho\|\psi^{(1)} - \psi^{(1)}\|$ with $\rho < 1$, when T is small enough. Let $\psi^{(1)} \in S, \psi^{(2)} \in S$. Then one has

$$\left|A_1\psi^{(1)} - A_1\psi^{(2)}\right| \le \frac{1}{2}\left|\int_{\frac{x-(t+s)}{2}}^{\frac{x+(t+s)}{2}}\left\{\left(\psi_2^{(1)} - \psi_2^{(2)}\right)\left(\xi, t-|x-\xi|\right)\right.\right.$$

$$\left\{\psi_2^{(1)}\left(\xi, t-|x-\xi|, s\right) + \frac{1}{8}\left[\psi^{(1)}{}_2\left(\frac{\xi+t-|x-\xi|-s}{2},\right.\right.\right.$$

$$\left.\frac{\xi+t-|x-\xi|+s}{2}\right) + \psi^{(1)}{}_2\left(\frac{\xi-t+|x-\xi|+s}{2},\right.$$

$$\left.\left.\left.\frac{-\xi+t-|x-\xi|+s}{2}\right)\right]\right\} + \psi_2^{(2)}\left(\xi, t-|x-\xi|, s\right)$$

$$\times\left\{\left(\psi_1^{(1)} - \psi_1^{(2)}\right)\left(\xi, t-|x-\xi|, s\right) + \frac{1}{8}\left[\left(\psi_2^{(1)} - \psi_2^{(2)}\right)\right.\right.$$

$$\left(\frac{\xi+t-|x-\xi|-s}{2}, \frac{\xi+t-|x-\xi|+s}{2}\right)$$

$$+\left(\psi_2^{(1)}-\psi_2^{(2)}\right)$$

$$\left(\frac{\xi-t+|x-\xi|+s}{2},\frac{-\xi+t-|x-\xi|+s}{2}\right)\Big]\Big]\Big\}$$

$$d\xi\Big|\le\frac{5T}{2}\alpha_0\left\|\psi^{(1)}-\psi^{(2)}\right\|_T,$$

$$\left|A_2\psi^{(1)}-A_2\psi^{(2)}\right|\le 4\left|\int_{-|x|}^{|x|}\left\{\left(\psi_2^{(1)}-\psi_2^{(2)}\right)\right.\right.$$

$$(\xi,t+|x|-\xi)\ \left\{\psi_1^{(1)}(\xi,t+|x|-\xi,t-|x|)\right.$$

$$\left.+\frac{1}{8}\left[\psi_2^{(1)}(|x|,t)+\psi_2^{(1)}(\xi-|x|,t-\xi)\right]\right\}$$

$$+\psi_2^{(2)}(\xi,t+|x|-\xi)\times\left\{\left(\psi_1^{(1)}-\psi_1^{(2)}\right)\right.$$

$$(\xi,t+|x|-\xi,t-|x|)+\frac{1}{8}\left[\left(\psi_2^{(1)}-\psi_2^{(1)}\right)\right.$$

$$\left.\left.\left.(|x|,t)+\left(\psi_2^{(1)}-\psi_2^{(1)}\right)(\xi-|x|,t-\xi)\right]\right\}\right\}$$

$$d\xi\Big|\le 40T\alpha_0\left\|\psi^{(1)}-\psi^{(2)}\right\|_T.$$

It follows from the preceding estimates that if $T_0=1/40\,\alpha_0$, then for $T\in(0,T_0)$ the operator A is a contraction operator with $\rho=T/T_0$ on the set *S*. Therefore, the Equation (11) has a unique solution which belongs to *S* according to the contraction mapping principle. The solution is the limit of the sequence $\psi^{[n]}$, $n=0,1,2,...,$ where $\psi^{[0]}=\psi(0)$, $\psi^{[n+1]}=A\psi^{[n]}$, and the series

$$\psi^{[0]}+\sum_{n=0}^{\infty}\left(\psi^{[n+1]}-\psi^{[n]}\right)$$

converges not slower than the series

$$\left\|\psi^{[0]}\right\|_T+\sum_{n=0}^{\infty}\rho^n\left\|\psi^{[1]}-\psi^{[0]}\right\|_T$$

We now prove Theorem 2. Since the conditions Theorem 1 hold, the solution belong to the set *S* and $\|\psi_i\|_T\le 2\alpha_0$, $i=1,2.$ Let $\psi^{(k)}$, $k=1,2$ be vector functions which are the solution of the Equation (11) with the data $f_k(t,s)$, $k=1,2,$ respectively, *i.e.*,

$$\psi^{(k)}=A\psi^{(k)}$$

From the previous results in the proof of Theorem 1, it follows that

$$\left|\psi_1^{(k)}-\psi_2^{(k)}(x,t,s)\right|\le 4\left\|f_1(t,s)-f_2(t,s)\right\|_{C_t^1(Q_T)}$$

$$+40T\alpha_0\left\|\psi_1-\psi_2\right\|_T,\ k=1,2.$$

Therefore, one has

$$\left\|\psi_1-\psi_2\right\|_T\le 4\left\|f_1(t,s)-f_2(t,s)\right\|_{C_t^1(Q_T)}+\rho\left\|\psi_1-\psi_2\right\|_T$$

The last inequality gives

$$\left\|\psi_1-\psi_2\right\|_T\le\frac{4}{1-\rho}\left\|f_1(t,s)-f_2(t,s)\right\|_{C_t^1(Q_T)}\qquad(12)$$

The stability estimate (4) follows from the inequality (12).

4. References

[1] V. G. Romanov, "Inverse Problems of Mathematical Physics," in Russian, Publishing House "Nauka", Moscow, 1984.

[2] V. G Romanov, "Stability in Inverse Problems," in Russian, Nauchnyi Mir, Moscow, 2005.

[3] D. K. Durdiev, "A Multidimensional Inverse Problem for an Equation with Memory," *Siberian Mathematical Journal*, Vol. 35, No. 3, 1994, pp. 514-521.

[4] D. K. Durdiev, "Some Multidimensional Inverse Problems of Memory Determination in Hyperbolic Equations," *Journal of Mathematical Physics, Analysis, Geometry*, Vol. 3, No. 4, 2007, pp. 411-423.

[5] D. K. Durdiev, "Problem of Determining the Nonstationary Potential in a Hyperbolic-Type Equation," *Journal of Theoretical and Mathematical Physics,* Vol. 2, No. 156, 2008, pp. 1154-1158.

Applied Mathematics, **2010, 1, 128-136**
doi:10.4236/am.2010.12017 Published Online July 2010 (http://www. SciRP.org/journal/am)

Vibration of Visco-Elastic Parallelogram Plate with Parabolic Thickness Variation

Arun Kumar Gupta*, Anuj Kumar, Yogesh Kumar Gupta
Maharaj Singh College, Saharanpur, India
E-mail: *gupta_arunnitin@yahoo.co.in*
Received April 7, 2010; *revised May* 10, 2010; *accepted May* 17, 2010

Abstract

The main objective of the present investigation is to study the vibration of visco-elastic parallelogram plate whose thickness varies parabolically. It is assumed that the plate is clamped on all the four edges and that the thickness varies parabolically in one direction *i.e*. along length of the plate. Rayleigh-Ritz technique has been used to determine the frequency equation. A two terms deflection function has been used as a solution. For visco-elastic, the basic elastic and viscous elements are combined. We have taken Kelvin model for visco-elasticity that is the combination of the elastic and viscous elements in parallel. Here the elastic element means the spring and the viscous element means the dashpot. The assumption of small deflection and linear visco-elastic properties of "Kelvin" type are taken. We have calculated time period and deflection at various points for different values of skew angles, aspect ratio and taper constant, for the first two modes of vibration. Results are supported by tables. Alloy "Duralumin" is considered for all the material constants used in numerical calculations.

Keywords: Vibration, Parallelogram Plate, Visco-Elastic Mechanics, Parabolic Thickness, Aspect Ratio

1. Introduction

The materials are being developed, depending upon the requirement and durability, so that these can be used to give better strength, flexibility, weight effectiveness and efficiency. So some new materials and alloys are utilized in making structural parts of equipment used in modern technological industries like space craft, jet engine, earth quake resistance structures, telephone industry etc. Applications of such materials are due to reduction of weight and size, low expenses and enhancement in effectiveness and strength. It is well known that first few frequencies of structure should be known before finalizing the design of a structure. The study of vibration of skew plate structures is important in a wide variety of applications in engineering design. Parallelogram elastic plates are widely employed nowadays in civil, aeronautical and marine structures designs. Complex shapes with variety of thickness variation are sometimes incorporated to reduce costly material, lighten the loads, and provide ventilation and to alter the resonant frequencies of the structures. Dynamic behavior of these structures is strongly dependent on boundary conditions, geometric shapes, material properties etc.

Dhotarad and Ganesan [1] have considered vibration analysis of a rectangular plate subjected to a thermal gradient. Amabili and Garziera [2] have studied transverse vibrations of circular, annular plates with several combinations of boundary conditions. Ceribasi and Altay [3] introduced the free vibration analysis of super elliptical plates with constant and variable thickness by Ritz method. Gupta, Ansari and Sharma [4] have analyzed vibration analysis of non-homogenous circular plate of non linear thickness variation by differential quadrature method. Jain and Soni [5] discussed free vibrations of rectangular plates of parabolically varying thickness. Singh and Saxena [6] discussed the transverse vibration of rectangular plate with bi-directional thickness. Free vibrations of non-homogeneous circular plate of variable thickness resting on elastic foundation are discussed by Tomar, Gupta and Kumar [7]. Yang [8] has considered the vibration of a circular plate with varying thickness. Gupta, Ansari and Sharma [9] discussed the vibration of non-homogeneous circular Mindlin plates with variable thickness. Bambill, Rossit, Laura and Rossi [10] have analyzed transverse vibration of an orthotropic rectangular plate of linearly varying thickness with a free edge.

Sufficient work [11,12] is available on the vibration of a rectangular plate of variable thickness in one direction, but none of them done on parallelogram plate. Recently Gupta, Kumar and Gupta [13] studied the vibration of visco-elastic parallelogram plate of linearly varying thickness. A simple model presented here is to study the effect of parabolic thickness variation on vibration of visco-elastic parallelogram plate having clamped boundary conditions on all the four edges. The hypothesis of small deflection and linear visco-elastic properties are made. Using the separation of variables method, the governing differential equation has been solved for vibration of visco-elastic parallelogram plate. An approximate but quite convenient frequency equation is derived by using Rayleigh-Ritz technique with a two-term deflection function. It is assumed that the visco-elastic properties of the plate are of the "Kelvin Type". Time period and deflection function at different point for the first two modes of vibration are calculated for various values of taper constant, aspect ratio and skew angle and results are presented in tabular form.

2. Equation of Transverse Motion

The parallelogram (skew) plate is assumed to be non-uniform, thin and isotropic and the plate R be defined by the three number a, b and θ as shown in **Figure 1**.

The skew coordinates are related to rectangular coordinates are

$$\xi = x - y\tan\theta, \eta = y\sec\theta$$

The boundaries of the plate in skew coordinates are

$$\xi = 0, \xi = a, \eta = 0, \eta = b$$

The governing differential equation of transverse motion of visco-elastic parallelogram plate of variable thickness, ξ- and η- coordinates is given by [13]:

$$T_{max} = \frac{1}{2}\rho p^2 \cos\theta \iint hW^2 d\xi d\eta \tag{1}$$

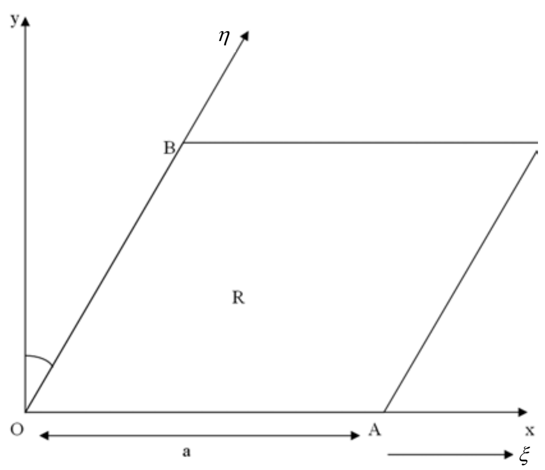

Figure 1. Geometry of parallelogram plate.

and

$$V = \frac{1}{2}\cos\theta \iint D\Big[(\nabla^2 W)^2 - 2(1-\nu)\cdot \sec^2\theta (W_{,\xi\xi} W_{,\eta\eta} - W_{,\xi\eta}^2)\Big] d\xi d\eta$$

or

$$V = \frac{1}{2\cos^3\theta}\iint D\Big[W_{,\xi\xi}{}^2 - 4\sin\theta W_{,\xi\xi}W_{,\xi\eta} + 2(\sin^2\theta + \nu\cos^2\theta)W_{,\xi\xi}W_{,\eta\eta} + 2(1+\sin^2\theta - \nu\cos^2\theta)\cdot W_{,\xi\eta}{}^2 - 4\sin\theta W_{,\xi\eta}W_{,\eta\eta} + W_{,\eta\eta}{}^2\Big] d\xi d\eta \tag{2}$$

and

$$T_{,tt} + p^2 \check{D} T = 0 \tag{3}$$

A comma followed by a suffix denotes partial differential with respect to that variable. Here p^2 is a constant.

Here solution $w(\xi, \eta, t)$ can be taken in the form of products of two functions as for free transverse vibration of the parallelogram plate so that

$$w(\xi, \eta, t) = W(\xi, \eta)T(t) \tag{4}$$

where $T(t)$ is the time function and W is the maximum displacement with respect to time t.

Assuming thickness variation of parallelogram plate parabolically in ξ-direction as

$$h = h_0\{1 + \beta(\xi / a)^2\} \tag{5}$$

where β is the taper constant in ξ-direction and $h_0 = h\big|_{\xi=0}$.

The flexural rigidity D of the plate can now be written as

$$D = Eh_0^3(1 + \beta(\xi / a)^2)^3 / 12(1 - \nu^2), \tag{6}$$

3. Solution and Frequency Equation

In using the Rayleigh-Ritz technique, one requires maximum strain energy be equal to the maximum kinetic energy. So it is necessary for the problem consider here that

$$\delta(V - T_{\max}) = 0 \tag{7}$$

for arbitrary variations of W satisfying relevant geometrical boundary conditions.

For a parallelogram plate, clamped (c) along all the four edges, the boundary conditions are

$$\begin{aligned} W = W_{,\xi} = 0 \ \ at \ \ \xi = 0, \ a \ \ and \\ W = W_{,\eta} = 0 \ \ at \ \ \eta = 0, b \end{aligned} \tag{8}$$

and the corresponding two-term deflection function is taken as

$$W = \left[(\xi/a)(\eta/b)(1-\xi/a)(1-\eta/b)\right]^2 \cdot \left[A_1 + A_2(\xi/a)(\eta/b)(1-\xi/a)(1-\eta/b)\right] \tag{9}$$

Using Equations (5) and (6) in Equations (1) and (2), one obtains

$$T_{\max} = \frac{1}{2} h_0 \rho p^2 \cos\theta \int_{\eta=0}^{b}\int_{\xi=0}^{a} (1+\beta(\frac{\xi}{a})^2) W^2 d\xi d\eta \tag{10}$$

and

$$V = \frac{Eh_0^3}{24(1-\nu^2)\cos^3\theta} \int_{\eta=0}^{b}\int_{\xi=0}^{a} (1+\beta(\frac{\xi}{a})^2)^3 \Big[W_{,\xi\xi}{}^2 - 4(\frac{a}{b}) \cdot \sin\theta W_{,\xi\xi} W_{,\xi\eta} + 2(\frac{a}{b})^2(\sin^2\theta + \nu\cos^2\theta) W_{,\xi\xi} W_{,\eta\eta} + 2(\frac{a}{b})^2(1+\sin^2\theta - \nu\cos^2\theta) W_{,\xi\eta}{}^2 - 4(\frac{a}{b})^3 \cdot \sin\theta W_{,\xi\eta} W_{,\eta\eta} + (\frac{a}{b})^4 W_{,\eta\eta}{}^2 \Big] d\xi d\eta \tag{11}$$

Using Equations (10) and (11) in Equation (7), one obtains

$$(V_1 - \lambda^2 p^2 T_1) = 0 \tag{12}$$

where

$$V_1 = \int_{\eta=0}^{b}\int_{\xi=0}^{a} (1+\beta(\frac{\xi}{a})^2)^3 \Big[W_{,\xi\xi}{}^2 - 4(\frac{a}{b}) \cdot \sin\theta W_{,\xi\xi} W_{,\xi\eta} + 2(\frac{a}{b})^2(\sin^2\theta + \nu\cos^2\theta) W_{,\xi\xi} W_{,\eta\eta} + 2(\frac{a}{b})^2(1+\sin^2\theta - \nu\cos^2\theta) W_{,\xi\eta}{}^2 - 4(\frac{a}{b})^3 \sin\theta W_{,\xi\eta} W_{,\eta\eta} + (\frac{a}{b})^4 W_{,\eta\eta}{}^2 \Big] d\xi d\eta \tag{13}$$

and

$$T_1 = \cos^4\theta \int_0^b\int_0^a (1+\beta(\frac{\xi}{a})^2) W^2 d\xi d\eta \tag{14}$$

Here,

$$\lambda^2 = \frac{12 a^4 \rho (1-\upsilon^2)}{E h_0^2} \tag{15}$$

is a constant.

But Equation (12) involves the unknown A_1 and A_2 arising due to the substitution of $W(\xi, \eta)$ from Equation (9). These two constants are to be determined from Equation (12), as follows:

$$\partial(V_1 - \lambda^2 p^2 T_1)/\partial A_n = 0, \quad n = 1,2 \tag{16}$$

Equation (16) simplifies to the form

$$b_{n1}A_1 + b_{n2}A_1 = 0, \quad n = 1,2 \tag{17}$$

where b_{n1}, b_{n2} (n =1,2) involve parametric constants and the frequency parameter.

For a non-trivial solution, the determinant of the coefficient of Equation (17) must be zero. So one gets the frequency equation as

$$\begin{vmatrix} b_{11} & b_{12} \\ b_{21} & b_{22} \end{vmatrix} = 0 \tag{18}$$

Here,

$$b_{11} = (F_1 - \lambda^2 p^2 B_1),$$

$$b_{12} = b_{21} = (F_2 - \lambda^2 p^2 B_2),$$

and $$b_{22} = (F_3 - \lambda^2 p^2 B_3)$$

where F_1, F_2, F_3, B_1, B_2, B_3 involves parametric constants, skew angle and aspect ratio and given as

$$F_1 = I_1 + 2(\frac{a}{b})^2(\sin^2\theta + \nu\cos^2\theta)I_2 + 2(\frac{a}{b})^2(1+\sin^2\theta - \nu\cos^2\theta)I_3 + (\frac{a}{b})^4 I_4,$$

$$B_1 = \cos^4\theta I_5,$$

$$F_2 = I_6 + 2(\frac{a}{b})^2(\sin^2\theta + \nu\cos^2\theta)I_7 + 2(\frac{a}{b})^2(1+\sin^2\theta - \nu\cos^2\theta)I_8 + (\frac{a}{b})^4 I_9,$$

$$B_2 = \cos^4\theta I_{10},$$

$$F_3 = I_{11} + 2(\frac{a}{b})^2(\sin^2\theta + \nu\cos^2\theta)I_{12} + 2(\frac{a}{b})^2(1+\sin^2\theta - \nu\cos^2\theta)I_{13} + (\frac{a}{b})^4 I_{14},$$

$$B_3 = \cos^4\theta I_{15},$$

Here,

$$I_1 = \frac{2}{1575} + \frac{16}{11025}\beta + \frac{4}{3675}\beta^2 + \frac{113}{363825}\beta^3,$$

$$I_2 = \frac{4}{11025} + \frac{1}{3675}\beta + \frac{8}{121275}\beta^2 + \frac{2}{675675}\beta^3,$$

$$I_3 = \frac{4}{11025} + \frac{1}{3675}\beta + \frac{8}{121275}\beta^2 + \frac{2}{675675}\beta^3,$$

$$I_4 = \frac{2}{1575} + \frac{2}{1925}\beta + \frac{4}{10725}\beta^2 + \frac{4}{75075}\beta^3,$$

$$I_5 = \frac{1}{396900} + \frac{1}{1455300}\beta,$$

$$I_6 = \frac{1}{8085} + \frac{1}{5390}\beta + \frac{4}{53361}\beta^2 + \frac{37}{1981980}\beta^3,$$

$$I_7 = \frac{1}{22050} + \frac{4}{121275}\beta + \frac{1}{150150}\beta^2 + \frac{1}{194040}\beta^3,$$

$$I_8 = \frac{1}{22050} + \frac{1}{23100}\beta + \frac{1}{42900}\beta^2 + \frac{1}{210210}\beta^3,$$
$$I_9 = \frac{1}{8085} + \frac{1}{10010}\beta + \frac{6}{175175}\beta^2 + \frac{1}{216580}\beta^3,$$
$$I_{10} = \frac{1}{3841992} + \frac{1}{14270256}\beta,$$
$$I_{11} = \frac{1}{210210} + \frac{1}{220220}\beta + \frac{5}{2004002}\beta^2 + \frac{17}{30060030}\beta^3,$$
$$I_{12} = \frac{1}{592900} + \frac{19}{15415400}\beta + \frac{1}{3853850}\beta^2 + \frac{3}{524123600}\beta^3,$$
$$I_{13} = \frac{1}{592900} + \frac{3}{1926925}\beta + \frac{3}{3853850}\beta^2 + \frac{3}{20158600}\beta^3,$$
$$I_{14} = \frac{1}{210210} + \frac{2}{525525}\beta + \frac{3}{2382380}\beta^2 + \frac{1}{6172530}\beta^3,$$
$$I_{15} = \frac{1}{144288144} + \frac{1}{541080540}\beta,$$

From Equation (18), one can obtains a quadratic equation in p^2 from which the two values of p^2 can found. After determining A_1 & A_2 from Equation (17), one can obtain deflection function W. Choosing $A_1 = 1$, one obtains $A_2 = (-b_{11}/b_{12})$ and then W comes out as

$$W = \left[XY(a/b)(1-X)(1-Y\,a/b)\right]^2 \left[1+(-b_{11}/b_{12})XY(a/b)(1-X)(1-Y\,a/b)\right]. \tag{19}$$

Here

$$X = \xi/a \quad and \quad Y = \eta/a.$$

4. Differential Equation of Time Function and its Solution

Time functions of free vibrations of viscoelastic plates are defined by the general ordinary differential Equation (3). Their form depends on the viscoelastic operator $\check{D}$. For Kelvin's model, one has

$$\check{D} = \left\{1+(\check{n}/G)(d/dt)\right\} \tag{20}$$

where, $\check{n}$ is viscoelastic constant and G is shear modulus.

The governing differential equation of time function of a parallelogram plate of variable thickness, by using Equation (20) in Equation (3), one obtains as

$$T_{,tt} + p^2(\check{n}/G)T_{,t} + p^2 T = 0 \tag{21}$$

Equation (21) is a differential equation of order two for time function T. Solution of Equation (21) comes out as

$$T(t) = e^{kt}(C_1\cos k_1 t + C_1 \sin k_1 t) \tag{22}$$

where,

$$k = -p^2\,\check{n}/2G \tag{23}$$

and

$$k_1 = p\left\{1-(p\check{n}/2G)^2\right\}^{1/2} \tag{24}$$

Let us take initial conditions as

$$T = 1 \quad \text{and} \quad dT/dt = 0 \quad \text{at} \quad t = 0 \tag{25}$$

Using initial conditions from Equation (25) in Equation (22), one obtains

$$T(t) = e^{kt}\left[\cos(k_1 t) + (-k/k_1)\sin(k_1 t)\right] \tag{26}$$

Thus, deflection w may be expressed, by using Equations (26) and (19) in Equation (4), to give

$$W = \left[XY(a/b)(1-X)(1-Y\,a/b)\right]^2 \cdot \left[1+(-b_{11}/b_{12})XY(a/b)(1-X)(1-Y\,a/b)\right] \cdot \left[e^{kt}\left\{\cos(k_1 t)\right\} + (-k/k_1)\sin(k_1 t)\right] \tag{27}$$

Time period of vibration of the plate is given by

$$K = 2\pi/p, \tag{28}$$

where p is frequency given by Equation (18).

5. Results and Discussion

Time period and deflection are computed for visco-elastic parallelogram plate, whose thickness varies parabolically, for different value of skew angle (θ), taper constant (β), and aspect ratio (a/b) at different points for first two mode of vibration. The material parameters have been taken as [14]: $E = 7.08 \times 10^{10}$ n/m^2, $G = 2.682 \times 10^{10}$ n/m^2, $\check{n} = 1.4612 \times 10^6$ n.s/m^2, $\rho = 2.80 \times 10^3$ kg/m^3, $\nu = 0.345$ and $h_0 = 0.01$ meter.

All the results are presented in the **Tables 1-11**.

The value of time period (K) for $\beta = 0.6$, $\theta = 45^\circ$ have been found to decrease 35.89% for first mode and 34.74% for second mode in comparison to rectangular plate at fixed aspect ratio ($a/b = 1.5$).

The value of time period (K) for $\beta = 0.6$, $\theta = 45^\circ$ have been found to decrease 20.54% for first mode and 21.23% for second mode in comparison to parallelogram plate of uniform thickness at fixed aspect ratio ($a/b = 1.5$) .

Table 1 shows the results of time period (K) for different values of taper constant (β) and fixed aspect ratio ($a/b = 1.5$) for two values of skew angle (θ) *i.e.* $\theta = 0^\circ$ and $\theta = 45^\circ$ for first two mode of vibration. It can be seen that the time period (K) decrease when taper constant (β) increase for first two mode of vibration.

Table 2 shows the results of time period (K) for different values of skew angle (θ) and fixed aspect ratio (a/b = 1.5) for two values of taper constant (β) *i.e.* β = 0.0, β = 0.2 for first two mode of vibration. It can be seen that the time period (K) decrease when skew angle (θ) increase for first two mode of vibration. .

Table 3 shows the results of time period (K) for different values of aspect ratio (a/b) and fixed taper constant (β = 0.0 and β = 0.6) for two values of skew angle (θ) *i.e.* $\theta = 0^\circ$ and $\theta = 45^\circ$ for first two mode of vibration. It can be seen that the time period (K) decrease when aspect ratio (a/b) increase for first two mode of vibration.

The value of deflection (w) for β = 0.6 and $\theta = 45^\circ$ have been found to increase 14.19% for first mode and 1.07% for second mode in comparison to parallelogram plate of uniform thickness for initial time 0.K at X = 0.2, Y = 0.4 and a/b = 1.5.

The value of deflection (w) for β = 0.6 and $\theta = 45^\circ$ have been found to decrease 4.76% for first mode and 0.53% for second mode in comparison to rectangular plate for initial time 0.K at X = 0.2, Y = 0.4 and a/b = 1.5.

The value of deflection (w) for β = 0.6 and $\theta = 45^\circ$ have been found to increase 11.91% for first mode and decrease 6.03% for second mode in comparison to parallelogram plate of uniform thickness for time 5.K at X = 0.2, Y = 0.4 and a/b = 1.5.

The value of deflection (w) for β = 0.6 and $\theta = 45^\circ$ have been found to decrease 7.91% for first mode and 11.96% for second mode in comparison to rectangular plate for time 5.K at X = 0.2, Y = 0.4 and a/b = 1.5.

Tables 4-11 show the results of deflection (w) for different values of X, Y and fixed taper constant (β = 0.0 and β = 0.6), and aspect ratio (a/b = 1.5) for two values of skew angle (θ) *i.e.* $\theta = 0^\circ$ and $\theta = 45^\circ$ for first two mode of vibration with time 0.K and 5.K. It can be seen that deflection (w) start from zero to increase then decrease to zero for first two mode of vibration (except second mode at Y = 0.2 and 0.4) and second mode of vibration deflection (w) at (Y = 0.2 and Y = 0.4) start zero to increase, decrease, increase, decrease and finally become to zero for different value of X.

6. Conclusions

The Rayleigh-Ritz technique has been applied to study the effect of the taper constants on the vibration of clamped visco-elastic isotropic parallelogram plate with parabolically varying thickness on the basis of classical plate theory.

Table 1. Time period K (in second) for different taper constant (β) and a constant aspect ratio (a/b = 1.5).

β	$\theta = 0^\circ$		$\theta = 45^\circ$	
	First Mode	**Second Mode**	**First Mode**	**Second Mode**
0.0	0.142648	0.036357	0.090306	0.023976
0.2	0.131780	0.033664	0.084639	0.022199
0.4	0.121820	0.030664	0.078029	0.020376
0.6	0.112958	0.028060	0.072148	0.018465
0.8	0.104063	0.025895	0.067140	0.017093

Table 2. Time period K (in second) for different skew angle (θ) and a constant aspect ratio (a/b = 1.5).

θ	β = 0.0		β = 0.2	
	First Mode	**Second Mode**	**First Mode**	**Second Mode**
0°	0.142648	0.036357	0.131780	0.033664
15°	0.137773	0.035762	0.127248	0.032985
30°	0.121041	0.031427	0.112004	0.029016
45°	0.090306	0.023976	0.084639	0.022199
60°	0.051089	0.013211	0.047425	0.012143
75°	0.014111	0.003431	0.013235	0.003491

Table 3. Time period K (in second) for different aspect ratio (a/b).

a/b	$\beta = 0.0, \theta = 0^\circ$		$\beta = 0.0, \theta = 45^\circ$		$\beta = 0.6, \theta = 0^\circ$		$\beta = 0.6, \theta = 45^\circ$	
	First Mode	**Second Mode**	**First Mode**	**Second Mode**	**First Mode**	**Second Mode**	**First Mode**	**Second Mode**
0.5	0.172515	0.042510	0.1189167	0.029103	0.133024	0.032025	0.091918	0.022024
1.0	0.159377	0.040155	0.106213	0.027055	0.124312	0.030879	0.083221	0.020997
1.5	0.142648	0.036357	0.090306	0.023976	0.112958	0.028060	0.072148	0.018465
2.0	0.125147	0.033092	0.075399	0.020193	0.100177	0.026135	0.061061	0.016145
2.5	0.108096	0.028951	0.061982	0.016358	0.087268	0.023080	0.050393	0.013274

Table 4. Deflection *w* for different *X*, *Y* and β = 0.0, θ = 0˚ and *a*/*b* = 1.5 at initial time 0.K.

X	Y = 0.2		Y = 0.4		Y = 0.6		Y = 0.8	
	First Mode	**Second Mode**	**First Mode**	**Second Mode**	**First Mode**	**Second Mode**	**First Mode**	**Second Mode**
0.0	0.000000	0.000000	0.000000	0.000000	0.000000	0.000000	0.000000	0.000000
0.2	0.001085	0.000390	0.001411	0.000371	0.000201	0.000145	0.001533	0.002571
0.4	0.002398	0.000055	0.003102	–0.000385	0.000452	0.000268	0.003522	0.007022
0.6	0.002398	0.000055	0.003102	–0.000385	0.000452	0.000268	0.003522	0.007022
0.8	0.001085	0.000390	0.001411	0.000371	0.000201	0.000145	0.001533	0.002571
1.0	0.000000	0.000000	0.000000	0.000000	0.000000	0.000000	0.000000	0.000000

Table 5. Deflection *w* for different *X*, *Y* and β = 0.0, θ = 45˚ and *a*/*b* = 1.5 at initial time 0.K.

X	Y = 0.2		Y = 0.4		Y = 0.6		Y = 0.8	
	First Mode	**Second Mode**	**First Mode**	**Second Mode**	**First Mode**	**Second Mode**	**First Mode**	**Second Mode**
0.0	0.000000	0.000000	0.000000	0.000000	0.000000	0.000000	0.000000	0.000000
0.2	0.001055	0.000390	0.001365	0.000372	0.000201	0.000146	0.001580	0.002571
0.4	0.002296	0.000051	0.002953	–0.000392	0.000444	0.000270	0.003679	0.007028
0.6	0.002296	0.000051	0.002953	–0.000392	0.000444	0.000270	0.003679	0.007028
0.8	0.001055	0.000390	0.001365	0.000372	0.000201	0.000146	0.001580	0.002571
1.0	0.000000	0.000000	0.000000	0.000000	0.000000	0.000000	0.000000	0.000000

Table 6. Deflection *w* for different *X*, *Y* and β = 0.6, θ = 0˚ and *a*/*b* = 1.5 at initial time 0.K.

X	Y = 0.2		Y = 0.4		Y = 0.6		Y = 0.8	
	First Mode	**Second Mode**	**First Mode**	**Second Mode**	**First Mode**	**Second Mode**	**First Mode**	**Second Mode**
0.0	0.000000	0.000000	0.000000	0.000000	0.000000	0.000000	0.000000	0.000000
0.2	0.001233	0.000392	0.001634	0.000380	0.000212	0.000150	0.001310	0.002565
0.4	0.002910	0.000063	0.003870	–0.000371	0.000493	0.000271	0.002760	0.007007
0.6	0.002910	0.000063	0.003870	–0.000371	0.000493	0.000271	0.002760	0.007007
0.8	0.001233	0.000392	0.001634	0.000380	0.000212	0.000150	0.001310	0.002565
1.0	0.000000	0.000000	0.000000	0.000000	0.000000	0.000000	0.000000	0.000000

Table 7. Deflection *w* for different *X*, *Y* and β = 0.6, θ = 45˚ and *a*/*b* = 1.5 at initial time 0.K.

X	Y = 0.2		Y = 0.4		Y = 0.6		Y = 0.8	
	First Mode	**Second Mode**	**First Mode**	**Second Mode**	**First Mode**	**Second Mode**	**First Mode**	**Second Mode**
0.0	0.000000	0.000000	0.000000	0.000000	0.000000	0.000000	0.000000	0.000000
0.2	0.001182	0.000391	0.001560	0.000376	0.000210	0.000150	0.001386	0.002570
0.4	0.002731	0.000061	0.003610	–0.00036	0.000481	0.000271	0.003022	0.007014
0.6	0.002731	0.000061	0.003610	–0.00036	0.000481	0.000271	0.003022	0.007014
0.8	0.001182	0.000391	0.001560	0.000376	0.000210	0.000150	0.001386	0.002570
1.0	0.000000	0.000000	0.000000	0.000000	0.000000	0.000000	0.000000	0.000000

Table 8. Deflection *w* for different *X*, *Y* and $\beta = 0.0$, $\theta = 0^\circ$ and $a/b = 1.5$ at time 5.K.

X	*Y* = 0.2		*Y* = 0.4		*Y* = 0.6		*Y* = 0.8	
	First Mode	**Second Mode**	**First Mode**	**Second Mode**	**First Mode**	**Second Mode**	**First Mode**	**Second Mode**
0.0	0.000000	0.000000	0.000000	0.000000	0.000000	0.000000	0.000000	0.000000
0.2	0.001035	0.000325	0.001344	0.000313	0.000193	0.000123	0.001462	0.002141
0.4	0.002287	0.000044	0.002962	–0.000322	0.000431	0.000225	0.003361	0.005850
0.6	0.002287	0.000044	0.002962	–0.000322	0.000431	0.000225	0.003361	0.005850
0.8	0.001035	0.000325	0.001344	0.000313	0.000193	0.000123	0.001462	0.002141
1.0	0.000000	0.000000	0.000000	0.000000	0.000000	0.000000	0.000000	0.000000

Table 9. Deflection *w* for different *X*, *Y* and $\beta = 0.0$, $\theta = 45^\circ$ and $a/b = 1.5$ at time 5.K.

X	*Y* = 0.2		*Y* = 0.4		*Y* = 0.6		*Y* = 0.8	
	First Mode	**Second Mode**	**First Mode**	**Second Mode**	**First Mode**	**Second Mode**	**First Mode**	**Second Mode**
0.0	0.000000	0.000000	0.000000	0.000000	0.000000	0.000000	0.000000	0.000000
0.2	0.000980	0.000292	0.001267	0.000280	0.000185	0.000111	0.001465	0.001940
0.4	0.002131	0.000040	0.002741	–0.000294	0.000412	0.000202	0.003414	0.005295
0.6	0.002131	0.000040	0.002741	–0.000294	0.000412	0.000202	0.003414	0.005295
0.8	0.000980	0.000292	0.001267	0.000280	0.000185	0.000111	0.001465	0.001940
1.0	0.000000	0.000000	0.000000	0.000000	0.000000	0.000000	0.000000	0.000000

Table 10. Deflection *w* for different *X*, *Y* and $\beta = 0.6$, $\theta = 0^\circ$ and $a/b = 1.5$ at time 5.K.

X	*Y* = 0.2		*Y* = 0.4		*Y* = 0.6		*Y* = 0.8	
	First Mode	**Second Mode**	**First Mode**	**Second Mode**	**First Mode**	**Second Mode**	**First Mode**	**Second Mode**
0.0	0.000000	0.000000	0.000000	0.000000	0.000000	0.000000	0.000000	0.000000
0.2	0.001162	0.000311	0.001541	0.000301	0.000201	0.000115	0.001231	0.002030
0.4	0.002740	0.000051	0.003645	–0.000294	0.000465	0.000213	0.002600	0.005541
0.6	0.002740	0.000051	0.003645	–0.000294	0.000465	0.000213	0.002600	0.005541
0.8	0.001162	0.000311	0.001541	0.000301	0.000201	0.000115	0.001231	0.002030
1.0	0.000000	0.000000	0.000000	0.000000	0.000000	0.000000	0.000000	0.000000

Table 11. Deflection *w* for different *X*, *Y* and $\beta = 0.6$, $\theta = 45^\circ$ and $a/b = 1.5$ at time 5.K.

X	*Y* = 0.2		*Y* = 0.4		*Y* = 0.6		*Y* = 0.8	
	First Mode	**Second Mode**	**First Mode**	**Second Mode**	**First Mode**	**Second Mode**	**First Mode**	**Second Mode**
0.0	0.000000	0.000000	0.000000	0.000000	0.000000	0.000000	0.000000	0.000000
0.2	0.001080	0.000274	0.001420	0.000263	0.000191	0.000102	0.001261	0.001792
0.4	0.002490	0.000042	0.003283	–0.000263	0.000436	0.000190	0.002752	0.004896
0.6	0.002490	0.000042	0.003283	–0.000263	0.000436	0.000190	0.002752	0.004896
0.8	0.001080	0.000274	0.001420	0.000263	0.000191	0.000102	0.001261	0.001792
1.0	0.000000	0.000000	0.000000	0.000000	0.000000	0.000000	0.000000	0.000000

On comparison with [13], it is concluded that:

Time period K is more for non-uniform thickness in case of parabolic variation as comparison to linear variation.

Deflection w is less for non-uniform thickness in case of parabolic variation as comparison to linear variation.

In this way, authors concluded that parabolic variation is more useful than linear variation.

7. References

[1] M. S. Dhotarad and N. Ganesan, "Vibration Analysis of a Rectangular Plate Subjected to a Thermal Gradient," *Journal of Sound and Vibration*, Vol. 60, No. 4, 1978, pp. 481-497.

[2] M. Amabili and R. Garziera, "Transverse Vibrations of Circular, Annular Plates with Several Combinations of Boundary Conditions," *Journal of Sound and Vibration*, Vol. 228, No. 2, 1999, pp. 443-446.

[3] S. Ceribasi and G. Altay, "Free Vibration of Super Elliptical Plates with Constant and Variable Thickness by Ritz Method," *Journal of Sound and Vibration*, Vol. 319, No. 1-2, 2009, pp. 668-680.

[4] U. S. Gupta, A. H. Ansari and S. Sharma, "Vibration Analysis of Non-Homogenous Circular Plate of Non-Linear Thickness Variation by Differential Quadrature Method," *Journal of Sound and Vibration*, Vol. 298, No. 4-5, 2006, pp. 892-906.

[5] R. K. Jain and S. R. Soni, "Free Vibrations of Rectangular Plates of Parabolically Varying Thicknesses," *Indian Journal of Pure and Applied Mathematics*, Vol. 4, No. 3, 1973, pp. 267-277.

[6] B. Singh and V. Saxena, "Transverse Vibration of Rectangular Plate with Bidirectional Thickness Variation," *Journal of Sound and Vibration*, Vol. 198, No. 1, 1996, pp. 51-65.

[7] J. S. Tomar, D. C. Gupta and V. Kumar, "Free Vibrations of Non-Homogeneous Circular Plate of Variable Thickness Resting on Elastic Foundation," *Journal of Engineering Design*, Vol. 1, No. 3, 1983, pp. 49-54.

[8] J. S. Yang, "The Vibration of a Circular Plate with Varying Thickness," *Journal of Sound and Vibration*, Vol. 165, No. 1, 1993, pp. 178-184.

[9] U. S. Gupta, A. H. Ansari and S. Sharma, "Vibration of Non-Homogeneous Circular Mindlin Plates with Variable Thickness," *Journal of Sound and Vibration*, Vol. 302, No. 1-2, 2007, pp. 1-17.

[10] D. V. Bambill, C. A. Rossit, P. A. A. Laura and R. E. Rossi, "Transverse Vibrations of an Orthotropic Rectangular Plate of Linearly Varying Thickness and with a Free Edge," *Journal of Sound and Vibration*, Vol. 235, No. 3, 2000, pp. 530-538.

[11] A. W. Leissa, "Recent Research in Plate Vibrations: Classical Theory," *The Shock and Vibration Digest*, Vol. 9, No. 10, 1977, pp. 13-24.

[12] Z. Sobotka, "Free Vibration of Visco-Elastic Orthotropic Rectangular Plates," *Acta Technica* (*Czech Science Advanced Views*), No. 6, 1978, pp. 678-705.

[13] A. K. Gupta, A. Kumar and Y. K. Gupta, "Vibration Study of Visco-Elastic Parallelogram Plate of Linearly Varying Thickness," *International Journal of Engineering and Interdisciplinary Mathematics*, accepted for publication.

[14] K. Nagaya, "Vibrations and Dynamic Response of Viscoelastic Plates on Non-Periodic Elastic Supports," *Journal of Engineering for Industry*, Vol. 99, 1977, pp. 404-409.

Appendix: List of Symbols

a	length of the plate,	$\check{n}$	Visco-elastic constants,
b	width of the plate,	$w(\xi, \eta, t)$	deflection of the plate *i.e.* amplitude,
ξ and η	co-ordinates in the plane of the plate,	$W(\xi,\eta)$	deflection function,
h	thickness of the plate at the point (ξ, η),	$T(t)$	time function,
E	young's modulus,	β	taper constant,
G	shear modulus,	K	time period,
v	Poisson's ratio,	h_0	h at $\xi = 0$,
$\tilde{D}$	visco-elastic operator,	a/b	aspect ratio,
D	$Eh^3/12(1-v^2)$, flexural rigidity,	θ	skew angle,
ρ	mass density per unit volume of the plate material,	$T_{\max}$	Kinetic energy,
		V	Strain energy,
t	time,	λ^2	$12\rho\,(1-v^2)a^4/Eh_0^2$, a frequency parameter

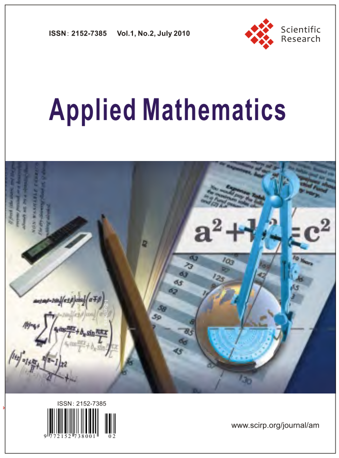

Call for Papers

Applied Mathematics (AM)

ISSN 2152-7385 (Print) ISSN 2152-7393 (Online)
http://www.scirp.org/journal/am

Applied Mathematics (AM) is an international journal dedicated to the latest advancement of applied mathematics. The goal of this journal is to provide a platform for scientists and academicians all over the world to promote, share, and discuss various new issues and developments in different areas.

Subject Coverage

This journal invites original research and review papers that address the following issues. Topics of interest include, but are not limited to:

- Approximation Theory
- Chaos Theory
- Combinatorics
- Complexity Theory
- Computability Theory
- Control Theory
- Cryptography
- Discrete Geometry
- Dynamical Systems
- Financial Mathematics
- Game Theory
- Graph Theory
- Information Theory
- Mathematical Biology
- Mathematical Chemistry
- Mathematical Economics
- Mathematical Physics
- Mathematical Psychology
- Mathematical Sociology
- Numerical Analysis
- Operations Research
- Optimization
- Probability Distribution
- Probability Theory
- Statistics
- Stochastic Processes
- Theoretical Computer Science

We are also interested in short papers (letters) that clearly address a specific problem, and short survey or position papers that sketch the results or problems on a specific topic. Authors of selected short papers would be invited to write a regular paper on the same topic for future issues of ***Applied Mathematics***.

Notes for Intending Authors

Submitted papers should not have been previously published nor be currently under consideration for publication elsewhere. Paper submission will be handled electronically through the website. All papers are refereed through a peer review process. For more details about the submissions, please access the website.

Website and E-Mail

http://www.scirp.org/journal/am **E-mail: am@scirp.org**

Applied Mathematics, 2010, 1, 87-136
Published Online July 2010 in SciRes (http://www.SciRP.org/journal/am/).

TABLE OF CONTENTS

Volume 1 Number 2 July 2010

